

Immune Response Markers are Prevalent in the mRNA Expression Profile of Maturing Dystrophic Murine Skeletal Muscle

Thomas Gregory Gainer

Thesis submitted to the Faculty at Virginia Polytechnic Institute and State University in partial fulfillment of the requirements for the degree of

Master of Science

in

Human Nutrition, Foods, and Exercise

Dr. Robert W. Grange, Committee Chair

Dr. Jay H. Williams, Committee Member

Dr. John L. Robertson, Committee Member

May 10, 2005

Blacksburg, Virginia

Keywords: Duchenne Muscular Dystrophy, Mdx-Utrophin Knockout Mouse, Affymetrix

Immune Response Markers are Prevalent in the mRNA Expression Profile of Maturing Dystrophic Murine Skeletal Muscle.

Thomas Gregory Gainer

(ABSTRACT)

Duchenne muscular dystrophy (DMD) is a severe and fatal muscle wasting disease characterized by a high mutation rate in the gene that encodes the membrane-associated protein dystrophin that results in absence of expressed protein. Although the primary genetic defect for DMD is known, the mechanisms that initiate the onset of DMD are not currently understood. This study tested the hypothesis that pathophysiological processes involved in DMD could be identified by the global expression of mRNA in maturing dystrophin- and utrophin-deficient mouse (*mdx:utrn*^{-/-}) muscles. Two potential dystrophic onset mechanisms targeted for analysis were (1) disrupted expression of calcium handling proteins; and, (2) increased expression of immune response markers.

An mRNA expression profile was developed following isolation of total RNA from control and *mdx:utrn*^{-/-} triceps surae (TS) muscles at ages 9-10 and 20-21 days using Affymetrix® Mu74Av2 GeneChips®. Compared to control, the mRNA expression profile in *mdx:utrn*^{-/-} muscles revealed there was a 3-fold increase in the number of gene transcripts differentially expressed more than 2-fold (53 transcripts at ages 9-10 days; 153 at ages 20-21 days). However, there were no changes in the mRNA transcripts for calcium handling proteins. In distinct contrast, there was up-regulation of transcripts that corresponded to an immune response (40 transcripts), extracellular matrix activity (14), and proteolysis (8). Up-regulation of several transcripts corresponded to cytokines and their receptors (11), chemokines and their receptors (5), and lymphoid and myeloid markers (16) suggesting that dystrophic muscle is susceptible to invasion by macrophages, leukocytes, B- and T-cells. These results are consistent with several reports (Spencer et al., 1997; Chen et al., 2000; Porter et al., 2002; Porter et al., 2003a; Porter et al., 2003b; Porter et al., 2004) that indicate the immune system may play an important role in the early pathophysiology of DMD. Understanding the functional aspects of an immune response in DMD onset should lead to more effective therapeutics.

Acknowledgements

First and foremost, I would like to thank my parents Tom and Sheila Gainer. They have provided unconditional love and support throughout all the challenges I have taken on in life and have especially been supportive during stressful and difficult times. Thanks for your support (and help with tuition and the costs of living)!

Next, I would like to thank my graduate advisor, Dr. Robert W. Grange, undergraduate advisor and committee member, Dr. Jay H. Williams and committee member, Dr. John L. Robertson (Dr. Bob). They have provided great encouragement and advice and have provided the interests and motivation to pursue my career in the biological sciences. Thank you for your patience!

Special thanks go to Amanda McWatters and Hanna Craig at the Virginia Bioinformatics Institute. Amanda helped guide me through the Affymetrix® procedures and Hanna assisted with the complex analysis of the data sets.

Special thanks also go to Kathy Reynolds, Laboratory Specialist in the Department of Human Nutrition, Foods, and Exercise. Kathy provided assistance teaching me molecular techniques, guided me throughout my project, and provided invaluable advice.

Thank you to all my graduate colleagues, especially Todd Distler, Simon Lees, Jeffery Otis, and Matthew Rittler. They made lab time much more enjoyable and provided assistance with all aspects of my data collection. They especially provided great entertainment outside of our academic lives.

Without the assistance of the Human Nutrition, Foods, and Exercise Staff, Sophia Leedy, Sherry Saville, Sherry Terry, and Wes Brusseau, I would not have been able to get through the everyday hustles and bustles of school life. Thank you all for keeping our records and paper work straight. You made sure we were all well cared for.

Table of Contents

Abstract.....	ii
Acknowledgements	iii
List of Figures and Tables.....	vii
List of Important Definitions	viii
Chapter 1. Introduction.....	1
Introduction	2
Statement of the problem.....	3
Significance of the study.....	4
Specific Aims	5
Research Hypotheses.....	6
Basic Assumptions	7
Limitations	8
Chapter 2: Literature Review.....	9
Introduction	10
Dystrophin.....	10
The Dystrophin Glycoprotein Complex.....	12
DMD Pathophysiology	13
Clinical Presentation	14
Animal Models	14
Hypotheses of DMD pathology.....	17
Membrane stability hypothesis.....	17
Evidence that supports the membrane hypothesis.....	18
Evidence that disputes the membrane hypothesis.....	20
Excitation Contraction Coupling	25
Calcium Hypothesis.....	27
The Signaling Hypothesis.....	31
Integrins.....	32
Nitric oxide synthase.....	32
Proteolysis.....	33
Immune Response.....	33
Summary	38
Chapter 3: Methods	41
Mouse Genotypes.....	42
Genotyping	43
DNA Isolation from Tail Snips.....	43

Dystrophin Screen	43
Utrophin Screen	44
Muscle Preparation	45
Total RNA Isolation.....	45
Expression Profiling by Affymetrix® Murine Genome U74Av2 GeneChip®	46
Analysis.....	47
Chapter 4. Results.....	48
Mice.....	49
Quality Control Analysis.....	49
Normalization of Data and Statistical Analyses.....	52
Significant Changes in Overall mRNA Expression	53
Age comparisons	53
mRNA Expression of Transcripts for Proteins in the Dystrophin-Glycoprotein Complex	55
mRNA Expression of Transcripts for Proteins in Excitation Contraction Coupling.....	57
mRNA Expression of Transcripts for Proteins Involved in Immune Function	58
Immune response expression markers at age 9-10 days	59
Immune response expression markers at age 20-21 days	59
mRNA Expression of Other Transcripts.....	60
Chapter 5. Discussion	66
DMD onset mechanisms are not presently well understood	67
Major Findings	67
Changes in mRNA expression were detected in mdx:utrn ^{-/-} muscle and an age dependent increase in the number of transcripts differentially expressed was also found.....	68
The expression of mRNA transcripts corresponding to proteins involved in ECC were not differentially expressed in mdx:utrn ^{-/-} muscle	69
The mRNA expression profile of mdx:utrn ^{-/-} muscle demonstrated dominant over-expression of immune response markers that suggests an immune response dominates the mdx:utrn ^{-/-} muscle during the early stages of the disease.....	69
Cytokine and receptor expression.....	70
Chemokine and receptor expression.....	70
Lymphoid and myeloid marker expression.....	71
Complement system	72
Secreted phosphoprotein 1	72
Summary	73
Rejection/Non-Rejection of Research Hypotheses.....	74
Future Directions.....	75
References.....	77
Appendices.....	94
Appendix A. Mouse Morphological Data	95
Appendix B. Directions to download raw data.	96

Curriculum Vita..... 97

List of Figures and Tables

Figure 2.1. The Dystrophin Gene	11
Figure 2.2. The Dystrophin Protein	12
Figure 2.3. The Dystrophin Glycoprotein Complex.	13
Figure 2.4. The Mdx-Utrophin Knockout (mdx:utrⁿ^{-/-}) vs. C57BL/6 Mouse	16
Figure 3.1. Experimental Design	42
Figure 3.2. Dystrophin and Utrophin Screen by PCR	44
Figure 4.1. Assessment of total RNA quality	49
Table 4.1. Summary of Affymetrix® MicroArray Suite - Expression Report	52
Table 4.2. Number of gene transcripts significantly differentiated	53
Table 4.3. Classes of differentially regulated transcripts in mdx:utrⁿ^{-/-}	54
Table 4.4. Expression calls of gene transcripts corresponding to the proteins of the DGC	57
Table 4.5. Expression calls of gene transcripts corresponding to the proteins involved in ECC	58
Table 4.6. The gene transcripts differentially expressed greater than 2-fold	61
Table 4.6B. Increased expression in mdx:utrⁿ^{-/-} at age 7-10 days (≥ 2 fold)	62
Table 4.6C. Decreased expression in the mdx:utrⁿ^{-/-} at age 20-21 days (≥ 2 fold)	63
Table 4.6D. Increased expression in mdx:utrⁿ^{-/-} at age 20-21 days (≥ 2 fold)	64

List of Important Definitions

1. DMD: Duchenne muscular dystrophy
2. DGC: Dystrophin-glycoprotein complex
3. D: dystrophin
4. U: utrophin
5. *mdx*: dystrophin ($D^{-/-}$) deficient mouse ($D^{-/-};U^{+/+}$)
6. *mdx:utrn^{-/-}*: *mdx* ($D^{-/-}$) and utrophin ($U^{-/-}$) knockout mouse ($D^{-/-};U^{-/-}$)
7. Ca^{2+} : Calcium
8. $[Ca^{2+}]_i$: Intracellular free calcium concentration
9. $[Ca^{2+}]_o$: Extracellular free calcium concentration
10. CSQ: Calsequestrin
11. PARV: Parvalbumin
12. RyR: Ryanodine receptor type 1 isoform found predominantly in skeletal muscle
13. SERCA: Sarco-endoplasmic reticulum Ca^{2+} ATPase
 - a. SERCA 1: Type 1 isoform found predominantly in fast twitch skeletal muscle
 - b. SERCA 2: Type 2 isoform found predominantly in slow twitch skeletal muscle
14. SR: Sarcoplasmic reticulum

Chapter 1. Introduction

Introduction

Duchenne muscular dystrophy (DMD) is an X-linked recessive skeletal muscle disease. The disease results from mutations in the dystrophin gene that leads to the absence of its encoded protein product, dystrophin. In addition, in the absence of dystrophin, other associated muscle membrane proteins, collectively known as the dystrophin-glycoprotein complex, or DGC (Koenig et al., 1987; Hoffman et al., 1987a; Love et al., 1990) are also absent. One in thirty five hundred boys is affected by DMD (Hoffman et al., 1987a). The disease is characterized by severe muscle fiber degradation and compromised regeneration. The slow but progressive loss of muscle function results in an inability to walk by adolescence, and leads to premature death in the early 20s because of cardiac and/or respiratory failure. Although the primary genetic mutations in the dystrophin gene and the protein losses associated with the disease have been well characterized, the function of dystrophin and the pathophysiological event(s) that initiate the disease are not yet understood. Discovering and understanding this/these event(s) would help assist in the development of target-specific drugs that could slow or stop the disease.

Absence of the dystrophin protein results from spontaneous mutations in its gene, the longest gene characterized to date (Koenig et al., 1987, Hoffman et al., 1987a). The dystrophin gene is located on the short arm, locus p21, of the X chromosome. The protein product has several different isoforms that are distinctly localized in skeletal, cardiac and smooth muscles, and brain tissue. In DMD, the absence of the skeletal muscle isoform of dystrophin and the DGC cause severe pathophysiology.

The 427 kD skeletal muscle isoform of dystrophin consists of 3,685 amino acids and is localized in the cytoplasmic membrane and at the myotendinous junction (Hoffman et al., 1987a; Tidball and Law, 1991). The association of dystrophin with the transmembrane proteins of the DGC provides a direct stabilizing link between the cytoskeletal surface of the sarcolemma and the extracellular matrix (Campbell, 1995; Rybakova et al., 2000). The DGC consists of subcomplexes of integral membrane proteins, including the dystroglycans (α and β), and the peripheral membrane proteins, the sarcoglycans (α , β , γ and δ). Dystrophin interacts with the DGC by binding β -dystroglycan at its carboxyl domain. β -dystroglycan crosses the membrane binding α -dystroglycan, and α -dystroglycan links the DGC with the extracellular matrix by binding to agrin and laminin in the extracellular matrix. The sarcoglycans associate laterally with the dystroglycans and bind sarcospan and possibly dystrobrevin to form a separable

heterotetrameric transmembrane complex whose function is not clearly defined. In addition, other cytoplasmic adapter proteins exist. These proteins are the syntrophins ($\alpha 1$ and $\beta 1$) that bind directly to the carboxyl terminal of dystrophin and dystrobrevin. The PDZ domains in the syntrophins may bind neuronal nitric oxide synthase (nNOS) and voltage-gated sodium channels (Roberts, 2001).

The functions of dystrophin and its association with the DGC are not well understood. Dystrophin comprises approximately 0.002% of total muscle protein (Hoffman et al., 1987a) and accounts for 5% of the surface associated cytoskeletal membrane protein (Ohlendiek and Campbell, 1991). In DMD, its absence leads to the complete loss of the DGC (Ohlendiek et al., 1993) and a series of molecular events causing muscle degradation and a compromised ability for muscle to regenerate.

Since the discovery of the dystrophin protein (Hoffman et al., 1987a), research has focused on determining its function to develop therapeutic strategies to blunt the disease progression or prevent it. It is currently believed that dystrophin interacts with actin, the DGC, laminin, and other proteins to form a rib-like lattice, or costameres, that span the sarcolemmal membrane. The costameres function to mechanically stabilize the sarcolemma and transduce forces from the muscle fibers to the tendons (Tidball and Law, 1991; Petrof et al., 1993; Campbell 1995; Rybakova et al., 2000). In addition, dystrophin may interact with its adjacent proteins of the DGC to assist signal transmission between the extracellular matrix and cytosol (Tidball and Law, 1991). However, the precise function of dystrophin and the molecular events that initiate the disease pathophysiology are not presently understood. Thus, it is important to determine the function of dystrophin and the molecular event(s) that initiate DMD pathophysiology.

Statement of the problem

There are at least three hypotheses to explain how dystrophin deficiency leads to the onset of DMD. The first hypothesis is the loss of dystrophin and the DGC compromises the integrity of the sarcolemma making it more susceptible to damage by mechanical stress (Petrof et al., 1993). This hypothesis is supported by observations of compromised membrane integrity in older dystrophin-deficient mice (mdx mice; age 90-100 days) subjected to eccentric contractions (Petrof et al., 1993, Stedman et al., 1991) but is refuted by the observation that the same

magnitude of mechanical stress is not sufficient enough to initiate the dystrophic process in young mdx mice (age 9-12 days; Grange et al., 2002).

The second hypothesis of dystrophy onset is that loss of dystrophin and the DGC leaves the sarcolemma leaky to calcium (Ca^{2+}). Ca^{2+} homeostasis is altered in dystrophic muscle (Turner et al., 1988, Fong et al., 1990, Turner et al., 1991). The increase in cytosolic Ca^{2+} may initiate muscle fiber degradation by the activation of Ca^{2+} dependent proteases (i.e., calpains), Ca^{2+} -initiated apoptosis, or metabolic alterations (Turner et al., 1993; Alderton and Steinhardt, 2000; McCarter and Steinhardt, 2000; Chen et al., 2000).

Finally, the third hypothesis suggests the loss of dystrophin and the DGC disrupts signaling between the extracellular matrix and cytosol compromising important physiological activities (Tidball and Law, 1991, Grange et al., 2002). Recent studies have demonstrated a profound chronic immune response by macrophages, cytotoxic T lymphocytes, dendritic cells, and mast cells in 6-9 year old human and 8 week old mouse dystrophin deficient muscles (Chen et al., 2000; Spencer and Tidball, 2001; Porter et al., 2002). Altered signaling in the muscle may initiate an immune response that degrades the muscle (Spencer et al., 1997; Chen et al., 2000; Spencer and Tidball, 2001; Porter et al., 2002).

Overall, there is conflicting evidence of the mechanisms that initiate pathophysiology in DMD. Three hypotheses for onset have been suggested but it is unclear whether the proposed hypotheses mentioned above initiate the disease or if they act alone, in combination, or in combination in a distinct temporal pattern. Therefore, it is important to test these hypotheses and determine the event(s) that initiate DMD.

Significance of the study

Because the mechanisms that initiate DMD are not fully understood, it is important to clearly define the mechanism(s) of pathophysiological onset. This knowledge is necessary to develop therapeutic interventions to blunt or prevent the pathophysiology of the disease.

Most DMD research has focused on determining the functions of dystrophin through the characterization of changes in single pathophysiological biomarkers during the middle stages of the disease in mdx mice (ages 6-8 weeks), and few studies have examined markers around the overt signs of pathophysiological onset at ages 21-28 days (Deconinck et al., 1998; Rezvani et al., 1995). Recent advances in technology, such as DNA microarrays, have allowed scientists to

examine the global expression of mRNA to better understand the transcriptional events occurring in cells, tissue, and organs. Through careful experimental planning and stringent statistical methods, comparisons of the expression profiles between healthy and diseased tissue have allowed scientists the opportunity to better understand the pathophysiological mechanisms contributing to diseases.

Gene expression in human dystrophin-deficient muscle (Chen et al., 2000; Tkatchenko et al., 2001) and in the muscle of mdx mice (the most common mouse model of DMD; Tkachenko et al., 2000; Porter et al., 2002) have been examined with Affymetrix® GeneChip® microarrays. These groups have reported DNA microarrays to be an effective tool to examine multiple physiological processes at a given time and have suggested physiological processes involved in the dystrophic process that have been previously overlooked. However, although these studies have provided important information about factors involved in the dystrophic process, they characterize the middle stages of the disease and use the mdx mouse which in an animal model that does not exhibit the same disease pathophysiology, or phenotype, as the human. Thus, to determine the mechanisms responsible for the initiation of the dystrophic process, it is imperative to make these measurements prior to or around the onset of pathophysiology in a more appropriate model for the disease, the mdx-utrophin knockout (*mdx:utrn*^{-/-}) mouse. This study describes how a DNA microarray was used to assess the mechanisms of pathophysiological onset in DMD using RNA from maturing *mdx:utrn*^{-/-} at ages 9-10 and 20-22 days. Given the *mdx:utrn*^{-/-} mouse exhibits a disease phenotype similar to humans afflicted with DMD, mRNA expression changes measured in this model may provide better clues of the event(s) involved in the beginning stages of dystrophy.

Specific Aims

To determine the pathophysiological mechanisms associated with the initial stages of the dystrophic process, the Affymetrix® Mu74Av2 GeneChip® was used to examine and compare global mRNA expression in aged matched triceps surae muscles (TS), containing mixed fiber types, from normal and *mdx:utrn*^{-/-} mice at age 9-10 and 20-22 days. The specific aims of the present study were:

1. To test the hypothesis that DNA microarrays can provide information on pathophysiological processes associated with the initiation of the dystrophic process.

2. To test the hypothesis that the expression of mRNA transcripts corresponding to the proteins involved in Ca^{2+} handling during ECC are not altered in dystrophin-utrophin deficient muscle
3. To test the hypothesis that dystrophic muscle is associated with an immune response, and to identify potential molecules that may contribute to it.

Research Hypotheses

The following are the main research hypotheses tested in this study:

1. The mRNA expression profile of *mdx:utrn*^{-/-} muscle will differ from normal muscle at age 9-10 and 20-22 days and will provide clues to potential pathophysiological processes involved in the onset of dystrophy.
2. A greater number of significant mRNA expression changes will occur in *mdx:utrn*^{-/-} compared to control muscles around the age of apparent disease onset in the *mdx:utrn*^{-/-} at age 7-14 days.
3. No changes will occur between control and *mdx:utrn*^{-/-} muscle in mRNA expression corresponding to proteins involved in excitation contraction coupling.
4. Up-regulation in the mRNA expression of transcripts corresponding to factors involved in an immune response in *mdx:utrn*^{-/-} muscle around the age of disease onset at 7-14 days.

The following are the specific null hypotheses tested in this study:

H₀₁: mRNA expression profiles will not differ between control and *mdx:utrn*^{-/-} muscle at all ages.

H₀₂: mRNA expression profile will not differ between control muscle at 9 and 21 days of age.

H₀₃: mRNA expression profile will not differ between *mdx:utrn*^{-/-} muscle at 9 and 21 days of age.

H₀₄: mRNA expression corresponding to proteins of the DGC will not differ between control muscle at 9 and 21 days of age.

H₀₅: mRNA expression corresponding to proteins of the DGC will not differ between *mdx:utrn*^{-/-} muscle at 9 and 21 days of age.

H₀₆: mRNA expression corresponding to proteins of the DGC will not differ between control and *mdx:utrn*^{-/-} muscle at 9 days of age.

H₀₇: mRNA expression corresponding to proteins of the DGC will not differ between control and *mdx:utrn*^{-/-} muscle at 21 days of age.

H₀₈: mRNA expression corresponding to proteins involved in ECC will not differ between control muscle at 9 and 21 days of age.

H₀₉: mRNA expression corresponding to proteins involved in ECC will not differ between *mdx:utrn*^{-/-} muscle at 9 and 21 days of age.

H₁₀: mRNA expression corresponding to proteins involved in ECC will not differ between control and *mdx:utrn*^{-/-} muscle at 9 days of age.

H₁₁: mRNA expression corresponding to proteins involved in ECC will not differ between control and *mdx:utrn*^{-/-} muscle at 21 days of age.

H₁₂: mRNA expression corresponding to proteins involved in an immune response will not differ between control muscle at 9 and 21 days of age.

H₁₃: mRNA expression corresponding to proteins involved in an immune response will not differ between *mdx:utrn*^{-/-} muscle at 9 and 21 days of age.

H₁₄: mRNA expression corresponding to proteins involved in an immune response will not differ between control and *mdx:utrn*^{-/-} muscle at 9 days of age.

H₁₅: mRNA expression corresponding to proteins involved in an immune response will not differ between control and *mdx:utrn*^{-/-} muscle at 21 days of age.

Basic Assumptions

The following were the basic assumptions made by the investigator:

1. The mice were well fed and hydrated.
2. The control and *mdx:utrn*^{-/-} mice were free from disease except for the dystrophy evident in the *mdx:utrn*^{-/-} mice.
3. The skeletal muscle of the *mdx:utrn*^{-/-} was a suitable model for DMD.
4. The methods recommended by Affymetrix® were optimized for high quality sample yield.

5. The Affymetrix® Mu74aV2 GeneChip® contained specific probe sets for mouse DNA and the probe sets reflected the proper sequence for the corresponding protein product.

Limitations

The following were limitations of this investigation:

1. Because of resource limitations, the current study was limited only to the *mdx:utrn*^{-/-} model of dystrophic mice.
2. The current study was limited to the TS muscle of *mdx:utrn*^{-/-} mice.
3. The current study was limited to the 2 age periods of 9-10 and 20-21 days.
4. Due to resource limitations, the current study investigated only mRNA expression transcripts in normal and *mdx:utrn*^{-/-} muscle.

Chapter 2: Literature Review

Introduction

Duchenne muscular dystrophy (DMD) is a male auto recessive disorder that is inherited through a female carrier with a mutation in the gene encoding the dystrophin protein. It affects approximately 1 in 3500 boys (Hoffman et al., 1987a). Mutations in the dystrophin gene prevent the expression of the skeletal muscle product, dystrophin. In addition, the proteins of the transmembrane glycoprotein complex, collectively known as the dystrophin-glycoprotein complex (DGC), are also absent, even though their gene transcripts are present (Chang et al., 1996). The loss of these proteins in DMD causes debilitating muscle degradation leading to premature death from cardiac and/or respiratory failure (Hoffman et al., 1987a). Despite the known genetic basis for the disease, the pathophysiological events that result from the absence of dystrophin are not well understood. Identifying these events would provide insight to develop therapeutic strategies to slow or prevent DMD.

Dystrophin

The dystrophin gene is located on the short arm of the X chromosome at locus p21 and is composed of 79 exons distributed over 2.5 million base pairs (Koenig, 1987). The gene contains several promoters that generate 14 kb transcripts for distinct mRNAs regulating the expression of different dystrophin isoforms (Petrof, 1998). The isoforms are localized in skeletal, cardiac, and smooth muscles as well as the cerebral cortex and cerebellar Purkinje cells. Because of its large size, the gene has high mutation rates. Different mutations in the dystrophin gene account for two different forms of muscular dystrophy, Becker (BMD) and DMD (Koenig et al., 1987). Whereas partial deletions in the dystrophin gene in BMD result in the expression of a truncated but partially functional dystrophin protein, in DMD deletions and frame shift mutations in the dystrophin gene result in the absence of the skeletal muscle isoform (Figure 2.1; Koenig et al., 1987).

The 427 kD skeletal muscle isoform of dystrophin consists of 3,685 amino acids (Figure 2.2; Hoffman et al., 1987a) and is localized in the cytoskeletal membrane and at the myotendinous junction (Tidball and Law, 1991). Dystrophin comprises approximately 0.002% of total muscle protein (Hoffman et al., 1987a) and accounts for 5% of the surface associated cytoskeletal membrane (Ohlendiek and Campbell, 1991). The dystrophin protein has four distinct regions. The first region is a 240 amino acid globular cytoskeletal actin binding N-

terminal domain with similar homology to the actin binding regions of α -actinin and β -spectrin, a structural protein found in erythrocytes (Petrof, 1998; Roberts, 2001). The second region is a domain of 24 -109 amino acid spectrin-like repeats. The repeats form anti-parallel triple-helix bundles and confer an extended rod like shape on dystrophin (Roberts, 2001). The third region is cysteine rich with highly conserved motifs that bind with the intracellular region of spectrin. Finally, the fourth region consists of a 420 amino acid C-terminal domain that interacts with the syntrophin family (Roberts, 2001). The binding of dystrophin to β -dystroglycan and members of the syntrophin family establishes an important connection between dystrophin and the DGC.

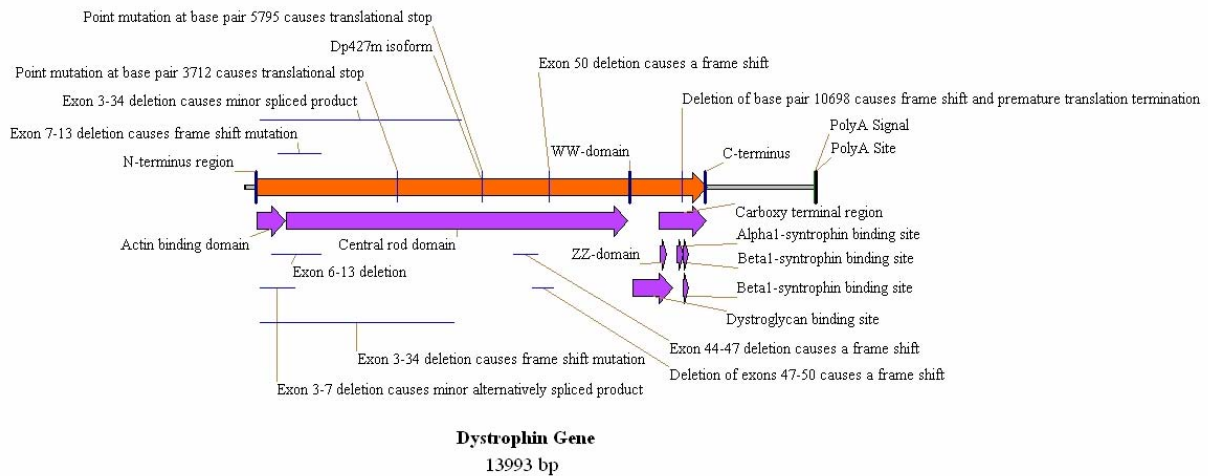


Figure 2.1. The Dystrophin Gene. The dystrophin gene is located on the short arm of the X chromosome at locus p21 and is composed of 79 exons distributed over 2.5 million base pairs (Koenig, 1987). The gene contains several promoters that generate 14 kb transcripts for distinct mRNAs regulating the expression of different dystrophin isoforms (Petrof, 1998). This figure illustrates the region of the gene encoding the 427 kD skeletal muscle isoform (Dp427m) and the different regions where mutations occur in DMD. This figure was created in Vector NTI using the mRNA sequence obtained from the National Center for Biotechnology Information (NCBI; Accession No. NM_004006, GI: 50322312).

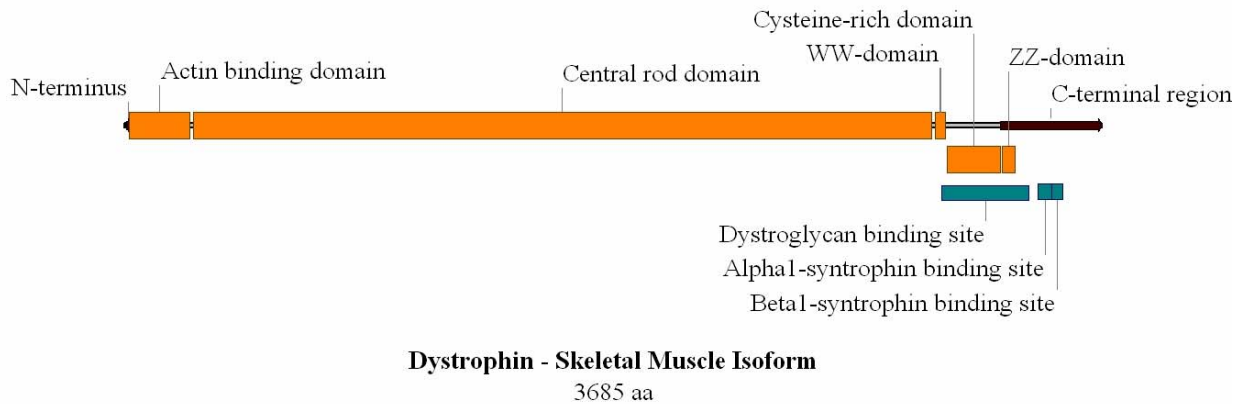


Figure 2.2. The Dystrophin Protein. The 427 kD skeletal muscle isoform of dystrophin consists of 3,685 amino acids (Hoffman et al., 1987a) and is localized in the cytoskeletal membrane and myotendinous junction (Tidball and Law, 1991). The protein has four distinct regions: 1) a 240 amino acid globular cytoskeletal actin binding N-terminal domain, 2) a central rod domain of 24 -109 amino acid spectrin-like repeats forming anti-parallel triple-helix bundles, 3) a cysteine rich region with highly conserved motifs, and 4) a 420 amino acid C-terminal domain that interacts with the syntrophin family, dystrobrevin, and β dystroglycan of the DGC (Petrof, 1998; Roberts, 2001). This figure was created in Vector NTI using the amino acid sequence obtained from NCBI (Accession No. NM_004006, NP_003997).

The Dystrophin-Glycoprotein Complex

The DGC is composed of distinct integral membrane protein sub-complexes that span the sarcolemma and link the cytoskeleton to the extracellular matrix. The members of the complex include the dystroglycans (α and β) and sarcoglycans (α , β , γ and δ). β -dystroglycan and the sarcoglycans cross the sarcolemma. β -dystroglycan binds to α -dystroglycan in the extracellular matrix and α -dystroglycan links the DGC to the extracellular matrix by binding to agrin and laminin. In addition, the sarcoglycans associate laterally with the dystroglycans to bind sarcospan and possibly β -dystrobrevin. This association forms a separable heterotetrameric transmembrane complex (Petrof, 1998). Dystrophin associates with the complex via its C-terminal interaction with β -dystroglycan. The cytoplasmic adapter proteins, syntrophins (α , β , γ and δ), also bind directly to the carboxyl terminals of dystrophin and dystrobrevin. They contain PDZ domains that may also bind neuronal nitric oxide synthase (nNOS) and voltage-gated sodium channels (Roberts, 2001). Figure 2.3 illustrates the composition of the DGC. The

linkage of dystrophin and the DGC between the cytoskeletal surface of the sarcolemma and extracellular matrix (Campbell, 1995; Rybakova et al., 2000) may serve both mechanical and signaling functions (Petrof et al., 1993; Campbell, 1995), but the nature of these potential functions is presently unclear.

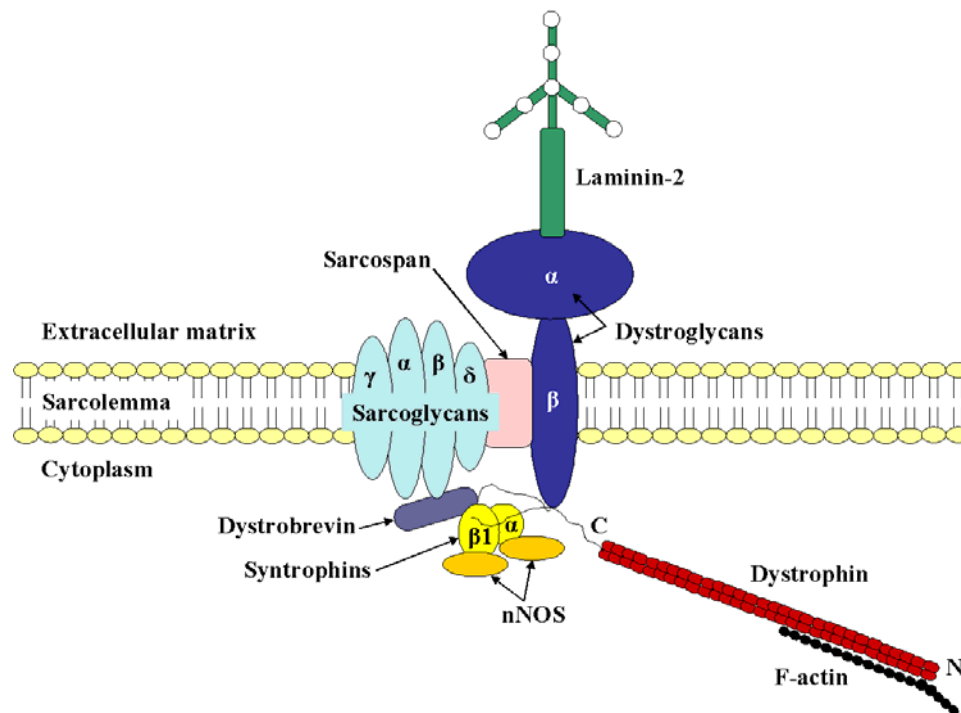


Figure 2.3. The Dystrophin-Glycoprotein Complex. The DGC is composed of distinct integral membrane protein sub-complexes that span the sarcolemma and link the cytoskeleton to the extracellular matrix. The members of the complex include the dystroglycans (α and β) and sarcoglycans (α , β , γ and δ) that cross the sarcolemma and bind to agrin and laminin-2 in the extracellular matrix via α -dystroglycan. The sarcoglycans associate laterally with the dystroglycans and bind sarcospan and possibly dystrobrevin. Dystrophin associates with the complex via its C-terminal interaction with β -dystroglycan. The cytoplasmic adapter proteins, syntrophins (α , β , γ and δ), also bind directly to the carboxyl terminals of dystrophin and dystrobrevin. The syntrophins contain PDZ domains that may also bind neuronal nitric oxide synthase (nNOS; Roberts, 2001). This figure was modified from Figure 1 (Durbeej and Campbell, 2002).

DMD Pathophysiology

In DMD, dystrophin and the associated proteins of the DGC are absent and cause a severe pathophysiological response. Progressive rounds of myofiber degeneration occur followed by regeneration. However, the capability of the myofiber to regenerate is compromised and extensive connective tissue proliferation occurs (Hoffman et al., 1987a).

Clinical Presentation

DMD was first described in 1852 by English physician Edward Meryon (Meryon, 1852) but was later named after French neurologist Guillaume Benjamin Amand Duchenne who published a series of illustrated articles in 1868 that described key features of the disease (Duchenne, 1868). Duchenne examined DMD muscle biopsies and established that the key abnormalities of the disease were hyperplasia of fibrous connective tissue and destruction of the muscle cellular architecture (Byrne et al., 2003).

Evidence of myofiber degeneration is evident in boys at approximately age 3 years. The muscles, especially the gastrocnemii, swell and appear larger than normal (pseudohypertrophy). The child uses the Gower's maneuver, which involves using the hands to walk to a standing position, because he has difficulties rising from a lying position, and he develops a waddling gait. Elevated levels of creatine kinase are observed in serum. With time, progressive muscle degeneration compromises the child's ability to support himself. At first, weakening of the limb muscles causes a postural change such that the stomach protrudes forward for stability. As a result, the spine curves forward and the child develops kyphosis, or severe curvature of the spine. Eventually the child loses all ability to support himself and becomes wheelchair bound at approximately age 12 years. The diaphragm and heart also undergo tissue degradation and weakening. Eventually, their function is compromised and death occurs around age 20 (Hoffman et al., 1987a).

Animal Models

Humans are not the only species that exhibit muscular dystrophy. Animal models are commonly used to study DMD because of ethical issues with human tissue samples. Mutations in the dystrophin gene also occur in chicken, hamster, cat, and dog and lead to mild to severely debilitating phenotypes. Several dog breeds, especially the golden retriever, are prone to develop canine X-linked muscular dystrophy (CXMD) which is genetically homologous to DMD. Like humans, myofiber necrosis and regeneration begin at an early age followed by extensive connective tissue proliferation and a premature death from cardiac and respiratory failure (Cozzi et al., 2001). The golden retriever has served a useful model for the study of DMD, but research has been limited as it is difficult to breed sufficient numbers for large studies.

The *mdx* mouse is the most common animal model for DMD research. It has a naturally occurring single point mutation along the 5' end of the dystrophin gene, in exon 23, which causes a premature transcriptional stop and results in the expression of a truncated protein product in skeletal muscle (Sicinski et al., 1989). At age 3-4 weeks, necrosis of *mdx* myofibers begins and lasts up to age 13 weeks (Deconinck et al., 1998; Rezvani et al., 1995). Thereafter, the hindlimb muscles compensate with fiber regeneration (Dimario et al., 1991). Myofiber degeneration in the diaphragm also occurs and continues throughout life with fibrotic and fatty tissue replacing muscle fibers. However, the weakening of the diaphragm does not impair function and the mouse is able to live a normal lifespan. Therefore, the pathophysiological consequences and clinical features of dystrophin deficiency in the *mdx* are not the same nor are they as severe as in the human.

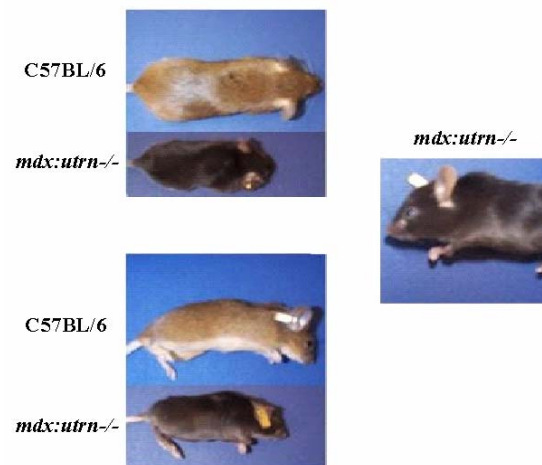
One possibility to explain the limited dystrophic pathophysiology in the *mdx* mouse is compensation by utrophin, a protein homolog of dystrophin. Utrophin is expressed in skeletal muscles and other tissues such as lung and kidney (Love et al., 1991). It is completely homologous to dystrophin (Tinsley et al., 1992) and like dystrophin, is transcribed from multiple promoters (Pearce et al., 1993, Blake et al., 1995). In adult skeletal muscle, utrophin is exclusively localized to the neuromuscular junction (Ohlendieck et al., 1991) and is believed to play a role in the formation and maintenance of acetylcholine receptors and synaptogenesis (Campanili et al., 1994; Grady et al., 1997). Utrophin expression is increased in dystrophin-deficient humans and *mdx* mice (Khurana et al., 1991; Matsumura et al., 1992). As expression increases, the pathophysiology becomes less severe, especially in *mdx* transgenic mice over-expressing utrophin (Matsumura et al., 1992; Tinsley et al., 1998). Tinsley et al. (1998) demonstrated that utrophin over-expressed in a transgenic *mdx* mouse line, localized at the sarcolemma, and prevented the dystrophic pathophysiology from occurring in hindlimb and diaphragm muscles. The extent of myofiber necrosis depended on the amount of utrophin present in the muscle. Therefore, in the absence of dystrophin, the localization of utrophin to the sarcolemma does compensate and rescue dystrophic animals from DMD (Tinsley et al., 1998). Unfortunately, there are no compensatory effects by utrophin in human DMD muscle (Tinsley et al., 1998).

Researchers have been eager to better understand the function of utrophin. Utrophin knockout mice have been generated. However, deleting the expression of skeletal muscle

utrophin had little effect on the mouse phenotype and quality of life compared to control (Grady et al., 1997). To better address the issue of a protective utrophin effect in dystrophin-deficient muscle, mice lacking dystrophin and utrophin were generated, as shown in Figure 2.4 (Grady et al., 1997; Deconinck et al., 1997). The mutation in these double knockout mutants (*mdx:utrn*^{-/-}) causes a severe pathological response and clinical phenotype similar to humans with DMD. At age 2-3 weeks, *mdx:utrn*^{-/-} hindlimb and diaphragm muscles develop severe muscle necrosis that is progressive until death at age 18-20 weeks (Grady et al., 1997). Regeneration of the muscle is compromised and myofibers are replaced with connective and fatty tissue. The mouse has a low weight and reduced growth. Its muscles are stiff making it difficult for the animal to move around. Limb contractures caused by stiffened muscles surrounding the joints of the hindlimb are evident when lifting the animal by the tail and severe kyphosis is evident. The *mdx:utrn*^{-/-} dies prematurely at age 18-20 weeks due to cardiac and/or respiratory failure (Grady et al., 1997). The *mdx:utrn*^{-/-} may be a better model to study DMD because of the similar phenotypic symptoms observed as the human. Carefully planned researched of both *mdx* and *mdx:utrn*^{-/-} mice can provide useful insight into characteristics of disease pathology. Examination of muscle prior to the overt signs dystrophy onset in both animals could provide information about mechanisms that initiate the disease pathophysiology. Understanding these mechanisms will inevitably suggest molecules or pathways to target for therapeutic interventions.

Figure 2.4. The *Mdx*-Utrophin Knockout (*mdx:utrn*^{-/-}) vs. C57BL/6 Mouse.

The *mdx:utrn*^{-/-} was created to better address the issue of a protective utrophin effect in dystrophin-deficient muscle (Grady et al., 1997; Deconinck et al., 1997). The mutation in these mice causes a severe pathophysiological response and the disease phenotype is similar to the human disease. Muscle degradation in the *mdx:utrn*^{-/-} hindlimb begins at age 2-3 weeks. Muscle regeneration becomes compromised and muscle fibers are replaced with connective and fatty tissue. As a result, muscles stiffen making it difficult for the animal to move. Limb contractures and kyphosis develop. The *mdx:utrn*^{-/-} has a low weight and reduced growth. The mouse dies prematurely at age 18-20 weeks due to cardiac and/or respiratory failure. Given the similar phenotype to the human disorder, the *mdx:utrn*^{-/-} may be a better model to study DMD.



Hypotheses of DMD pathology

The molecular events responsible for the initiation of pathophysiology in DMD remain unclear as research has focused on characterizing pathophysiology in patients and animals during middle disease stages. Thus, it is important to study patients or animals prior to the age of onset to identify the onset mechanisms. Currently, it is hypothesized that dystrophin and associated members of the DGC function to provide structural stability to the sarcolemma and/or support cellular signaling (Petrof et al., 1993, Campbell, 1995). The dystrophic mechanisms could be due to 1) compromised sarcolemmal integrity, 2) increased membrane permeability to calcium (Ca^{2+}), or 3) disrupted cellular signaling. Given the sophisticated nature of cellular activity, it is possible that one of these events could solely initiate the pathophysiology or act in a coordinated fashion in a specific sequence. In addition, evidence suggests an immune response is predominant in dystrophin-deficient fibers but have yet determined whether immune cells initiate and promote the pathophysiology in DMD (Spencer et al 1997; Porter et al., 2002).

Membrane stability hypothesis

Dystrophin is believed to be an important structural protein because of its localization and association with the proteins of the DGC. In addition to its cytoskeletal localization in the sarcolemma, dystrophin is also abundant in the myotendinous junction and is believed to help facilitate force transmission between the muscle fibers and tendons (Tidball and Law, 1991). Dystrophin in association with the DGC forms costameres. These are a rib-like lattice spanning across the cytoplasmic face of the sarcolemma that help stabilize the cytoskeleton to the extracellular matrix. Costameres serve as mechanical couplers to distribute contractile forces between the sarcomeres and basal lamina and help regulate the uniform length of sarcomeres within fibers of active and non-active motor units (Rybakova et al., 2000).

The absence of dystrophin and members of the DGC could compromise sarcolemmal integrity, making the sarcolemma more susceptible to damage by typical mechanical stresses derived from muscle contraction and stretch (McArdle et al., 1991, Petrof et al. 1993, Mendell et al., 1995). Thus, in DMD, the dystrophic process could be initiated by small tears in the membrane that leads to degradation of the muscle fibers. As the disease progresses the membranes become weaker still (Petrof et al., 1993). Membrane tensile strength is thought to be

compromised in the absence of dystrophin in *mdx* muscles; however, the experimental evidence is equivocal.

Evidence that supports the membrane hypothesis. Menke and Jockusch (1991) examined the stress resistance of dystrophin-deficient muscle fibers through hypo-osmotic shock. They enzymatically isolated fibers from interosseus muscle in C57BL/10 (control) and *mdx* mice and abruptly exposed them to a hypo-osmotic medium to examine osmotic cell damage. Cell damage was assessed in surviving muscle fibers by the formation of membrane blebs and potential changes in fiber diameter. *Mdx* muscle fibers were more sensitive (diameter $32 \pm 7 \mu\text{m}$) to osmotic shock than control (diameter $39 \pm 7 \mu\text{m}$). To determine if the increased sensitivity resulted from fiber degeneration and regeneration or the absence of dystrophin, bupivacaine was injected into *mdx* and control interosseus fibers *in situ* to induce muscle degradation to follow subsequent regeneration. Few *mdx* fibers regenerated after 30-40 days whereas control fibers regenerated, suggesting *mdx* fibers exhausted their pool of satellite cells from previous rounds of degeneration and regeneration. The precise mechanism that caused reduced stability in the *mdx* myotubes was unknown because osmotic stress involves both mechanical properties and ion fluxes. However, Menke and Jockusch concluded dystrophin deficiency contributed to the weakened stability of the *mdx* myotube (Menke and Jockusch, 1991).

Petrof et al. (1993) examined extensor digitorum longus (EDL) and diaphragm muscles for contraction-induced injury. They specifically wanted to determine if continuous degeneration observed for the diaphragm was due to the relatively greater work rate of the diaphragm compared to other muscles. Muscles were dissected from control and *mdx* mice aged 90-110 days. Whole EDL or diaphragm strips were attached to a dual-mode servomotor system, and immersed in an oxygenated bath of Ringer's solution. The muscles underwent one of four protocols. The first protocol was five tetanic stimulations for 700 ms with the muscle lengthened at 0.5 resting lengths (L_0) per second during the final 200 ms of the stimulation period. Second were five tetanic stimulations for 700 ms without muscle lengthening. The third was unstimulated muscle lengthening for 200 ms at 0.5 L_0 per second. The fourth was repeated unfused tetanic stimulations over a 5 minute period. A four minute rest period followed each stimulation period in the first 3 protocols. Muscle force was recorded and during stimulation protocols, procion orange (PO) in Ringer's solution was added to assess sarcolemmal damage.

PO is a small molecular weight (F.W. 631) fluorescent dye that penetrates damaged myofiber membranes but is impermeable to intact ones. The muscles were immediately mounted and frozen following PO incubation and transversely sectioned to determine fiber-cross sectional area and the proportion of damaged fibers (Petrof et al., 1993).

Control and dystrophic-deficient muscle fibers at age 90-110 days exhibited sarcolemmal breakage during isometric muscle contraction but damage was greatest with the stimulated eccentric contractions because these produced the greatest membrane stress. However, the *mdx* diaphragm and EDL suffered greater damage than control muscle and were even damaged with unstimulated stretches i.e., passive stretches. Passive stretches caused no damage to control muscle. It was reported that control and *mdx* muscle exhibited a linear relation between peak muscle force and the proportion of damaged fibers. However, the data supporting the linear relation appears widely distributed about the regression lines for each condition; therefore, the validity of this conclusion is questionable. Regardless, the linear relation was significantly greater in *mdx* diaphragm ($r=0.52$, $p < 0.05$; Petrof et al., 1993).

Based on these findings, the authors concluded that dystrophin could stabilize the sarcolemma during contraction by interacting with adjacent structural proteins to distribute force across the sarcolemma or by transmitting force beyond the membrane in the extracellular matrix through interactions with the DGC. Dystrophin-deficient muscle was more susceptible to damage for any given level of stress. Therefore, muscle degeneration could result from the cumulative effects of activity on the fragile membrane and compromise the ability for the muscle to regenerate (Petrof et al., 1993).

Lynch et al. (2000) examined the effects of contraction-induced injury on single skinned muscle fibers. The purpose of the study was to test the null hypothesis that skinning muscle membranes was so severe that fibers from normal, *mdx*, and *mdx* transgenic mice, which over-expressed dystrophin, would not suffer any force deficit differences from contraction-induced injury. EDL muscle fibers were chemically skinned from 6 month old control, *mdx*, and *mdx* transgenic mice. The *mdx* transgenic mice were chosen because they expressed sufficient levels of a truncated dystrophin construct to eliminate the pathophysiological effects of dystrophin deficiency (Lynch et al., 2000).

Muscle fibers in this study were attached between a sensitive force transducer and servomotor and maximally activated with Ca^{2+} (pCa 4.5) followed by a single stretch of 10%,

20%, and 30% strain at 0.5 fiber segment length (L_f) per second. The stretches were induced when the peak fiber force plateaued (P_o). Injury was determined by the force deficit or the difference between the normalized P_o immediately after stretch and P_o before stretch (Lynch et al., 2000).

The results showed no differences in cross-sectional area or P_o in fibers obtained from control, *mdx*, and *mdx* transgenic muscles. The peak force, the ratio of peak force during stretch to the P_o before stretch, normalized average force, the work during stretch, and power also did not differ between groups. Force deficits did increase linearly as a function of the stress magnitude but no differences in force deficit were observed between normal, *mdx*, and *mdx* transgenic muscle. Thus, the myofibrillar structure of fibers, i.e., actin and myosin, were not affected by the contraction-injury induced protocol and were not damaged in control, *mdx*, and *mdx* transgenic muscles. Therefore, the authors concluded the force deficits reported in whole muscle of *mdx* mice must be the result of a disrupted sarcolemma. Thus, sarcolemmal integrity is compromised in dystrophin-deficient muscle (Lynch et al., 2000).

While these studies provide evidence for compromised membrane integrity due to dystrophin-deficiency, contradictory results dispute the membrane hypothesis. The contradictory results may be due to the age of the animals studied.

Evidence that disputes the membrane hypothesis. Sacco et al. (1992) compared the contractile properties of *mdx* tibialis anterior muscle (TA) to normal muscle, as well as to damaged but regenerating muscles. The study tested the hypothesis that dystrophin-deficient muscle is more susceptible to stretch-induced muscle damage. Female *mdx* and control mice aged 16-26 weeks were anaesthetized and fixed so that the distal tendon of the TA muscle was attached to a force transducer while the proximal tendon remain attached *in situ*. The sciatic nerve was cut and bipolar electrodes were fixed on the peripheral sciatic nerve stump. Muscle length was then adjusted to provide maximum twitch tension and a force-frequency relationship was determined by stimulating the muscle at 1, 40, 60, and 100 Hz for a half second with 30 seconds rest between each stimulation. Following a 5 minute recovery, the muscles underwent a fatigue protocol of supramaximal stimulations at 40 Hz for 250 ms every second for 3 minutes. A tetanic stimulation was then applied and expressed as a percentage of the maximum tetanic force. *Mdx* muscle was 30% stronger (1.59 N) than control muscle (1.17 N) but when the force

produced was normalized to cross-sectional area, *mdx* muscle was significantly weaker than control muscle (0.24 N/mm², *mdx*; 0.30 N/mm², control; p<0.01). During the fatigue protocol, *mdx* muscle lost more force compared to control muscle during the first few contractions; however, the muscle was significantly more resistant to fatigue as it produced 48% its original force at the end of the protocol compared to 42% control muscle (p<0.05; Sacco et al., 1992).

Eccentric contractions were also applied to dorsiflexor muscles in *mdx* and control muscle. After being anaesthetized, the mice were fixed so that the knee from one leg was clamped and the foot was attached to a platform that provided full plantar and dorsi flexion in a 100 degree range of motion. The peroneal nerve of the TA was exposed and attached to a small hook electrode to apply 100 Hz stimulation for 300 ms just prior and throughout the entire lengthening phase. The protocol consisted of 240 repetitions of active lengthening and passive shortening with 5 seconds rest between each repetition. The contralateral muscle of the mice was not fixed to serve as a control. The mice were allowed to recover following the protocol and were anesthetized at 1, 6, or 12 days post protocol to determine contractile properties and fatigue resistance. They were then sacrificed and the TA muscles were removed to determine the extent of damage by counting the number of foci of mononuclear cells present in transverse sections stained with haematoxylin and eosin. Little change occurred histologically in *mdx* and normal muscle a day after the eccentric exercises. At 3 days, muscles were invaded by mononuclear cells that accompanied muscle destruction. The extent of invasion was significantly greater in *mdx* muscle (6.9 damage foci/field, *mdx*; 5.5 damage foci/field, control; p<0.05). However, the damage observed in the *mdx* was localized to fibers that had previously degenerated and were regenerating. At day 6, *mdx* muscle had fewer immune response cells and appeared to be regenerating based on the presence of small basophilic cells with central nuclei. Force frequency analysis showed a 55% decrease in force developed between stimulation frequencies of 40 and 100 Hz in *mdx* muscle compared to a 70% decrease in normal muscle. Both *mdx* and control muscles exhibited large losses of force up to 12 days following the eccentric contraction protocol. The largest deficit in force for both muscle groups was observed at 3 days following exercise (52%, *mdx*; 56%, control) which corresponded to the time of greatest fiber damage. However, muscle recovery was similar with the *mdx* producing 79% of maximal force and control muscle 76%. Control muscle was more resistant to fatigue at 3 days

as muscles produced 45% of maximal force compared to the *mdx*, 41%. The deficit observed in the *mdx* was the same in the contralateral muscle (Sacco et al., 1992).

Based on the contractile properties and fatigue resistance, Sacco et al. (1992) concluded that dystrophin-deficient *mdx* muscle aged 16-26 weeks was not more susceptible to stretch induced injury. These findings contradict observations made in *mdx* muscle, at ages 12-16 (Petrof et al., 1993) and 26 weeks (Menke and Jockusch, 1991; Lynch et al., 2000), and argue against the hypothesis that dystrophin structurally protects the sarcolemma from mechanical damage (Sacco et al., 1992).

McArdle et al. (1991) examined the *mdx* mouse to determine if contractile activity induced damage in dystrophin-deficient muscle and the role of Ca^{2+} and phospholipase activity in muscle damage. EDL muscles were dissected from control and *mdx* mice at approximately age 6 weeks. The muscles were mounted and attached to a rolling device in Ringer's solution at 37°C. The muscles were pre-incubated for 30 minutes then electrically stimulated at 100 Hz for 0.5 seconds every 5 seconds for 30 minutes, or repeatedly stretched over 30 minutes to 130% of resting muscle length for 0.5 seconds every 5 seconds with or without electrical stimulation. Other muscles were treated only in 20 μM calcium ionophore, a Ca^{2+} ion exchanger used to measure cytosolic Ca^{2+} concentrations, for 30 minutes. Following the protocol, the muscles were incubated in fresh Ringer's solution for 2 hr. The Ringer's solution was then collected for immediate analysis of creatine kinase (CK) activity or frozen for further determination of prostaglandin E_2 (PGE_2) content (McArdle et al., 1991).

Basal CK and PGE_2 during incubation did not rise in *mdx* mice. Muscle contractions induced by electrical activity caused a delayed release of CK from *mdx* and control muscle but the control release levels were significantly higher ($p < 0.05$) after 1.5 hrs. The repetitive contractions significantly fatigued both muscle groups with little recovery after 2 hours of rest. However, there was no difference in the severity of fatigue between the groups. PGE_2 release was significantly increased in the *mdx* compared to the control starting 1 hour after stimulation. Repetitive muscle stretches had no effect on CK release but caused a slight rise in PGE_2 release from both *mdx* and control muscles. When stimulation was applied during stretches, both muscles released great amounts of CK but levels were significantly greater from controls ($p < 0.05$) 1.5 hours after stimulation. *Mdx* muscles released significantly greater amounts of PGE_2 at 1 and 1.5 hours after stimulation ($p < 0.05$). Ca^{2+} ionophore induced a rapid and

substantial CK release from both control and *mdx* muscles and a significantly greater release of PGE₂ from the *mdx* (McArdle et al., 1991).

Given the observations that stimulated eccentric contractions caused a great release of CK from both tissue types but a greater release from control muscle, McArdle et al. (1991) concluded that dystrophin-deficient muscle was not necessarily more susceptible to damage by eccentric contractions. However, the rise of PGE₂ levels observed from *mdx* muscle suggested a potential alteration of Ca²⁺ influx in dystrophin-deficient fibers and the possibility that the removal of dystrophin affects the activity of phospholipase enzymes (McArdle et al., 1991).

Rezvani et al. (1995) tested the hypotheses that the absence of dystrophin in *mdx* skeletal muscle would reflect specific changes to contractile characteristics, endurance performance, and excitability. The differences observed would be age-dependent and relevant to the extent of muscle degeneration and regeneration. The gastrocnemius, plantaris, and soleus muscles (triceps surae, TS) were stimulated *in situ* (in 2, 5, and 13 week old control and *mdx* mice). The mice were anesthetized and fixed so that the TS were stimulated with an electrode probe at the end of the sciatic nerve. Twitch and tetanic contractions were elicited at L₀, followed by successive stimulations at 2, 10, and 20 Hz for 5 minutes. The time to peak tension, ½ relaxation time, maximal contraction rate, and maximal relaxation rate were compared. Muscles were also probed and stimulated to record the compound mass action potential which reflected the index of junctional transmission and sarcolemmal excitability. Following the stimulation protocols *in situ*, muscles were frozen and subsequently used to determine cytochrome C oxidase content by Western analysis (Rezvani et al., 1995).

Twitch and tetanic tensions as well as contractile speed increased with age in both genotypes while no difference in specific tension between control and *mdx* animals was evident until 5 weeks of age when the *mdx* muscle produced significantly less specific tension. At age 13 weeks, *mdx* muscle displayed a faster time to peak tension than control. An effect of contraction time on maximal contraction rate was observed at all ages but significantly declined in *mdx* muscle at age 13 weeks. The maximal relaxation rate did not differ at any age and progressive muscle fatigue occurred in both groups at all ages. The severity of fatigue was similar for *mdx* and control muscle at age 2 and 5 weeks, but at age 13 weeks, the *mdx* muscle was significantly less fatigable than control (p<0.05). This corresponded to greater electrical

activity. No differences in cytochrome C oxidase were observed between animals at any age (Rezvani et al., 1995).

Rezvani et al. (1995) concluded the lack of consideration for the onset of pathophysiology and periods of degeneration/regeneration may explain the inconsistent results on contractile properties in the *mdx* mouse. The lower twitch and tetanic properties observed in *mdx* fibers were due to fiber degeneration processes secondary to dystrophin deficiency. *Mdx* muscle became faster but less economical in utilizing ATP. Therefore, the lack of dystrophin had little effect on muscle excitability (Rezvani et al., 1995).

Grange et al. (2002) examined the effects of eccentric contractions in maturing *mdx* and *mdx:utrn*^{-/-} mice to determine if they rendered the sarcolemma more susceptible to contraction induced injury. EDL muscles were dissected from control, *mdx*, and *mdx:utrn*^{-/-} mice during early maturation at ages 9-12 days. The muscles were hung from a dual servomotor and subjected to stretch and no stretch protocols as described by Petrof et al. (1993). Briefly following the stretches, fiber damage was assessed by the uptake of procion orange. Before the stretches, isometric tension was significantly decreased compared to control (p<0.05). Muscle stiffness was similar in all groups following stretches, but tetanic tension was significantly reduced in both *mdx* and *mdx:utrn*^{-/-} animals (p<0.05). The uptake of procion orange dye suggested greater damage dystrophic compared to control EDL (p<0.05) but the damage was not different with each genotype between the no-stretch and stretch conditions. Therefore, damage to the sarcolemma did not appear to be increased by the stretch protocol and the onset of dystrophy in *mdx* and *mdx:utrn*^{-/-} mice was not due to contraction or injury induced by active eccentric contractions. Based on these results, the authors concluded increased membrane Ca²⁺ permeability at the membrane and/or compromised cellular signaling may play a more important role in the initiation of DMD pathophysiology during early maturation (Grange et al., 2002).

Overall, evidence for compromised membrane integrity due to dystrophin-deficiency is contradictory and calls into question the membrane hypothesis as an onset mechanism. While support exists for compromised membrane integrity in *mdx* muscle at ages 12-16 and 26 weeks (Petrof et al., 1993 and Lynch et al., 2000), others refute it in *mdx* muscle at ages 6 and 16-26 weeks (McArdle et al., 1991, and Sacco et al., 1992). However, evidence suggests that compromised sarcolemmal integrity does not contribute to the onset of dystrophy. Rezvani et al. (1995) demonstrated muscle excitability was unchanged in younger *mdx* mice near the age of

dystrophic onset at ages 2-5 weeks, but was reduced at age 13 weeks when muscles began repair. Grange et al. (2002) demonstrated that while maturing *mdx* and *mdx:utrn*^{-/-} are weaker and more damaged compared to control, active stretches did not damage the sarcolemma in young *mdx* and *mdx:utrn*^{-/-} mice prior to the onset of dystrophy at age 9-12 days. There are two possible reasons for the inconsistencies in the data that question the membrane hypothesis as an onset mechanism. First, the *mdx* may not be the best model for DMD since the hindlimb muscles are able to recover and the animal lives a normal life. Second, the ages of the animals examined varied between studies and the discrepancies in the data may reflect periods of muscle degeneration or regeneration in the *mdx*. Time course studies, starting with early maturation, that use common methods are necessary to critically examine the role of dystrophin in protecting sarcolemmal integrity. Thus, in the absence of a weaker membrane as an onset mechanism, increased Ca²⁺ permeability and/or altered cell signaling may play more important roles in the DMD onset.

Excitation Contraction Coupling

Calcium (Ca²⁺) is an important element that functions to initiate and regulate multiple physiological processes, including skeletal muscle contraction, where it acts as a signaling intermediate to regulate skeletal muscle contraction and relaxation during excitation contraction coupling (ECC).

Action potential generation is the first phase of ECC. Contraction is initiated by an action potential originating from a motor neuron that passes down the axon to the neuromuscular junction at the muscle fiber. Following release of the neurotransmitter acetylcholine from the axonal bouton, permeability of the muscle fiber end plate to sodium changes dramatically to yield fiber depolarization and generation of an action potential. The action potential is a wave of depolarization that spreads transversely across the sarcolemma and down the t-tubule. The Ca²⁺ release process is initiated when the depolarization reaches the t-tubule and activates L-type Ca²⁺ channels (dihydropyridine receptors, DHPR; Fleisher and Inui, 1989, Strube et al., 2000). Receptor activation causes the II-III loop of the DHPR to couple with the myoplasmic Ca²⁺ releasing ryanodine receptor (RyR) localized to the sarcoplasmic reticulum (SR; Felder et al., 2002). The SR functions as a Ca²⁺ storage organelle. DHPR-RyR coupling activates the RyR to release Ca²⁺ from the SR. RyRs are activated by the release of Ca²⁺ at low intracellular Ca²⁺ concentrations ([Ca²⁺]_i) and deactivated by high [Ca²⁺]_i. The negative and positive feedback

mechanisms of the RyR assist to regulate muscle contraction (Berchold et al., 2000). In addition, they prevent high $[Ca^{2+}]_i$, which could activate proteolysis through Ca^{2+} -dependent proteolytic pathways i.e., calpains. Therefore, the initial release of Ca^{2+} from the RyR during depolarization positively activates the RyR to further release Ca^{2+} from the SR.

Ca^{2+} released from the SR binds to Ca^{2+} sensitive troponin C (TnC) on the thin actin filament of the contractile apparatus. TnC, along with inhibitory troponin (TnI) and tropomyosin binding troponin (TnT), associates with tropomyosin to form the troponin-tropomyosin complex which acts to protect the myosin binding site. Ca^{2+} binding to the troponin-tropomyosin complex causes a conformational change such that TnI shifts to expose the myosin binding site on actin. Initial binding of ATP to its site on myosin results in a weak binding state between actin and myosin. In the process of ATP hydrolysis, and the subsequent release of ADP and P_i , actin and myosin first form a strong binding state, and then using the energy of ATP hydrolysis completes the power stroke. During the power stroke, the myosin thick filament pulls on the actin thin filament to generate movement. Repeated crossbridge cycles allow myosin to move along actin in a sliding motion (Berchtold et al., 2000). During the contraction phase of ECC, millions of cross bridges form throughout many muscle fibers to shorten the sarcomere and ultimately the muscle. This process continues as long as $[Ca^{2+}]_i$ remains elevated and ATP is available.

Relaxation occurs upon the detachment of the myosin head from the actin binding site and the dissociation of Ca^{2+} from TnC. The free Ca^{2+} translocates through the myoplasm to the SR. In fast type fibers, Ca^{2+} translocation is assisted by parvalbumin (PARV), a myoplasmic Ca^{2+} -binding protein (Berchtold 1989, Berchtold et al., 2000). Next, Ca^{2+} binds to the sarcoplasmic reticulum Ca^{2+} ATPase pump, SERCA, a Ca^{2+} ATP dependent pump localized to the SR membrane. Two isoforms of SERCA exist. SERCA1 is specifically expressed in fast twitch skeletal muscle fibers. SERCA2 is expressed in non-muscle tissue but also is predominantly expressed in slow twitch muscle fibers (Berchtold et al., 2000). Ca^{2+} binding to SERCA initiates ATP binding. ATP is hydrolyzed and causes a conformational change that pumps two- Ca^{2+} into the SR for each ATP hydrolyzed. Upon entry into the SR, Ca^{2+} is bound to calsequestrin (CSQ) for storage (Berchtold et al., 2000). Thus, the process of ECC is completed with the uptake and storage of Ca^{2+} in the SR.

Calcium Hypothesis

Dystrophin-deficient muscle fibers are unable to efficiently regulate Ca^{2+} , and Ca^{2+} leak channels at the membrane are more sensitive with a higher probability to remain open (Turner et al., 1991, Fong et al. 1990). Thus, dystrophin-deficient muscle contains higher resting levels of intracellular Ca^{2+} compared to normal muscle (Turner et al. 1988). It has been hypothesized the higher resting levels of intracellular Ca^{2+} initiate degradative proteolysis by Ca^{2+} sensitive proteases and phospholipases in dystrophin-deficient fibers, leaving them susceptible to necrosis (Turner et al., 1993). While research supports mechanisms for Ca^{2+} entry into the myoplasm, it remains uncertain when these changes occur and if they initiate the dystrophic process.

Turner et al. (1988) compared $[\text{Ca}^{2+}]_i$ in single flexor digitorum brevis fibers from normal and *mdx* mice, aged 1 to 4 months, using the fluorescent tetracarboxylate chelator fura-2. *Mdx* fibers contained greater $[\text{Ca}^{2+}]_i$ than control (92 ± 9.8 nM, *mdx*; 40 ± 2.8 nM, control) when the extracellular Ca^{2+} concentration ($[\text{Ca}^{2+}]_o$) was at physiological levels of 1.84 mM. When $[\text{Ca}^{2+}]_o$ was reduced ten-fold to 0.184 mM, $[\text{Ca}^{2+}]_i$ in *mdx* fibers was reduced 40% to a level close to normal resting fibers while control $[\text{Ca}^{2+}]_i$ was reduced 15%. Thus, dystrophin-deficient muscle fibers appear to have a reduced ability to regulate $[\text{Ca}^{2+}]_i$ (Turner et al., 1988).

To determine whether defects in the sarcolemma or the SR contributed to the increase in $[\text{Ca}^{2+}]_i$, the kinetics of Ca^{2+} release and uptake at the SR were investigated. Myofibers were loaded with fura-2 ester, a lipophilic Ca^{2+} binding indicator, and stimulated via platinum electrodes in a buffer at normal physiological $[\text{Ca}^{2+}]_o$. In control and *mdx* fibers, $[\text{Ca}^{2+}]_i$ levels were similar when maximally stimulated. However, in *mdx* fibers, basal and submaximal twitch levels remained significantly elevated. Therefore, it was concluded the SR was not defective in dystrophin-deficient muscle but potential defects in the sarcolemma provided the opportunity for increased Ca^{2+} influx (Turner et al., 1988).

The hypothesis that increased $[\text{Ca}^{2+}]_i$ could induce or increase protein degradation was also tested by the release of tyrosine, an amino acid that is not metabolized by muscle. At normal $[\text{Ca}^{2+}]_o$ concentrations, the rate of degradation was 80% higher in the *mdx* compared to control. Therefore, because *mdx* muscle between ages 1-4 weeks maintains elevated $[\text{Ca}^{2+}]_i$ at rest and during contraction, the net degradation of muscle proteins is significantly increased (Turner et al., 1988).

To determine the mechanism of Ca^{2+} entry into the myoplasm, Fong et al. (1990) tested the hypothesis that an alteration of Ca^{2+} leak channel properties was responsible. Intracellular Ca^{2+} concentrations were measured and compared in dystrophic myotubes cultured from human and mouse at 6-15 days after myoblast fusion. In normal human and mouse myotubes, resting $[\text{Ca}^{2+}]_i$ was 55 ± 5 nM and 82 ± 7 nM, respectively. The levels were significantly higher in human and mouse dystrophic myotubes (76 ± 5 nM, human; 110 ± 7 nM, mouse). Exposure of mouse myotubes to a ten-fold increase in $[\text{Ca}^{2+}]_o$ had no effect on normal $[\text{Ca}^{2+}]_i$ but significantly increased levels in *mdx*. In human myotubes, $[\text{Ca}^{2+}]_i$ increased with increased $[\text{Ca}^{2+}]_o$ in both normal and dystrophic myotubes, but the increase in the dystrophic myotubes was significantly greater. Therefore, these data suggest the ability to regulate $[\text{Ca}^{2+}]_i$ in dystrophin-deficient myotubes was impaired (Fong et al. 1990).

The activity of Ca^{2+} selective leak channels was tested in mouse and human myotubes using patch clamp techniques that record Ca^{2+} leak currents. Mean open times of the leak channels were similar in both normal and dystrophic myotubes. However, the mean channel closed times were reduced 2.5 to 3 times in both human and mouse dystrophin-deficient myotubes aged 6-15 days. The ability of myofibers to regulate $[\text{Ca}^{2+}]_i$ was related to the closed time of the channels. Normal mice, with high channel activity but long closed times, showed ability to tightly control $[\text{Ca}^{2+}]_i$ after exposure to a ten-fold higher extracellular concentration. Human and mouse dystrophic deficient fibers also showed high activity but the reduced closed channel times correlated to significantly higher $[\text{Ca}^{2+}]_i$ after exposure to a more concentrated extracellular Ca^{2+} solution (Fong et al., 1990).

Based on these findings, Fong et al. (1990) concluded there was increased activity of Ca^{2+} leak channels in human and mouse dystrophin-deficient myotubes that contributed to higher levels of $[\text{Ca}^{2+}]_i$. It was also postulated that downstream mechanisms involved in muscle protein degradation were influenced by the increased $[\text{Ca}^{2+}]_i$. Thus, the excess influx of Ca^{2+} through activated leak channels in dystrophic muscle could activate the myofiber degradation associated with dystrophic pathophysiology (Fong et al., 1990).

Turner et al. (1993) also investigated pathways that raise $[\text{Ca}^{2+}]_i$. Dystrophic muscle fibers from 3-6 week old *mdx* mice were studied in addition to DMD myotubes. *Mdx* fibers loaded with the Ca^{2+} indicator fura-2 were less able to regulate $[\text{Ca}^{2+}]_i$. At normal $[\text{Ca}^{2+}]_o$ of 1.8 mM, *mdx* and normal fibers showed no differences in regional $[\text{Ca}^{2+}]_i$; however, *mdx* fibers had

higher $[Ca^{2+}]_i$ (297 ± 34 nM) compared to normal fibers (209 ± 29 nM). When $[Ca^{2+}]_o$ was increased to 36 mM, $[Ca^{2+}]_i$ rapidly increased in *mdx* fibers and were localized to the sarcolemma region. Ca^{2+} levels near the sarcolemma were 385 ± 42 nM and 240 ± 27 nM in the center of the fiber. When the fibers were depolarized with 15 mM K^+ , the $[Ca^{2+}]_i$ became evenly distributed throughout the fiber. Ca^{2+} transient decay times measured in resting *mdx* and normal fibers were not different. Therefore, Ca^{2+} sequestering mechanisms in dystrophic myotubes were not altered but were slowed by increased $[Ca^{2+}]_i$. Resting free sodium levels and influx were measured with sodium-binding benzofuran isophthalate in the absence of Na^+/K^+ -ATPase activity. There were no differences in resting free sodium or sodium influx, indicating the Ca^{2+} defect observed in *mdx* muscle was Ca^{2+} -dependent (Turner et al., 1993).

Fong et al. (1990) previously found the probability of Ca^{2+} leak channels to remain open were significantly higher in *mdx* myotubes. Since Ca^{2+} leak channels in *mdx* myotubes are more abundant, specific, and more active, it was suggested that Ca^{2+} leak channels contribute to the higher $[Ca^{2+}]_i$ in dystrophin-deficient muscle (Turner et al., 1993).

Given the role of Ca^{2+} leak channels in Ca^{2+} influx into the myoplasm of dystrophin-deficient muscle, Alderton and Steinhardt (2000) investigated the role of Ca^{2+} leak channels in regulating proteolysis in dystrophin-deficient myotubes. Using a fluorogenic substrate, the hydrolysis rate of calpain, a Ca^{2+} -sensitive protease, was observed in normal and *mdx* cultured myotubes. The rates of hydrolysis were high in both normal and *mdx* cells during the periods of myocyte alignment and fusion. However, after contractile activity developed, hydrolysis rates decreased in normal myotubes but remained abnormally high in *mdx* myotubes. Hydrolysis rates became significantly lower in *mdx* myotubes when $[Ca^{2+}]_o$ was 0.09 mM compared to 1.8 mM ($p < 0.001$). At the lower $[Ca^{2+}]_o$, hydrolysis rates were not significantly different from normal myotubes in 1.8 mM Ca^{2+} . Thus, the decreased hydrolysis rate of the calpain substrate was likely due to decreased Ca^{2+} influx (Alderton and Steinhardt, 2000).

To determine whether Ca^{2+} influx through Ca^{2+} leak channels was responsible for increased hydrolysis rates of calpain substrate, the Ca^{2+} specific leak channel antagonist, AN1043, was added to the high concentration Ca^{2+} buffer before addition of the fluorogenic calpain substrate. AN1043 significantly reduced the rate of hydrolysis ($p < 0.0001$) to a level comparable to normal myotubes. Subsequently, the lysosomal and proteasome proteolytic pathways were blocked using ammonium chloride and clasto-lactacystin-activated protease,

respectively. There was no effect on the calpain substrate hydrolysis rate in high $[Ca^{2+}]_o$ concentrations in *mdx* myotubes but a decreased rates at low $[Ca^{2+}]_i$. Thus, these data suggested that Ca^{2+} activated proteolysis was due to abnormally active Ca^{2+} leak channels and calpain activation (Alderton and Steinhardt, 2000).

McCarter and Steinhardt (2000) tested the hypothesis that local membrane disruptions could increase the open probability of Ca^{2+} leak channels and initiate Ca^{2+} dependent proteolysis. Myotube cultures were prepared from 4-10 week old *mdx* mice. Single channel opening and closing events were recorded in 7-14 day old elongated cultured myotubes. Channel activity was significantly greater at sites close to transient sarcolemma ruptures (5 μ m), created by sudden withdrawal of a patch-clamp electrode, compared to sites further away (50 μ m). The high levels of activity remained constant during the duration of recordings, 1-12 minutes, and enhanced activity was observed 10 to 25 minutes after membranes were ruptured. The magnitude of membrane damage had no effect on channel activity. Increased activity was due to the increased open probability in a single channel instead of an increased density in channels on the membrane. Activation of the channel was determined to be a negative feedback response to shorter closing times near ruptures (McCarter and Steinhardt, 2000).

Since Ca^{2+} dependent proteolysis was higher in dystrophic muscle, McCarter and Steinhardt (2000) tested whether proteolysis was responsible for higher leak channel activity. Identical measurements of leak channel activity were made in myotubes at sites close and far away from transient ruptures in the presence of the cysteine protease inhibitor leupeptin. Inhibition of proteolysis prevented increased channel activity near ruptures. Thus, increased Ca^{2+} leak channel activity in dystrophin-deficient muscle was caused by increased proteolysis near membrane rupture sites. The authors concluded that because dystrophin-deficient muscle was more susceptible to transient membrane ruptures from contractile stresses in older *mdx* mice, initial leakage of Ca^{2+} activated Ca^{2+} dependent proteolysis, which then modified Ca^{2+} leak channels to increase Ca^{2+} leak. This results in a positive feedback loop to drive Ca^{2+} proteolysis. This chronic cycle eventually overwhelms the dystrophin-deficient muscle fibers and leads to myofiber necrosis (McCarter and Steinhardt, 2000).

In summary, Ca^{2+} regulates many biological processes. In skeletal muscle, a primary function for Ca^{2+} is to initiate muscle contraction and relaxation during ECC. Ca^{2+} also regulates proteolysis through activation of Ca^{2+} -dependent m- and u-calpain proteases. Protein

degradation is necessary for cell to growth and repair. In dystrophin-deficient muscle, cellular control of resting Ca^{2+} levels is compromised (Turner et al., 1988; Fong et al., 1990; Turner et al., 1993; Alderton and Steinhardt, 2000; McCarter and Steinhardt, 2000). It is apparent dystrophin-deficiency impairs the activity of Ca^{2+} sensitive leak channels localized to the sarcolemma (Fong et al., 1990, McCarter and Steinhardt, 2000). Leak channels become more active; potentially in response to transient disruptions along a weakened sarcolemma (McCarter and Steinhardt, 2000) with a higher open probability that permits the influx of external Ca^{2+} into the myoplasm. The elevated resting levels of Ca^{2+} activate the Ca^{2+} sensitive protease, calpain, which degrades muscle proteins and phospholipids (Alderton and Steinhardt, 2000). Proteolysis occurring near the sarcolemma further activates Ca^{2+} leak channels. Thus, a relentless cycle of protein degradation occurs that is believed to cause muscle necrosis (McCarter and Steinhardt, 2000). Deficiencies in Ca^{2+} handling may also involve the RyR and Ca^{2+} ATPase pump of the SR; however, these possibilities are not clearly defined at present. Thus, the mechanisms that compromise Ca^{2+} homeostasis are still not clear. Whether Ca^{2+} influx represents part of the onset mechanism in the pathophysiology in DMD remains to be determined. Studies around the age of overt disease onset may make this hypothesis conclusive.

The Signaling Hypothesis

Signaling pathways in dystrophin-deficient muscle are altered. The rise in intracellular Ca^{2+} and activation of calpains serve as an example of the disruption in signaling. It is hypothesized that dystrophin and members of the DGC function to support signaling processes within the myoplasm and across the membrane into the extracellular matrix (Tidball and Law, 1991). Therefore, in DMD, loss of dystrophin and the related DGC proteins may disrupt signaling functions, particularly mechanisms that respond to injury. However, it is not clear how the DGC proteins interact to coordinate cellular processes and whether a single or a coordinated series of events leads to the development of muscle necrosis. Recent studies on dystrophin-deficient muscle have closely examined the roles of molecules in signaling cascades and their impact on pathophysiology. These include but are not limited to the roles of 1) integrins in the extracellular matrix, particularly the $\alpha7\beta1$ integrin; 2) nitric oxide; and 3) two proteolytic pathways, the calpains, and the proteins associated with the ATP-dependent ubiquitin proteasome complex. Given the complexity of signaling pathways, it is difficult to examine

cellular signaling; thus, at present there is limited research to support the signaling hypothesis of dystrophy.

Integrins. Integrins are a family of transmembrane cell surface receptors that function by interacting with extracellular matrix proteins and receptors to play important roles in cell migration, cell shape formation, and cell-cell interactions. Integrins are heterodimers formed from α and β chains. Upon ligand binding, signals are transmitted from outside the cell to the cytosol, or from within the cell to the extracellular matrix and contribute to the modulation and activation of extracellular matrix ligand binding (Burkin and Kaufman, 1999).

In skeletal muscle, integrin $\alpha7\beta1$ is the predominant integrin that interacts with the DGC by binding laminin. It serves several roles during development. It is expressed on cells going into early limb budding, appears after differentiation during primary fiber formation, directs cells to laminin rich sites of secondary fibers surrounding primary fibers, and indirectly participates in myoblast fusion. In adult fibers, $\alpha7\beta1$ integrin is enriched at myotendinous and neuromuscular junctions and localizes peripherally around the myofiber. Overall, it is believed to promote terminal and peripheral muscle fiber cohesion that is important to neuromuscular connectivity, muscle integrity, and force generation (Burkin and Kaufman, 1999).

In patients with DMD as well as *mdx:utrn*^{-/-} mice, $\alpha7\beta1$ integrin is increased due to increased RNA expression of the $\alpha7$ chain. The protein is found in *mdx:utrn*^{-/-} hindlimb and diaphragm muscles normally confined to the junctional sites but expands out to extrajunctional regions. Enhancing the expression of the $\alpha7\beta1$ integrin reduces the symptoms associated with dystrophin-deficiency and restores muscle viability in the *mdx:utrn*^{-/-} $\alpha7\beta1$ transgenic mice (Burkin et al., 2001). It is not known whether the same effects occur in humans.

Nitric oxide synthase. Neuronal nitric oxide synthase (nNOS) is an important enzyme. It is a heme-containing oxidoreductase that catalyzes the conversion of L-arginine to L-citrulline and generates the free radical nitric oxide (NO[•]; Bredt and Snyder, 1994). NO[•] is involved in immune modulation and neural transmission. In skeletal muscle, it is involved in contractile function, SR Ca²⁺ release, and glucose metabolism. Most importantly, NO[•] functions to promote vasodilatation by stimulating guanylate cyclase and increasing cGMP production in vascular smooth muscle cells. In skeletal muscle, nNOS is associated with the DGC but is reduced in

dystrophin-deficient muscle (Chang et al., 1996). It is believed the reduction in nNOS decreases NO[·] production (Rando, 2002). During normal muscle activity, NO[·] likely contributes to functional hyperemia to ensure adequate blood flow to the working muscle (Lau et al., 1998; Grange et al., 2001, Crosbie, 2001)). In *mdx* mice as well as in young human DMD patients, the vasodilatory role of NO[·] may be compromised (Thomas et al., 1998; Sander et al., 2000). Furthermore, over-expression of an nNOS transgene in *mdx* mice diminished the dystrophic pathophysiology in soleus muscles, likely by providing NO[·] as an anti-inflammatory molecule (Wehling et al., 2001). Thus, the positive effects of NO[·] may be compromised in dystrophin-deficient muscle (Rando, 2002).

Proteolysis. Increased proteolysis is likely due to calpain activation in dystrophin-deficient muscles (Alderton and Steinhardt, 2000; McCarter and Steinhardt, 2000). Furthermore, evidence suggests proteolytic activity through proteasome activity is increased in dystrophin-deficient muscle. This was shown in DMD and BMD patients where increased proteasome content was observed localized in necrotic and regenerating muscle fibers (Kumamoto et al., 2000). In gene expression studies on human and murine dystrophin-deficient muscle, a number of proteasome specific mRNA transcripts have also been observed differentially over-expressed (Chen et al., 2002; Porter et al., 2002). It is still not clear when and by what mechanism proteasome activity is increased.

In summary, data to support the role of one or more signal pathways in DMD onset is unclear. Nevertheless, it is important to determine the functions of dystrophin and the DGC to understand how these proteins interact with each other and how their absence changes communication within and surrounding the muscle fiber. Gene expression analysis may be one viable approach to determine these pathways.

Immune Response

An immune response occurs when the body recognizes and responds to antigens. An antigen is any substance that causes the immune system to produce specific antibodies against that substance.. The antigen may be a foreign substance like bacteria, viruses, or molds, or it may be formed within the organism by cells or bacterial toxins. Inflammation is that part of the immune response that occurs when tissues are injured by bacteria, trauma, toxins, heat, or other

perturbations that stimulate tissues to release specific chemicals, such as histamine, that cause blood vessels to leak fluid into the tissues. The characteristic tissue swelling helps isolate the foreign substance from further contact with other body tissues. In addition, the chemicals released attract white blood cells that degrade the invading microorganism and/or the damaged cells (MedlinePlus, 2005).

Immune responses are classified as either a humoral antibody response or a cell-mediated immune response. A humoral antibody response involves the production of specific antibodies that circulate the bloodstream and bind to their specific antigen target. The antibody-antigen binding allows phagocytic cells, such as neutrophils, monocytes and macrophages, to ingest the antigen, and often activates blood proteins, called complement, that help destroy the antigen. A cell-mediated immune response involves the production of specialized cells, such as T-cells and B-cells, which react to the antigen presented on the surface of a host cell. These specialized cells then kill the host cell or induce other cells, such as macrophages or cytotoxic T-lymphocytes, to destroy the antigen (Alberts et al., 1983).

Six to nine year old DMD and 4-8 week old *mdx* muscles are infiltrated by a variety of specialized immune cells including cytotoxic T-lymphocytes, B-cells, macrophages, and dendritic cells (Spencer et al., 1997, Chen et al., 2000; Porter et al., 2002). This evidence suggests that a cell-mediated immune response is clearly present in young and older dystrophin-deficient muscles. However, it remains unclear whether an immune response is involved during the disease onset of DMD and whether it initiates the disease pathophysiology. Examining global gene expression in human and *mdx* muscle has provided some clues to identify mechanisms that potentially promote an immune response. Spencer et al. (1997) examined cytotoxic T-lymphocytes (CTLs or CD8⁺ cells) to determine if they were present in dystrophin-deficient muscle and if they initiated myonuclear apoptosis. Apoptosis, or programmed cell death, is the earliest detectable stage of muscle fiber necrosis, or degeneration, in *mdx* muscle (Tidball et al., 1995). At ages 4 and 8 weeks, *mdx* fibers contained a significantly greater number of CTLs compared to age matched controls. By age 14 weeks, the number of CTLs decreased. Since CTLs depend on interleukin-2 (IL-2) activation from helper T cells (CD4⁺ cells), helper T cell content was measured in *mdx* muscle. Helper T cells were increased compared to control muscles at ages 2 to 8 weeks. Collectively, these observations showed

CTLs and helper T-cells infiltrate dystrophin-deficient muscle and suggested CTLs become activated during the early stages of disease onset in dystrophin-deficiency (Spencer et al., 1997).

To determine if CTLs contributed to apoptosis, *mdx* mice were injected with anti-CD8 at age 10-12 days, prior to the overt signs of DMD pathophysiology. Muscles injected with anti-CD8 showed a decreased presence of apoptotic nuclei and significantly reduced tissue necrosis during the 2-8 week age range investigated. In addition, a 60% reduction in macrophage fiber infiltration was observed in CD8 depleted *mdx* mice although the overall concentration of macrophages was unaffected. Thus, these data suggested CTLs mediate apoptosis and macrophage infiltration in dystrophin-deficient fibers (Spencer et al. 1997)

Perforin is a pore forming protein contained in lysosomal-like structures within CTLs. To determine the mechanism that mediates apoptosis by CTLs, perforin-expression was examined in *mdx* and *mdx*-perforin knockout mice. In *mdx* mice, perforin expressing cells invaded muscle at the time apoptosis began increasing at age 4 weeks. However, in *mdx*-perforin knockout mice, myonuclear apoptosis was eliminated and tissue inflammation was significantly decreased by 44% along with muscle fiber necrosis by 79%. Thus, it was concluded perforin mediated the events leading to myofiber apoptosis and necrosis by CTLs in dystrophin-deficient muscle.

Chen et al. (2000) utilized gene expression profiling with Affymetrix® GeneChips® to determine downstream pathophysiological events in patients with DMD (aged 6-9 years) and α -sarcoglycan deficiency (α SGD, aged 8-11 years) compared to normal human muscle (aged 6-9 years). Of the 7,095 genes examined, 275 were found differentially regulated by a pairwise comparison of DMD and control muscle responses. While cell surface and extracellular matrix genes were the largest functional groups of genes up-regulated (42%), 20% of the transcripts corresponded to genes involved in immune responses (Chen et al., 2000).

Factor XIIIa is a fibrin cross-linker in coagulation. Immunostaining of DMD muscle showed an 11-26 fold increase in epimysial and endomysial connective tissue of DMD muscle. However, changes were undetectable at the gene expression level. HLA-DR is a histocompatibility antigen present on antigen presenting cells. At the gene expression level, a 3-fold increase was observed in DMD muscle and strong immunolocalization was observed near cells immunostained for factor XIIIa. Collectively, the positive stains observed for these two proteins represented dendritic cells that appeared to be infiltrating dystrophic muscle. Thus,

these results suggested dendritic cells and mast cells coordinately acted to mediate acute and chronic microenvironmental changes in the dystrophic fiber during the middle stages of the disease (Chen et al., 2000).

Thrombospondin 4 is an extracellular matrix Ca^{2+} binding protein localized primarily in the tendon and early osteogenic tissue. Its function is not well understood. In DMD muscle, thrombospondin 4 was found up-regulated 15-fold and immunostaining showed it localized to areas of macrophage infiltration. This finding suggested thrombospondin was expressed in interstitial cells in response to macrophage infiltration or cellular damage in older DMD muscle (Chen et al., 2000).

Porter et al. (2002) examined gene expression in the *mdx* mouse, aged 8 weeks, to establish a molecular profile of dystrophin myopathy. Using Affymetrix® GeneChips® arrays of approximately 10,000 genes, 249 genes were found differentially expressed in *mdx* compared to control muscles based on data obtained from stringent algorithmic comparisons in Affymetrix analysis software. Two hundred forty two genes were found differentially expressed from genes identified as significantly changed in Affymetrix algorithmic comparisons to genes identified in the microarray statistical software SAM (Significant Analysis of Microarrays). The expression changes found were consistent with documented markers of muscle degeneration and regeneration. The changes indicated a variety of events were involved in dystrophin-deficiency but found an immune response (29.8% of differentially expressed genes) to be a predominant disease process.

Gene expression patterns exhibited a coordinated immune and repair response in *mdx* muscle; mRNAs for proteins relevant to mast cells, macrophages, T and B cells were significantly elevated. The robust profiling indicated a chronic and persistent inflammatory reaction in dystrophin-deficient muscle (Porter et al., 2002).

Evidence for cytokine-dependent activity was indicated by increased expression for TNF α receptor and Stat6, an IL-4 mediating factor. TNF α , IL-1, and IL-4 are key inflammatory cytokines; however, they were not found differentially expressed (Porter et al., 2002).

Vascular cell adhesion molecule 1 (Vcam1) and P2x receptor (P2rx4) were vascular endothelium factors for an immune response found up-regulated. P2rx4 participates in signaling responses mediated by ATP in mast cells and Vcam1 acts as a chemoattractant for leukocytes, especially monocytes and lymphocytes (Porter et al., 2002).

Chemokines and their receptors were also up-regulated. This included the C-X-C class chemokine Scyb14, the C-X-C class chemokine receptor Cmkar4, the C-C class chemokines Scya2, scya6, scya7, and Scya9, and the C-C class receptor Cmkbr2. The up-regulated C-C class chemokines are chemotaxic for monocytes, eosinophils, basophils, and lymphocytes. C-X-C class chemokines are chemotaxic for neutrophils and lymphocytes. Therefore, the up-regulation of these genetic markers suggested *mdx* muscle was infiltrated by monocytes, leukocytes, eosinophils, basophils, lymphocytes, and neutrophils (Porter et al., 2002).

In summary, evidence suggests that dystrophin-deficient muscle is affected by an immune response. Spencer et al. (1997) showed cytotoxic T-lymphocytes were present in *mdx* muscle during the early stages of pathophysiological onset and were contributing to myofiber necrosis via apoptosis, likely mediated by perforin. Chen et al. (2000) examined gene expression in older human DMD and α SGD muscle and showed that a variety of markers corresponding to an immune response were up-regulated. Immunostaining confirmed that dendritic cells, mast cells, and macrophages were present in DMD fibers during the middle stages of the disease and gene expression changed for markers that were involved in collecting these immune cells around the muscle. Finally, Porter et al. (2002) showed a variety of inflammatory markers were up-regulated in older *mdx* mice, aged 8 weeks. This included a variety of cytokines, chemokines, and myeloid and lymphoid markers that suggested dystrophin-deficient muscle was affected by macrophages, neutrophils, lymphocytes, mast cells, and T- and B-cells. Because antigen presentation is necessary for the activation of immune cells, Spencer et al. (1997) has suggested dystrophin-deficient muscle must present an antigen that attracts immune cells. Although the source of the antigen is unknown, several potential sources exist. Muscle damage caused by a weakened membrane could cause a cytosolic leak of proteins into the extracellular matrix. The proteins or material released, which are not normally seen by the immune system, could activate immune cells, i.e., T-lymphocytes. Alternatively, dystrophin-deficient muscle may express proteins on the membrane that are recognized as antigens because they are not normally expressed in normal tissue (Spencer et al., 1997). It is important scientists understand the impact of the immune system on the pathophysiology of DMD and learn how the muscle is targeted for an immune response. Targeting the immune system with therapeutic agents may significantly attenuate the progression of DMD.

Summary

Dystrophin is an important protein in the cytoskeletal structure of skeletal muscle fibers. In DMD, mutations in the dystrophin gene eliminates the expression of dystrophin that causes severe progressive skeletal muscle wasting that ultimately kills young men by their early 20s. The function of dystrophin is not presently understood, nor are the events that initiate the severe pathophysiology of DMD.

Dystrophin is believed to function as a mechanical stabilizer that provides integrity to the sarcolemma. Although evidence exists to support this hypothesis in older *mdx* mice and myotubes (Petrof et al., 1993, Lynch et al., 2000), results from several studies in *mdx* mice suggest the membrane is not weaker (Sacco et al., 1992; McArdle et al., 1991; Rezvani et al., 1995). The membrane hypothesis has been difficult to confirm because the methods used to determine sarcolemmal properties varied between studies. Furthermore, the studies were often conducted on muscles of dystrophic mice at ages corresponding to the middle stages of the disease which are characterized by cycles of degeneration and regeneration, or at older ages (e.g., ages >10-11 weeks), when these cycles have slowed or ceased altogether. Grange et al. (2002) examined the contractile properties of muscle in *mdx* and *mdx:utrn*^{-/-} mice at age 9-12 days, prior to the overt signs of DMD. Although tetanic tension was significantly reduced and fiber damage was greater in *mdx* and *mdx:utrn*^{-/-} compared to control mice, no differences were found in the extent of fiber damage in dystrophic fibers after compared with before a stretch injury protocol. Thus, a weaker membrane does not appear to be an onset mechanism of DMD.

Calcium homeostasis is altered in dystrophin-deficient muscles (Turner et al., 1988). It is clearly evident that Ca²⁺ leak channel activity in older *mdx* mice is increased and contributes to the observed elevation of intracellular Ca²⁺ in the myofiber that increases calpain activity (Turner et al., 1988; Fong et al., 1990; Turner et al., 1993; Alderton and Steinhardt, 2000; McCarter and Steinhardt, 2000). However, it is not known why leak channel activity is increased or when proteolysis by calpains begins. Furthermore, it is still not clear if Ca²⁺ handling by the SR is compromised during early maturation that could lead to DMD onset. Thus, it is important to understand the mechanisms that compromise Ca²⁺ homeostasis in dystrophic-deficient muscle and to understand how Ca²⁺ contributes to the pathophysiology in DMD.

Dystrophin and the proteins of the DGC may coordinate signaling between the myoplasm and extracellular matrix. In the dystrophin-deficient muscle, signaling may be disrupted and

cause a variety of pathophysiological events that are, at present, not well understood. $\alpha7\beta1$ integrin and nNOS may be involved in onset of DMD because they associate with the DGC. In skeletal muscle, $\alpha7\beta1$ integrin is believed to promote terminal and peripheral muscle fiber cohesion that is important to neuromuscular connectivity, muscle integrity, and force generation (Burkin and Kaufman, 1999). Over-expression of $\alpha7\beta1$ in *mdx:utrn*^{-/-} muscle has been shown to reduce the symptoms of pathophysiology and restore the viability of the muscle (Burkin et al., 2001). Nitric oxide, a product of nNOS activity, is produced in skeletal muscle and contributes to the regulation of functional hyperemia (Chang et al., 1996, Lau et al., 1998). In *mdx* mice nNOS content is reduced (Chang et al., 1996), and this may compromise the hyperemic response in dystrophic muscles (Thomas et al., 1998; Sanders et al., 2000). Despite these possibilities, at present, it is still not clear how dystrophin and the DGC function as a signaling scaffold.

Recent evidence suggests an immune response dominates older dystrophin-deficient human and mouse muscle (Spencer et al., 1997; Chen et al., 2000; Porter et al., 2002). Based on data from immunohistochemical studies and DNA microarrays, dystrophin-deficient muscle is infiltrated by a variety of immune cells that contribute to muscle necrosis. However, neither the time course nor the mechanisms that initiate the immune response are well understood. Identifying molecules that target immune cells may be the most promising method to develop therapeutic agents that counteract an immune response to slow or prevent the progression of DMD.

Despite the volume of research published on DMD, the onset mechanisms are not clearly defined. This limitation in our understanding may be due to the age at which dystrophic mice are studied and/or the absence of a representative disease model. The *mdx* mouse has been the primary model studied. Although this genotype exhibits the overt signs of the disease between ages 3-10 weeks, the muscles recover from the rounds of degeneration and regeneration, and the mouse then lives a normal lifespan. The *mdx:utrn*^{-/-} mouse is another model of DMD, but has been less studied. Unlike the *mdx* mouse, but similar to the human DMD, the *mdx:utrn*^{-/-} suffers progressive muscle wasting that is initiated at approximately age 2 weeks and results in an early death at age 18-20 weeks. Thus, two critical requirements for identifying onset mechanisms of DMD are to study responses during early maturation (e.g., 7-21-days), and to use a more representative disease model.

The advent of the DNA microarray has enabled scientists to examine the global post transcriptional expression of mRNA to help identify molecules and physiological events in DMD (Chen et al., 2000; Tkatchenko et al., 2000; Tkatchenko et al., 2001; Porter et al., 2002). It has also identified an immune response as a predominant profile of the disease (Chen et al., 2000; Porter et al., 2002). However, the expression profile of dystrophin-deficient muscle has not been well studied in dystrophic mice prior to or just at the overt signs of dystrophic pathophysiology. Thus, the purpose of this study was to utilize the Affymetrix® GeneChip® to identify the expression profile of *mdx:utrn*^{-/-} muscle prior to the overt stages of disease onset to determine if (1) SR Ca²⁺ handling was altered, and (2) if an inflammatory signature was predominant. Understanding the physiological state of the muscle during early maturation may help identify the mechanisms of dystrophic onset.

Chapter 3: Methods

Mouse Genotypes

This investigation used male control C57BL/6 and *mdx:utrn*^{-/-} mice at ages 9-10 days and 20-21 days (n=5/genotype/age) to examine gene expression as shown in Figure 3.1. All mice were obtained from our colony in the Lab Animal Resources facility at Virginia Tech and all procedures were approved by the Virginia Tech Animal Care Committee. *Mdx:utrn*^{-/-} mice were obtained by crossing male and female *mdx:utrophin* heterozygote (*mdx:utrn*^{+/-}) breeders because the *mdx:utrn*^{-/-} mice are not fertile. The genotype of each mouse was determined by PCR analysis of DNA isolated from tail snips (Grange et al., 2002).

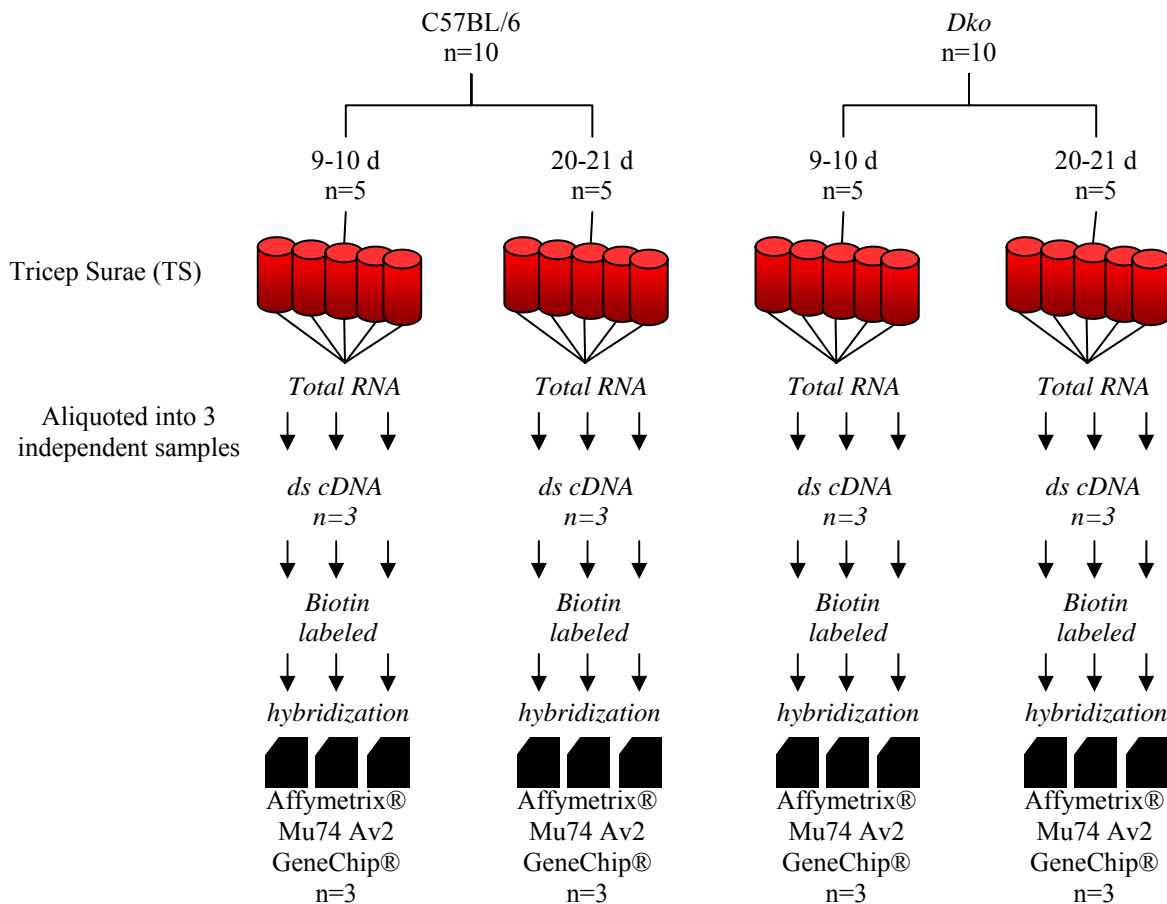


Figure 3.1. Experimental Design. Triceps surae (TS) muscles were excised from anesthetized control and *mdx:utrn*^{-/-} mice at ages 9-10 and 20-21 days (n=5 per age). The TS were pooled together to extract total RNA. Thereafter, the pooled RNA samples were divided into 3 independent samples for hybridization preparation. Briefly, each RNA sample was reverse transcribed into double-stranded copy DNA (ds cDNA) using T7 RNA polymerase. The ds-cDNA was then fragmented into 200 bp transcripts and labeled with biotin. The biotinylated samples were then hybridized with the oligo probes on the Affymetrix® Mu74Av2 GeneChip® and stained with streptavidin-phycoerythrin.

Genotyping

DNA Isolation from Tail Snips. The methods of Laird et al. (1991) were used to isolate DNA from mouse tail snips of approximately 0.5 cm length. Tail snips were digested at 55°C overnight in 0.5 ml lysis buffer (5 mM EDTA, 0.2% SDS, 200 nM NaCl, 100 nM Tris (pH 8.5), and 0.2 mg/ml Proteinase K). Samples were vortexed for approximately 1 minute and spun at 13,000 rpm for 10 minutes. The supernatant from each sample was transferred to a clean microcentrifuge tube and equal volume of 100% ice-cold isopropanol was added to precipitate the DNA. The precipitated DNA was transferred to a clean microcentrifuge tube, re-suspended in 10 mM Tris-EDTA (pH 7.4), and stored at -20°C until PCR was conducted.

Dystrophin Screen. Specific forward and reverse primers, obtained from Invitrogen, were used to screen each DNA sample for the dystrophin mutation, *mdx*, (Amalfitano and Chamberlain, 1996) and the utrophin knockout (Grady et al., 1997). The dystrophin screening for the wild type and *mdx* genotypes was performed in separate tubes. The reverse primer for the wild type (260E) was 5'-GTCACCTCAGATAGTTGAAGCCATTTAG-3'. The reverse primer for the *mdx* (302F) was 5'-GTCACCTCAGATAGTTGAAGCCATTTAA-3'. Each reaction used a common forward primer (9427) 5'-AACTCATCAAATATGCGTGTTAGTG-3', (Amalfitano and Chamberlain, 1996). The PCR reaction was performed using 0.5 µl of DNA in 24.5 µl of 1x PCR Buffer containing 1.5 mM MgCl₂, 0.4 mM dNTPs, 0.025 U/ µl platinum Taq, 200 nM primers (Invitrogen). The final cocktail volume was 25 µl. A PTC-150 Minicycler™ with Hot Bonnet™ (MJ Research, Inc.) was used to run the PCR reaction. The following conditions were used for the dystrophin screen: (1) 5 minutes at 94°C for the initial denaturation of the DNA, (2) 40 cycles with three 25 second steps per cycle (39°C, annealing; 72°C, extension; and, 94°C, denaturation), and (3) 5 minutes at 72°C for the final extension.

To examine the PCR products, samples were run at 100 V for 60 minutes on a 3% agarose gel (Invitrogen) stained with 0.001 mg/ml ethidium bromide in 0.5X Tris-Borate-EDTA running buffer (Fischer Scientific). The band products in the gel were visualized under the ultraviolet light of an Alpha Innotech Imager. Determination of the wild type and *mdx* genotype were based on the presence or absence of a 105 bp (bp) band from the reverse primer of the respective PCR products. Presence of bands from both screens indicated a dystrophin heterozygote, as shown in Figure 3.2 (Amalfitano and Chamberlain, 1996).

Utrophin Screen. The utrophin genotype screen was performed in a single tube with forward primers for the utrophin wild type and utrophin knockout. The utrophin wild type forward primer (554) was 5'-CTGAGCAAACAGCTTGGAAGCCTCC-3' and the utrophin knockout primer (553) was 5'-TTGCAGTGTCTCCCAATAAGGTATGAAC-3'. The common reverse primer was (22803), 5'-TGCCAAGTTCTAATTCCATCCATCAGAAGCTG-3' (Grady et al., 1997). The utrophin screen used similar conditions as the dystrophin screen except the annealing temperature was 48°C.

PCR products were examined under the same conditions as the dystrophin screen. A band of 640 bases indicated a utrophin wild type and a band of 450 bases indicated a utrophin knockout. As with the dystrophin screen, presence of both bands in the utrophin screen indicated a utrophin heterozygote (Grady et al., 1997). Figure 3.2 provides examples of both dystrophin and utrophin screens.

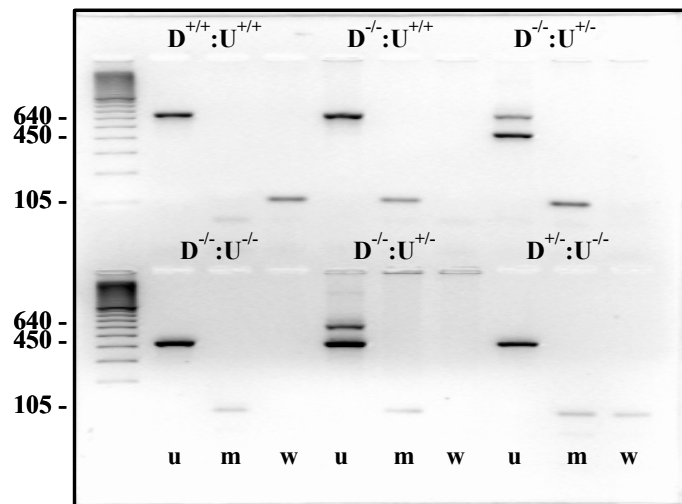


Figure 3.2. Dystrophin and Utrophin Screen by PCR. Control and *mdx:utrn*^{-/-} mice were screened for specific PCR products on DNA extracts from tail snips. Specific reverse primers were designed to identify the *mdx* mutations. The *mdx* mutation ($D^{-/-}$) was determined by a 105 bp PCR product (band; m) and the absence of a 105 bp band indicating wild type dystrophin ($D^{+/+}$) (w). Wild type expression ($D^{+/+}$) was determined by the presence of the wild type band only. Presence of both the *mdx* and wild type bands indicated a wild type heterozygote ($D^{+/-}$). The utrophin mutation ($U^{-/-}$) was determined with specific forward primers. The mutation was determined by presence of a 450 bp band and absence of a 640 bp wild type band (u). Wild type utrophin ($U^{+/+}$) was determined by the presence of the wild type band only. The *mdx:utrn*^{-/-} mice ($D^{-/-}:U^{-/-}$) were obtained by breeding *mdx* / utrophin heterozygotes ($D^{-/-}:U^{+/-}$) and identified by the expression of the *mdx* and utrophin mutant PCR products (from Grange et al., 2002).

Muscle Preparation

Mice were anesthetized using an intraperitoneal injection of 2 mg xylazine and 20 mg ketamine per 100 g body mass. The triceps surae (TS), which collectively refers to the left and right heads of the gastrocnemius and plantaris muscles, was dissected from each hindlimb of the mouse. The muscles were immediately washed in ice-cold 0.9% saline, blotted dry, frozen in liquid nitrogen, and stored at -80°C until isolation for total RNA. Proper precautions were taken to sterilize the instruments and area for dissection and RNaseZap[®] (Ambion) was used to inhibit RNase activity to avoid RNA degradation.

Total RNA Isolation

Total RNA was isolated from a pooled sample of frozen TS muscles obtained from five animals at their respective age and genotype. One TS muscle was randomly selected from each of the five chosen animals. The frozen muscles were placed in TRIZOL[®] reagent (Invitrogen) at a volume (μ l) approximately five times the muscle mass (mg) of the combined samples. Samples were incubated at room temperature (RT) for 5 minutes and homogenized for 45 seconds using a Pro250 homogenizer (PRO Scientific) pretreated with RNaseZap[®]. Next, the homogenized sample was transferred to a pre-spun 2 ml Heavy Phase Lock Gel (Brinkman, Inc) and a half TRIZOL[®] volume (μ l) of chloroform was added. The combination was mixed by inversion then spun at RT for 15 minutes at 10,000 rpm. Following the spin, the aqueous phase of the sample was transferred to a clean microcentrifuge tube. An equal volume of ice cold 100%-isopropanol was added to the sample then incubated at RT for 20 minutes. The precipitated RNA was collected by spinning the sample at RT for 15 minutes at 10,000 RPM. The pelleted RNA was isolated by discarding the supernatant after the spin then washed with 1 ml of 70% ethanol. Finally, the RNA pellet was air dried and re-suspended in 75 μ l of DEPC-treated water.

To ensure the procedure provided the proper and sufficient yield of RNA, 10 μ l of the sample was diluted, in the ratio of 1:100, in DEPC-treated water (final volume 1000 μ l). Five hundred microliters of the dilution were taken to a UV-transparent cuvette and the absorbance of the sample was determined at wavelengths of 260 nm (A_{260}) and 280 nm (A_{280}) using a GeneQuant spectrophotometer (Pharmacia Biotech). The RNA concentration was determined (μ g/ μ l) as the product of: 1) the sample A_{260} , 2) the coefficient of one A_{260} unit of single-stranded

RNA (40 µg) and 3) the dilution factor (100). Purity of the sample was determined by the A_{260}/A_{280} ratio. Only those samples yielding a ratio of 1.8-2.0 were used in this study.

To visualize the selected products, 5 µg of total RNA from each sample were run on an agarose/MOPS gel containing 1.0% agarose, 9.5% MOPS, 4.5% formaldehyde, and 85% water. If this step gave a clear visual presence of the 18S and 26S subunits of RNA, then a successful yield of RNA was ensured.

Finally, those samples selected were further purified using an RNeasy® Midi column (Qiagen Inc.) and the instructions for RNA cleanup provided by the manufacturer. After purification, the samples were again quantified and visualized to further ensure that an adequate yield and a high quality product were available to use on the microarrays .

Expression Profiling by Affymetrix® Murine Genome U74Av2 GeneChip®

A total 30 µg of purified total RNA was used for each genotype at each age. The RNA was divided equally into three independent samples to provide three replicate GeneChips® for each genotype at its given age. All procedures to perform expression profiling were carried out according to the Affymetrix® protocol with the materials recommended or supplied by the company.

The first step of this protocol utilized the SuperScript Choice system (Invitrogen) with an oligo-dT primer containing a T7 RNA polymerase promoter (Genset Corp.) to convert 10 µg of total RNA from each sample to double-stranded cDNA (ds-cDNA). Next, the ds-cDNA was purified by phenol/chloroform extraction and converted to biotin-labeled cRNA in an *in vitro* transcription reaction using the Enzo BioArray™ RNA transcript labeling kit (Enzo Life Sciences). The biotin-labeled cRNA was then purified by an RNeasy® mini kit (Qiagen Inc.) and randomly divided into approximately 200 bp fragments using a 5X fragmentation buffer (200 mM Tris-acetate, pH 8.2, 150 mM MgOAc, 500 mM KOAc). The fragmented sample was then hybridized to an Affymetrix® Mu74Av2 GeneChip®. The Mu74Av2 is a mouse specific microarray with 12,489 gene transcripts representing approximately 1/3 of the mouse genome. The samples were hybridized for 16 hours at 45°C in an Affymetrix® Hybridization Oven 640. Following hybridization, the chip was washed to remove non-hybridized material and stained in the Affymetrix® Fluidics Station 400 using the protocol provided in the Affymetrix® Microarray Suite 5.0.

Two separate staining steps were involved. In the first step, the chip sample was incubated with phycoerythrin-streptavidin (Affymetrix®) to detect bound cRNA. In the second step, signal intensity of bound cRNA was amplified with biotin-labeled anti-streptavidin antibody (Affymetrix®) followed by phycoerythrin-streptavidin (Affymetrix®) staining.

After the staining, the chips were scanned using the Affymetrix® GeneChip® Scanner for subsequent analysis.

Analysis

Signal intensity values from raw GeneChip® images were determined using Affymetrix® Microarray Suite 5.0. Signal values on each chip were scaled to a total global target intensity value (TGT) of 500 to normalize the data for comparison. Transcripts were then scaled to the median signal value on the chip to account for the detection efficiency among spots and to allow comparison among transcripts between chips on a similar scale. Gene expression was then normalized by the median expression of all transcripts in all samples as baseline. The normalized gene expression values were statistically compared between groups by ANOVA using the microarray analysis program, GeneSpring (Silicon Genetics).

The significantly changed gene transcripts were determined by comparing each *mdx:utrn*^{-/-} chip (n=3/age) with each control chip (n=3/age) at its respective age (10 or 21 days) to examine changes in transcription levels of a gene at a particular age. Then, each *mdx:utrn*^{-/-} chip (n=3/age) and each control chip (n=3/age) were compared between ages to determine changes in gene transcription during maturation. Information on the selected genes was gathered online from NetAffx® (www.affymetrix.com) to identify physiological roles and functions of the proteins encoded by the selected genes.

Chapter 4. Results

Mice

Analyses were performed on total RNA isolated from a pool of triceps surae (TS) obtained from control (C57BL/6, n=5/age) and mdx-utrophin knockout mice (*mdx:utrn*^{-/-}, n=5/age) at ages 9-10 and 20-21 days. Total RNA was extracted from the muscle pool and divided into 3 independent samples for preparation and hybridization on the Affymetrix® Mu74Av2 GeneChip®. The average mass of the control and *mdx:utrn*^{-/-} mice at 9-10 days were significantly different at 4.8±0.4 and 4.3±0.3 grams, respectively (p<0.05). At 20-21 days, the average weight of the control was greater than the *mdx:utrn*^{-/-} mice (9.5±1.7 vs 8.5±0.4 grams, respectively). The morphological data for the mice are presented in Appendix A.

Quality Control Analysis

To control for experimental variability, quality control analyses were performed throughout the sample preparation process on each RNA sample and GeneChip®. RNA samples were assessed for degradation by running 5 µg of sample on an agarose/MOPS gel to determine the presence of 18S and 28S RNA subunits. Sample purity was checked by determining the absorbance ratio (A_{260}/A_{280}) of the optical density readings at 260 nm to optical density reading at 280 nm. For RNA, the absorbance ratio should be between 1.8 to 2.0 which reflects a sample that has few impurities, such as protein. Thus, samples with absorbance ratios of 1.8 to 2.0 were chosen for the Affymetrix® expression assay. As shown in Figure 4.1, the samples chosen showed no visible signs of RNA degradation because distinct 18S and 28S mRNA bands were present.

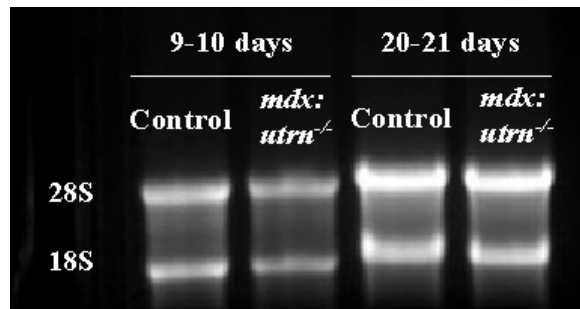


Figure 4.1. Assessment of total RNA quality. Total RNA obtained from pooled TS from *mdx:utrn*^{-/-} and control mice at ages 9-10 and 20-21 days was run on an agarose/MOPS gel to determine sample purity. The samples displayed no signs of degradation because distinct 28S and 18S mRNA bands were present, and all samples had A_{260}/A_{280} ratios of 1.8 -2.0.

Initial quality control analysis of the assay and hybridization performance, shown in Table 4.1, was assessed in the Affymetrix® MicroArray Suite - Expression Report generated after signal values of the raw image data were determined and scaled to the Affymetrix default total global target intensity value (TGT) of 500 to normalize the signals to facilitate microarray comparisons. Scaling each microarray, or chip, yields a scaling factor that should be within 3-fold of all the microarrays being compared within and between conditions. The TGT scaling factors were within the 3-fold range recommended by Affymetrix. However, the scaling factors varied more than 10% between replicate samples and suggested variability in probe signal values between samples.

For the control and *mdx:utrn*^{-/-} groups at 9-10 days, the mean signal value (Mean SI) was approximately 550 AU units, as shown in Table 4.1. The mean background signal value (Mean BG) for controls was 86±22 and 92±34 for *mdx:utrn*^{-/-}. While the mean values of the background were similar between the groups, the background values within the group replicates were variable (25%, control; 37%, *mdx:utrn*^{-/-}). For the control and *mdx:utrn*^{-/-} groups at age 20-21 days, the mean signal values were slightly higher, compared to the age 9-10 day values. The mean background values were also higher at 149±84 for control and 174±30 for *mdx:utrn*^{-/-}. As with the younger group, the background values within the group replicates were variable (57%, control; 18%, *mdx:utrn*^{-/-}). An average 29±8% of the gene transcripts on the chip for the control group were called present and 28±2% of the transcripts on the chip for the *mdx:utrn*^{-/-} group were called present. Calling a gene present means the P-value of the detection signal was less than 0.04. Affymetrix reports the typical background value of arrays to be in the range of 20-100. While the background values for the 9-10 day groups were within this range, the values for the age 20-21 day groups were high and fell outside the range (149±84, control and 174±30, *mdx:utrn*^{-/-}). The background reflected the high variability observed in the percentage of transcripts called present between replicates within the *mdx:utrn*^{-/-} group at age 9-10 days and control group at age 20-21 days. There was an 18% range in the number of transcripts called present at 9-10 days in the *mdx:utrn*^{-/-} group and 29% range in the control group at 20-21 days. A variety of factors could contribute to the number of transcripts called present in an array. This includes the tissue type, biological or environmental stimuli, and overall RNA quality. It was important to consider other assay metrics of quality control to best determine the quality of the assay and ability to compare the data. The variation in the background signal and the number of

genes called present within the 9-10 day *mdx:utrn*^{-/-} and 20-21 day control samples may have an affect on gene call. Genes may be called absent if their signal intensity value is less than the background signal. While the expression of the transcript may be low, there may be statistically significant differences in expression between conditions. The expression differences may have significant physiological effects.

Chip background is affected by sample quality and the noise of the scanner (Raw Q). The Raw Q varies between instruments but when samples scanned on the same scanner are compared, the values should be similar. At 9-10 days, the Raw Q was 2.8±0.5 for control and 3.0±0.8 for *mdx:utrn*^{-/-}, and at 21 days, the values were 3.4±1.6 for control and 4.4±0.3 for *mdx:utrn*^{-/-} groups. Overall, the values were similar except for one control chip at 20-21 days. The Raw Q values for each sample are also listed in Table 4.1 (Q Score).

RNA sample and assay quality were assessed by comparing the ratio of the signal value for the 3' probe sets of the internal control transcripts, β -actin and GAPDH, to the signal value of the matching 5' probe sets. The optimal ratio should be close to 1 but no greater than 3. Values higher than 3 indicate degraded RNA or inefficient transcription of either double-stranded cDNA or biotinylated cRNA. The β -actin 3'/5' ratios for controls and *mdx:utrn*^{-/-} at 9-10 and 20-21 days were less than 3 as shown in Table 4.1 (β -actin 3'/5' and GAPDH 3'/5', respectively). Therefore, the quality of the sample mRNA was sufficient for this experiment and the transcription and biotinylation of cDNA were efficient.

Affymetrix[®] provided eukaryotic hybridization controls (bioB, bioC, bioD, and creX) that were spiked into the hybridization cocktail, independent of RNA preparation. The cRNA transcripts were labeled in staggered concentrations of 1.5 pM (bioB), 5.0 pM (bioC), 25 pM (bioD), and 100 pM (creX) and were used to evaluate sample hybridization efficiency. BioB was provided at the level of assay sensitivity (1:100,000 transcripts per cell) and was expected to be called present 50% of the time. BioC, bioD and creX were expected to always be present with increasing signal values. For all samples tested, the hybridization controls were called present and the signal values for bioC, bioD, and creX increased, as shown in Table 4.1. However, there was high variation in the signal values within sample replicates. This result indirectly indicated possible variations in RNA sample quality or inefficient sample amplification and labeling. However, because the quality of the RNA samples in this experiment

was sufficient and the replicates were obtained from a pooled tissue source, the variation observed was likely due to the sample amplification or the labeling process.

Given the sample variation between replicates during the initial quality control analysis of the metrics in this experiment, it was determined two of the three microarrays from each group were similar enough in their overall expression to group together for statistical comparison. Therefore, a total of eight microarray samples, two for each of the four conditions were normalized and analyzed as described below.

Table 4.1. Summary of Affymetrix® MicroArray Suite - Expression Report. Quality control analysis on the assay and hybridization efficiency were assessed for each GeneChip® after the signal was scaled and normalized to a total global target intensity (TGT) of 500. The MicroArray Suite software generates a report for each chip that provides the percent of gene transcripts called present (% Present), the average signal (Mean SI), the background signal (Mean BG), the background signal variation (BG SD), and the scale factor used to normalize each chip to a TGT of 500. mRNA sample and assay quality were assessed by the 3’/5’ ratios of GAPDH and β -actin and hybridization efficiency was assessed by the variation on the signal values of the eukaryotic expression controls BioB (BioB SI), BioC (BioC SI), BioD (BioD SI), and CreX (CreX SI). Scanning performance was assessed by the RawQ value (Q Score). The values in this table are the average values and standard deviations for the 3 chips in each condition.

Condition	Control		<i>Mdx:utrn</i> ^{-/-}	
	9-10 days	20-21 days	9-10 days	20-21 days
% Present	38±3	29±8	38±7	28±2
Mean SI	551±34	668±94	546±76	666±34
Mean BG	86±23	149±84	92±34	174±30
BG SD	2.1±1.5	4.7±3.4	2.5±2.0	5.2±1.7
TGT Scale Factor	2.1±0.3	2.6±0.5	2.3±0.6	2.8±0.4
GAPDH 3’/5’	0.9±0.03	0.9±0.08	0.9±0.05	0.9±0.04
B-actin 3’/5’	1.0±0.01	0.9±0.04	1.0±0.06	0.9±0.05
BioB SI	98±20	62±15	103±18	82±11
BioC SI	259±39	176±28	226±18	200±33
BioD SI	594±440	470±101	732±108	531±83
CreX SI	3073±562	2069±444	3086±332	2180±142
Q Score	2.8±0.5	3.4±1.6	3.0±0.8	4.4±0.3

Normalization of Data and Statistical Analyses

As mentioned, the signal values on each chip were scaled to the default TGT of 500 to normalize the data for comparison. Transcripts were then scaled to the median signal value on the chip to account for the detection efficiency among spots and to allow comparison among transcripts between chips on a similar scale. For groups 1-3, gene expression was normalized by

the median expression of all transcripts in all samples as baseline. For group 4, gene expression was normalized to the appropriate control samples, i.e., *mdx:utrn*^{-/-} to control expression at 9-10 days and *mdx:utrn*^{-/-} to control expression at 20-21 days. Following normalization, the normalized gene expression values were statistically compared between groups using the microarray analysis program, GeneSpring (Silicon Genetics).

Significant Changes in Overall mRNA Expression

Of the 12,489 gene transcripts on the Affymetrix[®] Mu74Av2 GeneChip[®], a subset of 6,152 transcripts was called present in one or more of the samples. A small subset of these present transcripts, 2,910, were found significantly differentiated ($p < 0.05$) in the comparison groups, with 762 transcripts differentiated at a 2-fold or greater value, as reported in Table 4.2. Those transcripts that were differentiated greater than 2-fold were classified according to the function of the proteins they encode and the proportion in a given functional category was determined as shown in Table 4.3. A 2-fold cutoff was chosen based on the microarray analysis performed by Chen et al. (2000) and Porter et al (2002) who considered genes differentially expressed greater than 2-fold biologically significant.

Table 4.2. Number of gene transcripts significantly differentiated. GeneSpring analysis determined the number of genes that were significantly differentiated ($p < 0.05$) for each group comparison. Transcripts that were differentiated greater than 2-fold were chosen for further analysis.

Comparison Group	Description	$p < 0.05$	$\Delta \geq 2$ fold
1	Control day 9-10 vs. Control day 20-21	665	192
2	Control day 9-10 vs. <i>Mdx:utrn</i> ^{-/-} day 9-10	489	53
3	Control day 20-21 vs. <i>Mdx:utrn</i> ^{-/-} day 20-21	495	153
4	<i>Mdx:utrn</i> ^{-/-} day 9-10 vs. <i>Mdx:utrn</i> ^{-/-} day 20-21	1,261	346

Age comparisons. For both groups at age 20-21 days, there were a greater number of transcripts differentially expressed compared to both groups at 9-10 days. For the control group, 192 transcripts were significantly differentiated greater than 2-fold at 20-21 days compared to 9-10 days. For the *mdx:utrn*^{-/-} group, 346 transcripts were differentially expressed greater than 2-fold at 20-21 days compared to 9-10 days. At 9-10 days, 53 transcripts were significantly expressed in the *mdx:utrn*^{-/-} compared to control. By 20-21 days, the number of transcripts differentially

expressed increased to 153. The largest portion of transcripts significantly differentiated at both ages in the *mdx:utrn*^{-/-} corresponded to an immune response and included a number of cytokines and chemokines as well as lymphoid and myeloid markers. At 9-10 days, most of the immune response markers exhibited decreased expression while at 20-21 days most of the transcripts were up-regulated compared to control. Other differentially expressed gene transcripts corresponded to proteins and/or enzymes that reside in the extracellular matrix, or are involved in calcium homeostasis and proteolysis, metabolism and energy production, growth and differentiation, and biogenesis. Some transcripts could not be classified but are listed in Table 4.6.

Table 4.3. Classes of differentially regulated transcripts in *mdx:utrn*^{-/-}. The gene transcripts that were differentially regulated in *mdx:utrn*^{-/-} muscle compared to control at 9-10 and 20-21 days corresponded to an immune response, proteins of the extracellular matrix, calcium homeostasis, metabolism, growth and differentiation and cellular organization and biogenesis. Some transcripts could not be classified into a functional category. Utrophin was the only muscle specific transcript differentially expressed at age 9-10 days (-3.0 fold). The values in this table also show the proportion of transcripts differentially regulated for each functional category. The proportions represent the number of transcripts per function differentiated per age over the total number of increased and decreased transcripts per age.

Function	# of Transcripts $\Delta > 2$ -fold (% of total # Δ / age)			
	Decreased		Increased	
	9-10 days	20-21 days	9-10 days	20-21 days
Immune Response –total transcripts	14 (26.4%)	5 (3.3%)	3 (5.6%)	35 (22.9%)
Cytokines and receptors	1 (1.9%)	1 (0.7%)	-	10 (6.5%)
Vascular response/permeability	-	-	-	1 (0.7%)
Chemokines and receptors	2 (3.8%)	-	-	5 (3.3%)
Lymphoid and myeloid markers	6 (11.3%)	3 (2.0%)	2 (3.8%)	13 (8.5%)
MHC antigens	5 (9.4%)	1 (0.6%)	1 (1.9%)	2 (1.3%)
Complement system	-	-	-	5 (3.3%)
Extracellular matrix	5 (9.4%)	1 (0.7%)	2 (3.8%)	13 (8.5%)
Calcium homeostasis and proteolysis	1 (1.9%)	2 (1.3%)	-	6 (3.9%)
Metabolism and energy production	-	6 (3.9%)	1 (1.9%)	1 (0.7%)
Growth and differentiation	1 (1.9%)	2 (1.3%)	2 (3.8%)	8 (5.2%)
Cellular organization and biogenesis	1 (1.9%)	7 (4.6%)	-	6 (3.9%)
Muscle specific development	1 (1.9%)	-	-	2 (1.3%)
Unclassified	-	10 (6.5%)	5 (9.4%)	8 (5.2%)
Total	37	38	16	115

As hypothesized, a greater number of gene transcripts were significantly differentiated in the *mdx:utrn*^{-/-} at 20-21 days compared to control muscles of the same age and *mdx:utrn*^{-/-} muscles at age 9-10 days. The number of differentially expressed transcripts was also greater in the *mdx:utrn*^{-/-} compared to control muscle at 9-10 days. This increase correlates with the time period when pathophysiological onset occurs in the *mdx:utrn*^{-/-} mouse at age 7-14 days (Grady et al., 1997). Thus, the observed differences in gene expression may indicate onset of the dystrophic process. In addition, these differences provided a good time point to examine gene expression patterns relevant to the physiological state of the diseased muscle. A list of the gene transcripts found significantly differentiated can be found in Table 4.6.

mRNA Expression of Transcripts for Proteins in the Dystrophin-Glycoprotein Complex

Transcripts corresponding to the proteins of the DGC (Table 4.4) were examined to determine if differences at the transcription level corresponded to the known expression profile evident in DMD. In DMD, the loss of dystrophin leads to loss of syntrophin, sarcoglycan, and dystroglycan proteins, but the mRNA expression levels are similar to control muscle (Matsumura and Campbell, 1994; Campbell, 1995). Based on the present data, the expression of the transcripts corresponding to α -syntrophin, the sarcoglycans (α , β , and γ) and α -dystroglycan were present. The transcripts were called present in both control and *mdx:utrn*^{-/-} muscles at both ages and the expression levels of the transcripts were not different between genotypes. In contrast to the known genetic expression levels, the transcripts corresponding to β 1-syntrophin were undetectable for both genotypes at each age and δ -sarcoglycan was called marginally present in control muscle at age 9-10 days but was present in *mdx:utrn*^{-/-} muscle. At age 20-21 days δ -sarcoglycan expression was undetectable in each genotype, as shown in Table 4.5. nNOS expression was also called absent in both control and *mdx:utrn*^{-/-} muscles at both ages. In *mdx* mice, nNOS mRNA expression is present in both control and *mdx* muscles but is significantly decreased in the *mdx* (Chang et al., 1996).

Dystrophin expression in the control and *mdx:utrn*^{-/-} muscle was low and called absent. Although the expression was low, the expression levels decreased 35% in the *mdx:utrn*^{-/-} compared to control at age 9-10 days and 52% at 20-21 days. Given the low expression values and signal variation within the sample groups, there were no significant differences between the groups at both ages. Utrophin expression was also low in both sample groups at each age but

called present. At age 9-10 days, utrophin expression significantly decreased 60% in the *mdx:utrn*^{-/-} compared to normal muscle ($p < 0.05$) for the muscle specific probe (Affymetrix® ID 92507_at) on the Mu74Av2 GeneChip®. At age 20-21 days, there was no difference in utrophin expression for this probe. For the second utrophin probe (Affymetrix® ID 92508_s_at), expression in the *mdx:utrn*^{-/-} was reduced 37% at age 9-10 days and 39% at age 20-21 days compared to control but were not significantly different. According to the Affymetrix database, the biological processes for the second utrophin probe are muscle contraction and development. However, this probe was designed from the sequence in GenBank (NCBI) that is specific for G-utrophin, an utrophin isoform localized in brain and sensory ganglia (Blake et al., 1995). Given the utrophin gene is present in control and *mdx:utrn*^{-/-} mice, these probes may have been called present in the *mdx:utrn*^{-/-} muscles because they were not specific to the mutation in the mouse that terminates protein expression.

Overall, the expression values of the transcripts corresponding to the proteins of the DGC were consistent with the known mRNA expression profiles of the DGC in dystrophic muscle (Matsumura and Campbell, 1994; Campbell, 1995). However, there were differences in the expression levels of dystrophin in the controls that varied from the expected expression levels observed in healthy human compared to DMD muscles examined on Affymetrix® GeneChip® arrays (Chen et al., 2000). The dystrophin probe available on the Mu74Av2 GeneChip is specific for the mouse muscle isoform in exon 23, where the *mdx* mutation occurs. Given PCR analysis of control tailsnips demonstrated the animals were wild-type homozygotes, it is difficult to explain these observations.

Table 4.4. Expression calls of gene transcripts corresponding to the proteins of the DGC. Overall, the expression of α -dystroglycan, the sarcoglycans, and syntrophin correspond with the known mRNA expression in *mdx* muscle. Dystrophin was not observed in control or *mdx:utrn*^{-/-} muscle at ages 9-10 and 20-21 days. Utrophin was expressed in control and *mdx:utrn*^{-/-} muscle at both ages but was found significantly decreased in the *mdx:utrn*^{-/-} at ages 9-10 days.

Accession No.	Gene	Abbreviated Name	Affymetrix Call			
			9-10 days		20-21 days	
			Control	<i>Mdx:utrn</i> ^{-/-}	Control	<i>Mdx:utrn</i> ^{-/-}
AV244370	α -dystroglycan	Dag1	Present	Present	Present	Present
U43512	α -dystroglycan	Dag1	Present	Present	Present	Present
U56724	Dystrophin	Dmd	Absent	Absent	Absent	Absent
D14552	Nitric oxide synthase 1, neuronal (nNOS)	nNos1	Absent	Absent	Absent	Absent
AV206713	α -sarcoglycan	Sgca	Present	Present	Present	Present
AB024921	β -sarcoglycan	Sgcb	Present	Present	Present	Present
AB024923	δ -sarcoglycan	Sgcd	Marginal	Present	Absent	Absent
AB24922	γ -sarcoglycan	Sgeg	Present	Present	Present	Present
AV356394	α 1-syntrophin	Snta1	Present	Present	Present	Present
U00677	α 1-syntrophin	Snta	Present	Present	Present	Present
U00678	β 1-syntrophin	Sntb2	Absent	Absent	Absent	Absent
X83506	G-Utrophin	Utrn	Present	Present	Present	Present
Y12229	Utrophin	Utrn	Present	<u>Present*</u>	Present	Present

* Significantly down-regulated in the *mdx:utrn*^{-/-} at 9-10 days (p<0.05).

mRNA Expression of Transcripts for Proteins in Excitation Contraction Coupling

Expression of mRNA transcripts corresponding to proteins in ECC was examined (Table 4.5). The probes corresponding to FKBP, SERCA-1 and -2, PARV, and CSQ were available on the Affymetrix® Mu74Av2 GeneChip®. Transcripts corresponding to RyR were not available. mRNA expression, as shown in Table 4.5, was present for the available transcripts corresponding to the ECC transcripts in both control and *mdx:utrn*^{-/-} muscle at both ages. As hypothesized, there were no significant differences in expression for any of these transcripts between control and *mdx:utrn*^{-/-} muscle at both ages.

Table 4.5. Expression calls of gene transcripts corresponding to the proteins involved in ECC. Overall, for those probes present on the Mu74Av2 GeneChip®, all ECC transcripts were called present and there were no significant differences in expression between control and *mdx:utrn*^{-/-} muscles at either age.

Accession No.	Gene	Abbreviated Name	Affymetrix Call			
			9-10 days		20-21 days	
			Control	<i>Mdx:utrn</i> ^{-/-}	Control	<i>Mdx:utrn</i> ^{-/-}
AJ006306	FK binding protein 1	Fkbp	Present	Present	Present	Present
L06234	FK binding protein, alpha 1S subunit	Fkbp1s	Present	Present	Present	Present
U73487	FK binding protein, alpha2/delta subunit 1	Fkbp2d1	Present	Present	Present	Present
AV241808	SERCA 1	Atp2a1	Present	Present	Present	Present
X67140	SERCA 1	Atp2a1	Present	Present	Present	Present
AF029982	SERCA 2	Atp2a2	Present	Present	Present	Present
X59382	Parvalbumin	Parv	Present	Present	Present	Present
AF087687	Calsequestrin	CSQ	Present	Present	Present	Present

mRNA Expression of Transcripts for Proteins involved in Immune Function

The mRNA expression profile at ages 9-10 and 20-21 days showed a large proportion of gene transcripts corresponding to an immune response significantly differentiated in *mdx:utrn*^{-/-} muscle (32%, age 9-10 days and 26%, age 20-21 days), see Table 4.3. At age 9-10 days, 17 of a total 36 transcripts were differentially regulated in the *mdx:utrn*^{-/-} compared to control. At age 20-21 days, 40 of a total 112 transcripts were differentially regulated in the *mdx:utrn*^{-/-}. A higher proportion of immune transcripts were down-regulated (14 transcripts) at age 9-10 days while at 20-21 days, the majority of immune function transcripts increased (35 transcripts). Three transcripts increased in expression compared to control muscle at age 9-10 days (interferon-inducible GTPase, MRP14, and GRO1 oncogene) and 5 transcripts decreased in expression at 20-21 days (Janus kinase, castaneous IgK chain gene, germline Ig lambda-2-chain, antigen-specific protein mKAP13, and MHC class III region RD gene).

The immune response transcripts were classified into 6 categories according to the function of the protein product. The classes of transcripts differentially expressed were cytokines and receptors, vascular response proteins, chemokines and receptors, lymphoid and myeloid markers, major histocompatibility (MHC) antigens, and complement system components.

Immune response expression markers at age 9-10 days. At age 9-10 days, interferon-inducible GTPase was the only transcript corresponding to cytokines that was down-regulated (-6.4-fold) in the *mdx:utrn*^{-/-} compared to control muscles. There were no cytokine markers up-regulated at this age. Two chemokine transcripts were decreased in the *mdx:utrn*^{-/-}. These transcripts were for MRP14 (-4.8-fold) and GRO oncogene (-4.3-fold). There were also no chemokine transcripts up-regulated at age 9-10 days. Several transcripts for lymphoid and myeloid markers were either down- or up-regulated at age 9-10 days (6 transcripts decreased, 2 transcripts increased). The transcripts decreased were T-cell specific GTPase (-15.5-fold), cathelin-like protein (-4.2-fold), acid phosphatase (-3.5-fold), MRP-8 (-3.4-fold), interferon induced 15 kDa protein (-2.8-fold), and mGBP-2 (-2.8-fold). The transcripts for Fc receptor type II and mRNA for lysozyme were up-regulated +2.5- and +2.3-fold, respectively. Finally, several major histocompatibility (MHC) antigens were decreased. The transcripts were histocompatibility 2, K (-2.6-fold), histocompatibility 2, D (-2.6-fold), class I MHC gene (-2.4-fold), H-2K gene for MHC class I antigen (-2.3-fold), and MHC class I antigen (-2.0-fold). Histocompatibility 2, class II antigen was the only MHC antigen with increased expression at age 9-10 days (+6.9-fold).

Immune response expression markers at age 20-21 days. At age 20-21, 10 transcripts for cytokines and receptors were up-regulated in *mdx:utrn*^{-/-} compared to control muscles. This included the suppressor for cytokine signaling (+11.2-fold), the macrophage colony stimulating factor 1 receptor (+2.8-fold), and TNF receptor p75 (+2.0-fold). Janus kinase 2 was the only cytokine transcript significantly down-regulated (-2.2-fold). Several transcripts for chemokines and receptors were up-regulated. This included transcripts for the macrophage chemoattractant proteins 1 and 2 (MCP-1 and -2; +14.1- and +12.2-fold, respectively), MCP-1 receptor (+7.2-fold), MRP-8 (+3.2-fold), and GRO1 oncogene (+2.9-fold). There were no chemokine transcripts down-regulated at age 20-21 days.

The majority of transcripts differentially expressed at age 20-21 days in the *mdx:utrn*^{-/-} were classified as lymphoid and myeloid markers. Thirteen transcripts were up-regulated. This included the macrophage factors Mac-2 antigen (+13.1-fold), macrophage expressed protein gene 1 (+5.7-fold) and CD68 antigen (+3.8-fold), T-cell factors CD48 antigen (+3.8-fold) and T-cell specific mRNA (+2.0-fold), and the B-cell factor Beta Fc receptor type II (+4.2-fold). In

addition, mRNA corresponding to lysozymes P and M were increased 9.1 and 4.4 fold, respectively. All the lymphoid and myeloid markers described have previously been found differentially increased in mice and humans (Chen et al., 2000, Porter et al., 2002).

Finally, a few MHC antigen and complement system transcripts were differentially expressed in the *mdx:utrn*^{-/-} at age 20-21 days. The MHC antigen transcripts histocompatibility 2, class II and histocompatibility 2, blastocyst were increased +3.2- and +2.3-fold, respectively, and MHC class III region RD gene was decreased -3.2-fold. The complement system transcripts C1qB, 1qA, and 1qc were up-regulated +5.9-, +3.7-fold, and +2.6-fold respectively as well as complement component 3a receptor (+2.7-fold) and acid phosphatase (+2.8-fold). There were no transcripts down-regulated that corresponded to the complement system in the *mdx:utrn*^{-/-} at age 20-21 days. Table 4.6 lists all the immune response genes differentially regulated at ages 9-10 and 20-21 days with corresponding GenBank Accession Numbers.

mRNA Expression of Other Transcripts

In addition to the large differentiation in immune response factors, several transcripts were differentiated that corresponded to proteins in the extracellular matrix. At age 20-21 days, the transcript for the extracellular matrix metalloproteinase 3 (MMP3) was up-regulated +3.6-fold and expression for secreted phosphoprotein 1 (Spp1) increased +52.5-fold. Spp1 demonstrate the greatest fold change of all the transcripts in the *mdx:utrn*^{-/-} at age 20-21. At age 9-10 days Spp1 expression was decreased -6.1 fold in the *mdx:utrn*^{-/-}. This large change in expression of Spp1 across age has also been observed in other studies on mouse and human dystrophin-deficient muscle (Chen et al., 2000 and Porter et al., 2002). Both MMP3 and Spp1 may play important roles in an immune response (Porter et al., 2002 and Porter et al., 2003). Table 4.6 lists these transcripts as well as all other gene transcripts differentially expressed greater than 2-fold. The Microsoft Excel files containing the original signal values calculated for all probes by MicroArray Suite 5.0 are available to download as described in Appendix B.

Table 4.6. The gene transcripts differentially expressed greater than 2-fold. Gene transcripts differentially expressed in the *mdx:utrn*^{-/-} compared to control muscles at ages 9-10 (A, decreased expression and B, increased expression) and 20-21 (C, decreased expression and D, increased expression) days. The transcript fold change value and GenBank Accession Nos. are provided for reference.

Table4.6A. Decreased expression in the *mdx:utrn*^{-/-} at age 9-10 days (≥ 2 fold)

Accession No.	Gene	Abbreviated Name	(-) Fold Difference
Cytokines and receptors			
AJ007971	Interferon-inducible GTPase	Iigp-pending	- 6.4
Chemokines and receptors			
M83219	MRP14	S100a9	- 4.8
J04596	GRO1 oncogene	Cxcl1	- 4.3
Lymphoid and myeloid markers			
L38444	T-cell specific GTPase	Tgtp	- 15.5
X94353	Cathelin-like protein	Camp	- 4.2
M99054	Acid phosphatase	Acp5	- 3.5
AA204579	MRP8	Vig1-pending	- 3.4
X56602	Interferon induced 15kDa protein	Isg15	- 2.8
AJ007970	mGBP-2	Gbp2	- 2.8
MHC antigens			
M27134	Histocompatibility 2, K	H2-Q10	- 2.6
M69069	Histocompatibility 2, D	H2-D1	- 2.6
X16202	Class I MHC gene	H2-Q7	- 2.4
V00746	H-2K gene for MHC class I antigen	H2-K	- 2.3
M58156	MHC class I antigen	H2-K	- 2.0
Extracellular matrix			
L20232	Integrin binding salioprotein	Ibsp	- 43.7
X72795	MMP 9	Mmp9	- 25.6
L24431	Bone gamma carboxyglutamate protein	Bglap1	- 7.7
X13986	Secreted phosphoprotein 1	Spp1	- 6.1
X66473	MMP 13	Mmp13	- 5.6
Calcium homeostasis and proteolysis			
L28836	Peroxisomal membrane protein	Abcd3	- 2.0
Growth and differentiation			
AI854029	p53 apoptosis effector related to Pmp22	Perp-pending	- 15.9
Cellular organization and biogenesis			
U53219	GTPase IGTP	Igtp	- 2.6
Muscle specific development			
AA816121	Utrophin		- 3.0

Table 4.6B. Increased expression in *mdx:utrn*^{-/-} at age 9-10 days (≥ 2 fold)

<i>Accession No.</i>	<i>Gene</i>	<i>Abbreviated Name</i>	<i>(+) Fold Difference</i>
<i>Lymphoid and myeloid markers</i>			
M31312	<i>Fc receptor type II</i>	<i>Fcgr2b</i>	+ 2.5
X51547	<i>mRNA for lysozyme</i>	<i>Lzp-s</i>	+ 2.3
<i>MHC antigens</i>			
X52643	<i>Histocompatibility 2, class II antigen A</i>	<i>H2-Aa</i>	+ 6.9
<i>Extracellular matrix</i>			
M93428	<i>Endothelial ligand for L-selectin</i>	<i>Glycam1</i>	+ 6.9
X04573	<i>Elastase 2</i>	<i>Ela2</i>	+ 2.6
<i>Metabolism and energy production</i>			
M21285	<i>Steroyl-coenzyme A desaturase 1</i>	<i>Scd1</i>	+ 2.1
<i>Growth and differentiation</i>			
AV315419	<i>Cell division cycle 25 homolog A (S. cerevisiae)</i>	<i>Cdc25a</i>	+ 6.5
V00727	<i>FBJ osteosarcoma oncogene</i>	<i>Fos</i>	+ 2.6
<i>Unclassified</i>			
AW125330	<i>Expressed sequence AL024210</i>	<i>AL024210</i>	+ 5.1
AW045753	<i>RIKEN cDNA 1110015E22 gene</i>	<i>1110015E22Rik</i>	+ 4.6
L12367	<i>Adenyl cyclase-associated protein</i>	<i>Cap1</i>	+ 2.3
U23781	<i>B-cell leukemia/lymphoma 2 related protein A1a</i>	<i>Bcla1a</i>	+ 2.2
K02236	<i>Methallothionein 2</i>	<i>Mt2</i>	+ 2.1

Table 4.6C. Decreased expression in the *mdx:utrn*^{-/-} at age 20-21 days (≥ 2 fold)

Accession No.	Gene	Abbreviated Name	(-) Fold Difference
Cytokines and receptors			
L16956	Janus kinase 2	Jak2	- 2.2
Lymphoid and myeloid markers			
M80423	Castaneous IgK chain gene		- 4.4
J00592	Germline Ig lambda-2-chain	2010309G21Rik	- 2.9
D85925	Antigen-specific protein mKAP13	Krtap14	- 2.6
MHC antigens			
AF109906	MHC class III region RD gene	Hspa1b	- 3.2
Extracellular matrix			
M93428	Endothelial ligand for L-selectin	Glycam1	- 2.6
Calcium homeostasis and proteolysis			
L28836	Peroxisomal membrane protein	Abcd3	- 5.3
X61232	Carboxypeptidase H	Cpe	- 2.3
Metabolism and energy production			
AB017026	Oxysterol-binding protein	Osbp1a	- 3.0
D29639	Embryonal carcinoma cell	Hadhsc	- 2.5
L42996	Mitochondrial acyltransferase	Dbt	- 2.5
X51905	Lactate dehydrogenase	Ldh2	- 2.3
AF037370	Cytochrome c oxidase subunit VIIa-H (Cox7ah)	Cox7a1	- 2.2
X51941	Methylmalonyl coenzyme A mutase	Mut	- 2.0
Growth and differentiation			
U09504	Thyroid hormone receptor alpha	Nr1d2	- 2.5
AF100171	Myelodysplasia/ myeloid leukemia factor 1	Mlf1	- 2.1
Cellular organization and biogenesis			
Y13569	Phosphatidylinositol 3-kinase	Pik3r2	- 2.9
D76440	Necdin	Ndn	- 2.9
L19953	ELK3	Elk3	- 2.4
AJ250489	Receptor activity modifying protein 1	Ramp1	- 2.4
D86037	Sulfonylurea receptor 2	Abcc9	- 2.2
X15373	Inositol 1,4,5-triphosphate receptor 1	Itpr1	- 2.1
X54327	Glutamyl-tRNA synthetase	Eprs	- 2.1
Unclassified			
AJ007909	Erythroid differentiation factor	Edr	- 4.3
U88623	Aquaporin 4	Aqp4	- 4.1
AB034693	Endomucin-1	Emcn-pending	- 2.6
AJ131398	MinK-like protein	Kcne11	- 2.3
AF060490	TLS-associated protein TASR-2	Nssr	- 2.2
D16580	Peptidyl arginine deaminase	Padi2	- 2.2
M11533	Myelin basic protein	Mbp	- 2.2
U35141	Retinoblastoma-binding protein	Rbbp4	- 2.1
U89489	LIM homeobox protein cofactor CLIM-1b	Ldb2	- 2.1
AB016080	Calcium binding protein Kip 2	Kip2-pending	- 2.1

Table 4.6D. Increased expression in *mdx:utrn*^{-/-} at age 20-21 days (≥ 2 fold)

Accession No.	Gene	Abbreviated Name	(+) Fold Difference
Cytokines and receptors			
U88328	Suppressor of cytokine signalling-3	Socs3	+ 11.2
M36579	S100 calcium binding protein	S100a4	+ 6.7
AJ007971	IIGP	Iigp-pending	+ 4.3
X03505	Serum amyloid A	Saa3	+ 4.3
X06368	Colony stimulating factor 1 receptor	Csf1r	+ 2.8
U04204	Fibroblast growth factor regulated protein	Akr1b8	+ 2.8
M31419	Interferon activated gene	Ifi204	+ 2.5
AF022371	Interferon activated gene 203	Ifi203	+ 2.1
X87128	TNF receptor p75	Tnfrsf1b	+ 2.0
Vascular response/permeability			
AF004858	Platelet-activating factor receptor	Par	+ 2.2
Chemokines and receptors			
M19681	Macrophage chemoattractant protein 1 (MCP-1)	Ccl2	+ 14.1
AB023418	Macrophage chemoattractant protein 2 (MCP-2)	Ccl8	+ 12.2
U56819	Macrophage chemoattractant protein 1 receptor (MCP-1 receptor)	Ccr2	+ 7.2
M83218	MRP-8	S100a8	+ 3.2
J04596	GRO1 oncogene	Cxcl1	+ 2.9
Lymphoid and myeloid markers			
X16834	Mac-2 antigen	Lgals3	+ 13.1
X51547	mRNA for lysozyme P	Lzp-s	+ 9.1
L20315	Macrophage expressed gene 1	Mpeg1	+ 5.7
M65027	Glycoprotein 49 A	Gp49a	+ 4.7
M21050	Lysozyme M	Lyzs	+ 4.4
M31312	Beta Fc receptor type II	Fcgr2b	+ 4.2
X53526	CD48 antigen	Cd48	+ 4.2
M96827	Haptoglobin	Hp	+ 3.9
X68273	CD68 antigen	Cd68	+ 3.8
AB007599	MD-1	Ly86	+ 2.3
M69260	Lipocortin 1	Anxa1	+ 2.3
X00246	Set 1 repetitive element for MGC antigen	H2-D1	+ 2.3
M94584	Secretary protein (YM-1)	Chi3l3	+ 2.3
L38444	T-cell specific mRNA	Tgtp	+ 2.0
MHC antigens			
U35330	Histocompatibility 2, class II	H2-DMb1	+ 3.2
U21906	Histocompatibility 2, blastocyst		+ 2.3
Complement system			
M22531	Complement C1qB	C1qb	+ 5.9
X58861	Complement component C1qA	C1qa	+ 3.7
U77461	Complement component 3a receptor	C3ar1	+ 2.7
X57199	Acid phosphatase 2	Acp2	+ 2.8
X66295	Complement C1qC	C1qg	+ 2.6
Extracellular matrix			
X13986	Secreted phosphoprotein protein 1	Spp1	+ 52.5
V00755	Tissue inhibitor of metalloproteinase 1	Timp1	+ 10.0

M16238	Fibrinogen-like protein 2	Fgl2	+ 5.1
D00466	Apolipoprotein E	Apoe	+ 3.7
X66402	MMP 3	Mmp3	+ 3.6
U22262	Apolipoprotein B editing complex 1	Apobec1	+ 3.4
L10244	Spermidine N1-acetyl transferase	Sat	+ 3.3
X75129	Xanthine dehydrogenase	Xdh	+ 3.2
X54511	Myc basic motif homologue 1	Capg	+ 2.8
X56304	Tenascin C	Tnc	+ 2.7
J03484	Gamma laminin	Lamc1	+ 2.7
X82648	Apolipoprotein D	Apod	+ 2.5
D16195	Granulin	Grn	+ 2.2
Calcium homeostasis and proteolysis			
AJ223208	Cathepsin S	Ctss	+ 10.9
U06119	Cathepsin H	Ctsh	+ 3.1
AJ000990	Legumain	Lgmn	+ 2.9
M65270	Cathepsin B gene	Ctsb	+ 2.4
U25844	Serine protease inhibitor	Serpinb6	+ 2.3
U22033	Large multifunctional protease 7	Psmb8	+ 2.0
Metabolism and energy production			
AF089751	ATP receptor P2X4	P2rx4	+ 3.6
Growth and differentiation			
U20735	Transcription factor junB	Junb	+ 16.2
AF041847	MCARP	Crap	+ 10.0
M34896	Ectropic viral integration site 2	Evi2	+ 6.6
AF099973	Schlafen 2	Slfn2	+ 4.3
X66449	Calcyclin	S100a6	+ 2.7
U09507	Cyclin dependent kinase inhibitor 1A	Cdkn1a	+ 2.2
Cellular organization and biogenesis			
AF084466	Ras-like GTP-binding protein	Rrad	+ 8.9
V00727	FBJ osteosarcoma oncogene	Fos	+ 7.2
U72680	Ion channel homolog RIC	Fxyd5	+ 4.4
AF009414	SOXII	Sox11	+ 2.8
U59807	Cystatin B	Cstb	+ 2.5
M28845	Early growth response 1	Egr1	+ 2.2
Muscle specific development			
L47600	Troponin T isoform	Tnnt2	+ 7.4
M74753	Myosin heavy chain, skeletal muscle	Myh3	+ 5.0
Unclassified			
V00835	Metallothionein	Mt1	+ 10.4
K02236	Metallothionein 2	Mt2	+ 9.8
M64086	Spi2 protease inhibitor	Serpina3n	+ 8.3
AF024637	TYRO protein tyrosine kinase binding protein	Tyrobp	+ 6.4
M88694	Thioether S-methyltransferase	Temt	+ 4.6
L27439	Protein S	Pros1	+ 2.1
X61800	CCAAT/enhancer binding protein	Cebpd	+ 2.1

Chapter 5. Discussion

DMD onset mechanisms are not presently well understood

Aside from the primary dystrophin defect in DMD, the events that lead to the pathogenesis of the disease are not well understood. At least two mechanisms are believed to be involved in the pathogenesis of dystrophin-deficient muscle. One is the activation of calcium-dependent proteases or apoptotic pathways caused by increased calcium in the myoplasm. This may occur either from leaky calcium channels at the sarcolemma or from dysfunctional calcium handling by proteins involved in muscle contraction, e.g., the SERCA pump (Turner et al., 1988, Fong et al., 1990). The second possible mechanism is an immune response (Spencer et al., 1997 and Porter et al., 2002). It is not clearly understood how these mechanisms become involved in the dystrophic process or if they are the specific pathophysiological mechanism(s) that initiate DMD. One reason for this lack of clear definition is many studies have not effectively characterized the disease in its early stages. In addition, the *mdx* mouse, the most commonly used animal model to investigate DMD, does not appear to adequately mimic human DMD. The purpose of the present study was to determine the pathophysiological processes involved in the initial stages of the dystrophic process. DNA microarrays were used to examine global mRNA expression in maturing *mdx:utrn*^{-/-} mouse skeletal muscle, a more appropriate model of DMD, at ages 9-10 and 20-21 days. Specific purposes for the study were to determine (1) if DNA microarrays can provide information on pathophysiological processes associated with the initiation of the dystrophic process.; (2) if the expression of mRNA transcripts corresponding to the proteins involved in Ca²⁺ handling during ECC are altered in dystrophin-utrophin deficient muscle ; (3) if dystrophic muscle is associated with an immune response at an age close to overt disease onset, and to identify potential molecules that could trigger onset.

Major Findings

There were three major findings in the present study. (1) DNA microarrays detected differences in mRNA expression in dystrophic *mdx:utrn*^{-/-} compared to control skeletal muscles. An age-dependent increase in the number of transcripts differentially expressed was also found. (2) The expression of mRNA transcripts corresponding to proteins involved in ECC were not differentially expressed in *mdx:utrn*^{-/-} compared to control muscles. (3) The mRNA expression profile of *mdx:utrn*^{-/-} compared to control utrophin muscles showed a dominant over-expression

of transcript markers that suggested dystrophin-deficient muscle is affected by an immune response associated with the time period of disease pathophysiological onset.

Changes in mRNA expression were detected in *mdx:utrn*^{-/-} muscle and an age dependent increase in the number of transcripts differentially expressed was also found.

At age 9-10 days, 53 transcripts were differentially regulated greater than 2-fold in *mdx:utrn*^{-/-} compared to control muscles. But by age 21 days, the number of transcripts differentially expressed greater than 2-fold had increased approximately 3-times to 153 transcripts. Porter et al. (2003a) reported a similar age effect in *mdx* hindlimb muscles. In the Porter (2003a) study, the number of mRNA transcripts differentially expressed in *mdx* hindlimb and diaphragm muscles was low at age 7 days. By age 14 days, the number of mRNA transcripts differentially expressed increased. Between the ages of 14 and 23 days the number of transcripts differentially expressed increased by ~ 17-fold. At age 56 days, the number of transcripts differentially expressed peaked and leveled off by age 112 days. Porter et al. (2003a) concluded the trend in the number of transcripts differentially expressed corresponded well with the pathophysiology of *mdx* muscle and the jump in the number of transcripts between ages 14 and 23 days correlated well with the age of histological disease onset in *mdx* muscle at age 3 weeks. (Porter et al., 2003a).

At age 7 days, Porter et al. (2003a) found the majority of transcripts differentially expressed were down-regulated but become up-regulated or unchanged by age 14 days through 112 days. Most of the transcripts were linked to an immune response, the extracellular matrix, and proteolysis. The present study also showed similar responses in expression patterns between ages 9-10 and 20-21 days. At age 9-10 days, the majority of transcripts in *mdx:utrn*^{-/-} compared to control hindlimb muscles were differentially down-regulated (64%), but this pattern was reversed at age 20-21 days where 70% of the transcripts were up-regulated or unchanged. These transcripts primarily were linked to an immune response and the extracellular matrix. For example, matrix metalloproteinases 9 and 12 (MMP9 and 12) were down-regulated 26- and 6-fold, respectively, in the present study, but were not differentially regulated at ages 14 through 112 days (Porter et al., 2003a). Secreted phosphoprotein 1 (Spp1) was down-regulated 6-fold in *mdx:utrn*^{-/-} muscle at ages 9-10 days but became up-regulated 53-fold by ages 20-21 days. In *mdx* muscle, MMP9 and MMP12 were also down-regulated 35- and 14-fold at age 7 days but

were unchanged at ages 14 through 112 days (Porter et al., 2003a). *Spp1* was also down-regulated 22-fold in *mdx* muscle at age 7 days but was up-regulated 2- to 74-fold at ages 14 through 112 days. These results confirm the second hypothesis of this study that a greater number of transcripts would be differentially regulated around the age of pathophysiological onset in the *mdx:utrn*^{-/-} muscle between age 7 and 14 days.

The expression of mRNA transcripts corresponding to proteins involved in ECC were not differentially expressed in *mdx:utrn*^{-/-} muscle.

The Affymetrix® Mu74Av2 GeneChip® contains probes for the following proteins involved in ECC: SERCA 1, SERCA 2, FK binding protein, parvalbumin, and calsequestrin, but not RyR. These transcripts were called present for control and *mdx:utrn*^{-/-} muscle at both 9-10 and 20-21 days but were not significantly differentially expressed between any condition. Rittler reported there were no differences in the content of ECC proteins in *mdx* and *mdx:utrn*^{-/-} limb muscle at ages 9-10 and 21 days (Rittler, 2002). High $[Ca^{2+}]_i$ is considered a potential effector of DMD pathogenesis (Turner et al., 1988; Fong et al., 1990; Turner et al., 1993). In the present study, $[Ca^{2+}]_i$ was not determined, but if it is assumed to be elevated, it did not appear to influence transcription levels for these calcium handling proteins. Therefore, increased $[Ca^{2+}]_i$ is more likely to activate calcium-dependent proteases and apoptotic processes (Turner et al., 1988, Fong et al., 1990). Based on the limited changes in the expression of transcripts encoding the specific calcium handling proteins on the GeneChip, there did not appear to be major differences in ECC between the *mdx:utrn*^{-/-} and control muscles.

The mRNA expression profile of *mdx:utrn*^{-/-} muscle demonstrated dominant over-expression of immune response markers that suggests an immune response dominates the *mdx:utrn*^{-/-} muscle during the early stages of the disease.

While at age 9-10 days, the majority of markers corresponding to an immune response were down-regulated, 26% of the total number of transcripts differentially expressed at 21 days corresponded to markers that suggest *mdx:utrn*^{-/-} muscle was affected by a variety of immune cells including mast cells, macrophages, and B- and T-lymphocytes. The markers for an immune response included a variety of transcripts corresponding to cytokines and receptors, chemokines and receptors, lymphoid and myeloid markers, MHC antigens, and complement components.

The results of the present study correspond well with the gene expression findings in investigations on 8 week *mdx* hindlimb muscle (Porter et al., 2002) and time course studies on *mdx* hindlimb and diaphragm at ages 7 to 112 days (Porter et al., 2003a and 2004).

Cytokine and receptor expression. Cytokines are a family of growth factors primarily secreted from leukocytes that stimulate vascular and cellular immune responses. Nine transcripts corresponding to cytokines and receptors were found up-regulated in the *mdx:utrn*^{-/-} muscle at age 20-21 days. Tumor necrosis factor alpha (TNF α) is a cytokine produced primarily by activated macrophages that modulates the immune response. TNF α induces the expression of other cytokines, is a key inducer of an immune response, and is invoked early after tissue damage. In DMD, injured myofibers may express TNF α and induce an immune response without a response from mononuclear cells (Tews and Goebel, 1996; Porter et al., 2002); however, TNF α expression is apparently not different in DMD patients or in *mdx* mice (Lundberg et al., 1995; Porter et al., 2002). Mast cells are found in muscle connective tissue and respond rapidly to mild injury (Gorospe et al., 1996). Mast cells store TNF α and are chronically present in DMD and transiently present in *mdx* muscle (Gorospe et al., 1994; Lefaucheur et al., 1996). Degranulation of mast cells in dystrophin deficient myofibers increases blood flow to the myofiber and causes direct proteolysis (Gorospe et al., 1994). TNF α expression was not different between *mdx:utrn*^{-/-} and control muscles in the present study, but expression of the transcript for TNF receptor p75 was increased 2-fold at age 21 days and was found up-regulated 2-fold in *mdx* leg muscle at age 8 weeks (Porter et al., 2002). An increase in TNF α secretion in muscle may not necessarily alter the expression of its transcript, but an increase in the expression of one of its receptors may indicate an adaptive response for mast cell localization to the site of injury in dystrophic muscle.

Chemokine and receptor expression. Chemokines are classes of small molecular weight cytokines that are characterized according to the patterns of cysteine residues at the N-terminus. They are induced by a wide range of stimuli and are involved in leukocyte extravasations, T-cell differentiation, and when coupled with G-protein coupling receptors, regulate the trafficking and migration of leukocytes and lymphocytes to injured sites (Tews et al., 1996; Gorospe et al., 1996; Porter et al., 2003). Five transcripts corresponding to chemokines and receptors were

found up-regulated in *mdx:utrn*^{-/-} muscle at age 21 days. Macrophage chemoattractant proteins 1 (MCP-1 or Ccl2) and 2 (MCP-2 or Ccl8) activate leukocyte adhesion molecules on endothelium and are important in macrophage and T-cell recruitment (Porter et al., 2003b). Expression for these transcripts was increased 14-fold (MCP-1) and 12-fold (MCP-2) in the present study and expression for the MCP-1 receptor (Ccr2) was found up-regulated 7-fold. Expression for MCP-1 was up-regulated 36-fold in 8 week old *mdx* limb muscle (Porter et al., 2002). Furthermore, MCP-1 in 8 week old *mdx* hindlimb muscle was found up-regulated 15-fold and MCP-2 receptor expression was increased 7-fold based on DNA microarray analysis (Porter et al., 2003b) Based on quantitative PCR, MCP-1 was up-regulated 63-fold, and its protein content was increased 4-fold by densitometric analysis of immunoblots (Porter et al., 2003b). Time course expression analysis also showed increased expression of MCP-1 in preneurotic *mdx* hindlimb muscle and histological analysis showed expression of MCP-1 in association with mononuclear cells surrounded by macrophages. In the same investigation, MCP-2 was up-regulated 29-fold by but changes in protein content were undetectable by densitometric analysis of immunoblots and immunolocalization analysis (Porter et al., 2003b). Moreover, expressions of transcripts corresponding to chemokines were not differentially regulated in *mdx* extraocular muscle (EOM, Porter et al., 2003a). Collectively, these data demonstrate that chemokines play an active and important role in macrophage and T-cell recruitment in *mdx* muscle prior to the overt signs of muscle necrosis. Up-regulated expression of MCP-1 and -2 in the present study also suggest that chemokines play an important role in the trafficking of macrophages and T-cells to damaged *mdx:utrn*^{-/-} muscle. Given the time course of MCP-1 expression, it is important to determine when and how these chemokines are expressed and how they affect muscle pathophysiology in DMD. MCP-1 may be an important target for drug therapy in DMD and, therefore, is something that warrants further study.

Lymphoid and myeloid marker expression. Further evidence of an immune response in *mdx:utrn*^{-/-} hindlimb muscle was shown in the present study by the significant increases in lymphoid and myeloid markers. Glycoprotein 49 A (Gp49a), which is expressed by mast cells, was up-regulated 5-fold in *mdx:utrn*^{-/-} muscle at age 21 days. It has also been found up-regulated, at higher levels (22-fold), in *mdx* hindlimb muscle at age 8 weeks (Porter et al., 2002). Macrophage expressed protein gene 1 (Mpeg1) and CD68 antigen (Cd68) were up-regulated

approximately 6-fold and 4-fold, respectively, and are expressed by macrophages. These genes were also up-regulated but at higher levels in 8 week old *mdx* muscle (34-fold, Mpeg1 and 12-fold, CD68; Porter et al., 2002). The mRNA markers for T-cells, CD48 antigen (Cd48) and T-cell specific mRNA (Tgtp), were increased approximately 4-fold and 2-fold, respectively, in the present study at age 21 days. In 8 week old *mdx* hindlimb, CD48 was found up-regulated 14-fold; however, Tgtp was not significantly differentially expressed (Porter et al., 2002). Finally, Beta Fc receptor type II (Fcgr2b) was increased 4-fold in *mdx:utrn*^{-/-} hindlimb muscle at 21 days and was also found increased in 8 week old *mdx* hindlimb but at higher levels (12-fold, Porter et al., 2002). Fcgr2b is specific for B-cells. Thus, the presence of similar myeloid and lymphoid markers in *mdx* and *mdx:utrn*^{-/-} muscle provide further evidence of an immune response in dystrophin-deficient and dystrophin- and utrophin-deficient hindlimb muscle. The higher levels of over-expression of these markers in the *mdx* mouse may reflect the older age of the *mdx* muscle investigated by Porter et al. (2002).

Complement system. The complement system is a group of soluble plasma proteins that attack cell membranes. Five transcripts corresponding to the complement system were found up-regulated in the present study. This included 3-C1q components (a, b, and c), the C3 receptor, and acid phosphatase. Other components of the complement system have also been found up-regulated in human DMD and α -sarcoglycan-deficient muscles (Chen et al., 2000), as well as in 8 week old *mdx* hindlimb muscles (Porter et al., 2002). Although the role of the complement system in the dystrophic process is not well understood, it is possible that this system exacerbates an already compromised dystrophin-deficient sarcolemma (Sewry et al., 1987; Porter et al., 2002). Understanding the involvement of the complement system and how it is activated in dystrophinopathy may provide important clues into the mechanisms that initiate muscle fiber necrosis.

Secreted phosphoprotein 1. Secreted phosphoprotein 1 (Spp1; minopontin) is dramatically elevated in 8 week old *mdx* hindlimb muscle (146-fold; Porter et al., 2002). In a time course investigation of *mdx* hindlimb muscle, Spp1 is down-regulated (-22-fold) at age 7 days but becomes dramatically up-regulated by age 23 days (30-fold) and remains elevated throughout the course of the disease (Porter et al., 2003a). In addition, it is up-regulated in human DMD muscle

biopsies (Haslett et al., 2002). The present study demonstrates a similar age-dependent expression in *mdx:utrn*^{-/-} muscle. Spp1 was down-regulated 6-fold at age 9-10 days but was up-regulated 53-fold at age 21 days. In the present investigation and the two mentioned above on *mdx* mice (Porter et al., 2002; Porter et al., 2003a), Spp1 became the most significantly up-regulated transcript. According to Porter et al. (2002 and 2003a), Spp1 is a macrophage product that enhances the turnover of the extracellular matrix and is believed to regulate collagen synthesis and accumulation. Up-regulation of Spp1 is believed to stimulate muscle repair in dystrophic muscle by macrophages and it is believed Spp1 exerts a chemotactic role in an immune response and fibrosis (Ashkar et al., 2000; Denhardt et al., 2001). Spp1 is activated by the cleavage of matrix metalloproteinase 3 (Mmp3). In the present study, the transcript for Mmp3 was found significantly up-regulated approximately 3-fold in the *mdx:utrn*^{-/-} at age 21 days. Our data and that of others indicate that Spp1 may be a viable therapeutic target for DMD (Porter et al., 2003a).

Summary

In the present study, the transcriptional state of normal and dystrophin-utrophin-deficient mouse muscle was compared by a DNA microarray approach to better understand the pathophysiological mechanisms involved in the onset of DMD. Comparison of mRNA expression in *mdx:utrn*^{-/-} to control muscles demonstrated that between ages 10 – 21 days, there is an increased number of gene transcripts differentially expressed that correlate with the age of dystrophic onset in the *mdx:utrn*^{-/-} at 7-14 days (Grady et al., 1997). The data indicate that expression levels for transcripts encoding specific calcium handling proteins were not different. This result suggests that problems with calcium handling may not be apparent at the transcription level. In contrast, there was significant up-regulation of transcripts that corresponded to immune markers and extracellular matrix activity. Up-regulation of several transcripts corresponding to cytokines and their receptors, chemokines and their receptors, and lymphoid and myeloid markers suggest that muscle is invaded by macrophages, leukocytes, B- and T-cells during the period of overt disease onset.

The evidence in these data and many other studies further implicate the immune system in the pathophysiology of DMD (Spencer et al., 1997; Chen et al., 2000; Porter et al., 2002; Porter et al., 2003a; Porter et al., 2003b; Porter et al., 2004). However, it is still unclear if an

immune response is the mechanism that initially damages DMD muscle. An immune response to muscle may occur in 2 different ways (1) immune cells respond to an already damaged muscle or (2) the molecular profile of dystrophin-deficient muscle, independent of initial muscle damage, changes such that the muscle becomes a target for invasion and subsequent necrosis. If an immune response is a response to damaged or a differentiated muscle, then other mechanisms are responsible for initiating muscle degradation in DMD. Stress does not appear to initiate damage in dystrophin-deficient muscle (Grange et al., 2002); therefore, DMD onset may occur by increased Ca^{2+} leak channel activity that increases $[\text{Ca}^{2+}]_i$ and causes muscle degradation to occur by increased proteolytic activity. Immune cells then respond to factors released by damaged muscle and further contribute to muscle degradation.

Alternatively, signaling through the DGC may be altered such that muscle becomes aberrantly elicited to an immune response that eventually traffics immune cells that cause necrosis. Therefore, given that a stimulus must be present, e.g., muscle damage or cell signaling, an immune response is not the mechanism that initiates the dystrophic process but appears to be a key physiological process contributing to muscle necrosis in DMD. Although an immune response may not initiate DMD, it plays an important role in necrosis. It is important to understand how the immune system responds to dystrophin-deficient muscle as therapeutic agents targeting the immune response may be important in slowing the disease progression.

Rejection/Non-Rejection of Research Hypotheses

The null hypothesis H_{01} was rejected. There were differences in mRNA expression between control and *mdx:utrn*^{-/-} muscle at both 9-10 and 21 days. Four hundred eighty nine transcripts were found differentially regulated between control and *mdx:utrn*^{-/-} muscle at age 9-10 days ($p < 0.05$) with 54 of the 489 transcripts significantly differentiated greater than 2-fold. Four hundred ninety five transcripts were found differentially regulated at ages 20-21 days ($p < 0.05$) with 152 of the 495 significantly differentiated transcripts expressed greater than 2-fold. The null hypotheses H_{02} and H_{03} were rejected. Six hundred sixty five transcripts were significantly differentiated between control groups at ages 9-10 and 21 days ($p < 0.05$) with 192 of 665 transcripts differentially regulated greater than 2-fold. For the *mdx:utrn*^{-/-} groups, 1,261 transcripts were significantly differentiated between ages 9-10 and 20-21 days ($p < 0.05$) with 346 of the 1,261 transcripts differentially expressed greater than 2-fold. The null hypotheses H_{04} , H-

05, H₀₆, H₀₇, H₀₈, H₀₉, H₁₀, and H₁₁ were not rejected as there were no effects of age or genotype on the expression of transcripts corresponding to the proteins of the DGC or ECC. The null hypothesis H₁₂ was not rejected as there were no differences in immune function genes in control muscle between ages 9-10 and 20-21 days. Finally, the null hypotheses H₁₃, H₁₄, and H₁₅ were rejected. There were differences between the number of transcripts corresponding to an immune response that were found significantly differentiated greater than 2-fold in the *mdx:utrn*^{-/-} between ages 9-10 and 20-21 days (p<0.05) as well as control and *mdx:utrn*^{-/-} muscle at ages 9-10 (p<0.05) and 20-21 days (p<0.05). Fourteen transcripts were found decreased in *mdx:utrn*^{-/-} muscle at age 9 days compared to 5 at age 21 days and 3 transcripts were found increased in *mdx:utrn*^{-/-} muscle at age 9-10 days compared to 35 at age 21 days. Seventeen transcripts corresponding to an immune response were differentially regulated in *mdx:utrn*^{-/-} muscle at age 9-10 days compared to control and 40 transcripts were differentially regulated in the *mdx:utrn*^{-/-} muscle at age 20-21 days compared to control.

Future Directions

More research is providing compelling evidence that an immune response to dystrophin-deficient muscle may have a specific role in the pathogenesis of DMD during the initial stages of the disease. However, it is still not clear if an immune response initially damages the muscle or if an immune response is a response to muscle damage. To better understand the onset of DMD, this must be determined. It is recommended that the up-regulation of the pro-inflammatory markers in this study be confirmed by other RNA quantification methods such as Real Time PCR. *Spp1* and *MMP3* appear to be important mediators in macrophage and T-cell recruitment. The chemokines, MCP-1 and -2, are also important mediators in macrophage recruitment. Given the significant up-regulation of expression in these transcripts in this study and others, further investigation is recommended. Future studies can determine the protein expression of these transcripts and determine the physiological activity these proteins have in recruiting immune cells during the onset and middle disease stages. These molecules may have specific roles in regulating necrosis in dystrophin-utrophin-deficient muscle and could be important targets for drug therapy.

Additional studies of mRNA expression in *mdx* and *mdx:utrn*^{-/-} muscle during the onset of the dystrophic process are also needed. These studies should examine mRNA expression over

a day by day timecourse from birth through the period of overt disease at ages 1-21 days and look at muscle histology to pinpoint when an immune response begins. The additional expression information may better pinpoint the exact time that onset occurs and better reveal the mechanism(s) of onset. In addition to an immune response, Ca^{2+} may have a significant role in initiating muscle degradation; therefore, further studies should also decipher if Ca^{2+} or an immune response is mediating initial muscle degradation in DMD.

References

1. Adams, B.A. and Beam, K.G. (1990). Muscular dysgenesis in mice: a model system for studying excitation-contraction coupling. *FASEB Journal*, 4(10):2809-16. Review.
2. Agnihotri, R., Crawford, H.C., Haro, H., Matrisian, L.M., Havrda, M.C. and Liaw, L. (2001). Osteopontin, a novel substrate for matrix metalloproteinase-3 (stromelysin-1) and matrix metalloproteinase-7 (matrilysin). *The Journal of Biological Chemistry*, 276(30):28261-28267.
3. Ahn, A.H. and Kunkel, L.M. (1993). The structural and functional diversity of dystrophin. *Nature Gene*, 3: 283-291.
4. Alderton, J.M. and Steinhardt, R.A. (2000). Calcium influx through calcium leak channels is responsible for the elevated levels of calcium-dependent proteolysis in dystrophic myotubes. *The Journal of Biological Chemistry*, 275(13): 9452-9460.
5. Amalfitano, A. and Chamberlain, J.S. (1996) The mdx-amplification-resistant mutation system assay, a simple and rapid polymerase chain reaction-based detection of the mdx allele. *Muscle Nerve*, 19(12):1549-1553.
6. Alberts, B., Bray, D, Lewis, J., Raff, M., Roberts, K., and Watson, J.D. (1983). *Molecular Biology of the Cell*. *Garland Publishing, Inc.*: 951-952.
7. Ashkar, S., Weber, G.F., Panoutsakopoulou, V., Sanchirico, M.E., Jansson, M., Zawaideh, S., Rittling, S.R., Denhardt, D.T., Glimcher, M.J and Cantor, H. (2000). Eta-1 (osteopontin): an early component of type-1 (cell-mediated) immunity. *Science*, 287(5454): 860-4.
8. Badalamente, M.A. and Stracher, A. (2000). Delay of muscle degeneration and necrosis in mdx mice by calpain inhibition. *Muscle & Nerve*, 23: 106-111.

9. Berchtold, M.W., Brinkmeier, H. and Muntener, M. (2000). Calcium ion in skeletal muscle: its crucial role for muscle function, plasticity, and disease. *Physiological Review*, 80(3): 1215-1265. Review.
10. Bernasconi, P., Torchiana, E., Confalonieri, P., Brugnoli, R., Barresi, R., Mora, M., Cornello, F., Morandi, L. and Mantegazza, R. (1995). Expression of transforming growth factor- β 1 in dystrophic patient muscles correlates with fibrosis: pathogenic role of a fibrogenic cytokine. *The Journal of Clinical Investigation*, 96: 1137-1144.
11. Blake, D.J., Schofield, J.N., Zuellig, R.A., Gorecki, D.C., Phelps, S.R., Barnard, E.A., Edwards, Y.H. and Davies, K.E. (1995). G-utrophin, the autosomal homologue of dystrophin Dp116, is expressed in sensory ganglia and brain. *Proceedings of the National Academy of Sciences of the United States of America*, 92(9): 3697-3701.
12. Bredt, D.S. and Snyder, S.H. (1994). Transient nitric oxide synthase neurons in embryonic cerebral cortical plate, sensory ganglia, and olfactory epithelium. *Neuron*, 13(2): 301-313.
13. Brooks, S.V., Zerba, E. and Faulkner, J.A. (1995). Injury to muscle fibres after single stretches of passive and maximally stimulated muscles in mice. *The Journal of Physiology*, 488(2): 459-469.
14. Burkin, D.J. and Kaufman, S.J. (1999). The α 7 β 1 integrin in muscle development and disease. *Cell Tissue Research*, 296: 183-190.
15. Burkin, D.J., Wallace, G.Q., Nicol, K.J., Kaufman, D.J. and Kaufman, S.J. (2001). Enhanced expression of the α 7 β 1 integrin reduces muscular dystrophy and restores viability in dystrophic mice. *The Journal of Cell Biology*, 152(6): 1207-1218.
16. Butcher, L.A. and Tomkins, J.K. (1986). Protein profiles of sarcoplasmic reticulum from normal and dystrophic mouse muscle. *Journal of the Neurological Sciences*, 72: 159-169.

17. Byrne, E., Kornberg, A.J. and Kapsa, R. (2003). Duchenne muscular dystrophy: hopes for the sesquicentenary. *The Medical Journal of Australia*, 179 (9): 463-464.
18. Cai, B., Spencer, M.J., Nakamura, G., Tseng-Ong, L. and Tidball, J.G. (2000). Eosinophilia of dystrophin-deficient muscle is promoted by perforin-mediated cytotoxicity by T cell effectors. *The American Journal of Pathology*, 156(5): 1789-1796.
19. Campanelli, J.T., Roberds, S.L., Campbell, K.P. and Scheller, R.H. (1994) A role for dystrophin-associated glycoproteins and utrophin in agrin-induced AChR clustering. *Cell*, 77(5): 663-674.
20. Campbell, K.P. (1995). Three muscular dystrophies: loss of cytoskeleton-extracellular matrix linkage. *Cell*, 80: 675-679.
21. Carnwath, J.W. and Shotton, D.M. (1987). Muscular dystrophy in the *mdx* mouse: histopathology of the soleus and extensor digitorum longus muscles. *Journal of the Neurological Sciences*, 80: 39-54.
22. Chang, W.J., Iannaccone, S.T., Lau, K.S., Masters, B.S., McCabe, T.J., McMillan, K., Padre, R.C., Spencer, M.J., Tidball, J.G. and Stull, J.T. (1996). Neuronal nitric oxide synthase and dystrophin-deficient muscular dystrophy. *Proceedings of the National Academy of Sciences of the United States of America*, 93(17): 9142-9147.
23. Chaubourt, E., Voisin, V., Fossier, P., Baux, G., Israël, M. and de La Porte, S. (2000). The NO way to increase muscular utrophin expression? *Life Sciences*, 323: 735-740.
24. Chang, W-J., Iannaccone, S.T., Lau, K.S., Masters, B.S., McCabe, T.J., McMillan, K., Padre, R., Spencer, M.J., Tidball, J.G. and Stull, T.J. (1996). Neuronal nitric oxide synthase and dystrophin-deficient muscular dystrophy. *The Proceedings for the National Academy of Sciences of the United States of America*. 93: 9142-9147.

25. Chen, Y., Zhao, P., Borup, R. and Hoffman, E.P. (2000). Expression profiling in the muscular dystrophies: identification of novel aspects of molecular pathophysiology. *The Journal of Cell Biology*, 151(6): 1321-1336.
26. Chu, G., Narasimhan, B., Tibshirani, R. and Tusher, V. (2001) *SAM: "Significance Analysis of Microarrays" Users Guide and Technical Document*. Stanford University. Retrieved from <http://www.utulsa.edu/microarray/Articles/sam%20manual.pdf>
27. Cole, M.A., Rafael, J.A., Taylor, D.J., Lodi, R., Davies, K.E. and Styles, P. (2002). A quantitative study of bioenergetics in skeletal muscle lacking utrophin and dystrophin. *Neuromuscular Disorders*, 12: 247-257.
28. Connolly, A.M., Keeling, R.M., Mehta, S., Pestronk, A. and Sanes, J.R. (2001). Three mouse models of muscular dystrophy: the natural history of strength and fatigue in dystrophin-, dystrophin/utrophin-, and laminin α 2-deficient mice. *Neuromuscular Disorders*, 11: 703-712.
29. Cozzi, F., Cerletti, M., Luvoni, G.C., Lombardo, R., Brambilla, P.G., Faverzani, S., Blasevich, F., Cornelio, F., Pozza, O. and Mora, M. (2001). Development of muscle pathology in canine X-linked muscular dystrophy. Quantitative characterization of histopathological progression during postnatal skeletal development. *Acta Neuropathologica*, 101: 469-478.
30. Danowski, B.A., Imanaka-Yoshida, K., Sanger, J.M. and Sanger, J.W. (1992). Costameres are sites of force transmission to the substratum in adult rat cardiomyocytes. *The Journal of Cell Biology*, 118(6): 1411-1420.
31. Denhardt, D.T., Noda, M., O'Regan, A.W., Pavlin, D., Berman, J.S. (2001). Osteopontin as a means to cope with environmental insults: regulation of inflammation, tissue

remodeling, and cell survival. *The Journal of Clinical Investigation*, 107(9): 1055-1061. Review.

32. De Luca, A., Pierno, S., Liantonio, A., Cetrone, M., Camerino, C., Simonetti, S., Papadia, F. and Camerino, D.C. (2001). Alteration of excitation-contraction coupling mechanism in extensor digitorum longus muscle fibres of dystrophic mdx mouse and potential efficacy of taurine. *British Journal of Pharmacology*, 132: 1049-1054.
33. Deconinck, N., Tinsley, J., De Backer, F., Fisher, R., Kahn, D., Phelps, S., Davies, K. and Gillis, J.M. (1997). Expression of truncated utrophin leads to major functional improvements in dystrophin-deficient muscles of mice. *Nature Medicine*, 3(11): 1216-1221.
34. Deconinck, N., Rafael, J.A., Beckers-Bleukx, G., Kahn, D., Deconink, A.E., Davies, K.E. and Gillis, J.M. (1998). Consequences of the combined deficiency in dystrophin and utrophin on the mechanical properties and myosin composition of some limb and respiratory muscles of the mouse. *Neuromuscular Disorders*, 8: 362-370.
35. DiMario, J.X., Uzman, A., and Strohman, R.C. (1991). Fiber regeneration is not persistent in dystrophic (mdx) mouse skeletal muscle. *Developmental Biology*, 148: 314-321.
36. Dubeej, M and Campbell, K.P. (2002). Muscular dystrophies involving the dystrophin-glycoprotein complex: an overview of current mouse models. *Current Opinions in Genetics and Development*, 12: 349-361.
37. Duchenne, G.B., (1868). Recherches sur la paralysie musculaire pseudo-hypertrophique ou paralysie myosclerosique. *Archives de medecine generale et tropicale*, 11, 5,178, 305, 421, 552.

38. Ebihara, S., Guibina, G.H., Gilbert, R., Nalbantoglu, J., Massie, B., Karpati, G. and Petrof, B.J. (2000). Differential effects of dystrophin and utrophin gene transfer in immunocompetent muscular dystrophy (mdx) mice. *Physiological Genomics*, 3: 133-144.
39. Emery, A.E. (1989). Clinical and molecular studies in Duchenne muscular dystrophy. *Progress in clinical and biological research*, 306: 15-28. Review.
40. Felder, E., Protasi, F., Hirsch, R., Franzini-Armstrong, C. and Allen, P.D. (2002). Morphology and molecular composition of sarcoplasmic reticulum surface junctions in the absence of DHPR and RyR in mouse skeletal muscle. *Journal of Biophysics*, 82(6): 3144-3149.
41. Fleischer, S. and Inui, M. (1989). Biochemistry and biophysics of excitation-contraction coupling. *Annual review of biophysics and biophysical chemistry*, 18: 333-364. Review.
42. Fong, P.Y., Turner, P.R., Denetclaw, W.F., and Steinhardt, R.A. (1990). Increased activity of calcium leak channels in myotubes of Duchenne human and *mdx* mouse origin. *Science*, 250(4981): 673-676.
43. Franco, A.J. and Lansman, J.B. (1990). Calcium entry through stretch-activated ion channels in mdx myotubes. *Nature*, 344: 670-673.
44. Gorospe, J.R., Tharp, M.D., Hinckley, J., Kornegay, J.N. and Hoffman EP. (1994). A role for mast cells in the progression of Duchenne muscular dystrophy? Correlations in dystrophin-deficient humans, dogs, and mice. *Journal of Neurological Sciences*, 122(1): 44-56.
45. Gorospe, J.R., Nishikawa, B.K. and Hoffman, E.P. (1996). Recruitment of mast cells to muscle after mild damage. *Journal of Neurological Sciences*, 135(1): 10-17.

46. Grady, R.M., Merlie, J.P. and Sanes, J.R. (1997). Subtle neuromuscular defects in utrophin-deficient mice. *The Journal of Cell Biology*, 136(4): 871-882.
47. Grady, R., Teng, H., Nichol, M., Cunningham, J., Wilkinson, R. and Sanes, J. (1997). Skeletal and cardiac myopathies in mice lacking utrophin and dystrophin: a model for Duchennes muscular dystrophy. *Cell*, 90: 729-738.
48. Grange, R.W., Gainer, T.G., Marschner, K.M., Talmadge, R.J. and Stull, J.T. (2002). Fast-twitch skeletal muscles of dystrophic mouse pups are resistant to injury from acute mechanical stress. *American Journal of Physiology. Cell Physiology*, 283(4): c1090-1101.
49. Hack, A.A., Lam, M.J., Cordier, L., Shoturma, D.I., Ly, C.T., Hadhazy, M.A., Hadhazy, M.R., Sweeney, H.L. and McNally, E.M. (2000). Differential requirement for individual sarcoglycans and dystrophin in the assembly and function of the dystrophin-glycoprotein complex. *Journal of Cell Science*, 113: 2535-2544.
50. Hartigan-O'Connor, D., Kirk, C.J., Crawford, R., Mulé, J.J. and Chamberlain, J.S. (2001). Immune evasion by muscle-specific gene expression in dystrophic muscle. *Molecular Therapy*, 4(6): 525-533.
51. Haslett, J.N., Sanoudou, D., Kho, A.T., Bennett, R.R., Greenberg, S.A., Kohane, I.S., Beggs, A.H. and Kunkel, L.M. Gene expression comparison of biopsies from Duchenne muscular dystrophy (DMD) and normal skeletal muscle. *The Proceedings for the National Academy of Sciences of the United States of America*, 99(23): 15000-15005.
52. Hoffman, E.P., Brown, R.H., Kunkel, L.M. (1987a). Dystrophin: the protein product of the Duchenne muscular dystrophy locus. *Cell*, 51: 919-928.
53. Hoffman, E.H., Monaco, A.P., Feener, C.A. and Kunkel, L.M. (1987b). Conservation of the Duchenne muscular dystrophy gene in mice and humans. *Science*, 238: 347-350.

54. Hutter, O.F., Burton, F.L., Bovells, D.L. (1991). Mechanical properties of normal and *mdx* mouse sarcolemma: bearing on function of dystrophin. *Journal of Muscle Research and Cell Motility*, 12(6): 585-589.
55. Hutter, O.F. (1992). The membrane hypothesis of Duchenne muscular dystrophy: quest for functional evidence. *Journal of Inherited Metabolic Disorders*, 15: 565-577.
56. Jackson, M.J., McArdle, A., Edwards, R.H.T. and Jones, D.A. (1991). Muscle damage in *mdx* mice. [Letter to the editor]. *Nature*, 350(6360): 2664.
57. Koenig, M., Hoffman, E.P., Bertelson, C.J., Monaco, A.P., Feener, C. and Kunkel, L.M. (1987). Complete cloning of the Duchenne muscular dystrophy gene in normal and affected individuals. *Cell*, 50: 509-517.
58. Khurana, T.S., Watkins, S.C., Chafey, P., Chelly, J., Tome, F.M., Fardeau, M., Kaplan, J.C. and Kunkel, L.M. (1991). Immunolocalization and developmental expression of dystrophin related protein in skeletal muscle. *Neuromuscular Disorders*, 1(3): 185-194.
59. Kwon, M.S., Park, C.S., Choi, K., Park, C.S., Ahn, J., Kim, J.I., Eom, S.H., Kaufman, S.J. and Song, W.K. (2000). Calreticulin couples calcium release and calcium influx in integrin-mediated calcium signaling. *Molecular Biology*, 11: 1433-1443.
60. Lagrota-Candido, J., Canella, I., Savino, W. and Quirico-Santos, T. (1999). Expression of extracellular matrix ligands and receptors in the muscular tissue and draining lymph nodes of *mdx* dystrophic mice. *Clinical Immunology*, 93(2): 143-151.
61. Laird, P.W., Zijderveld, A., Linders, K., Rudnicki, M.A., Jaenisch, R. and Berns A. (1991). Simplified mammalian DNA isolation procedure. *Nucleic Acids Research*, 19(15): 4293.

62. Lau, K.S., Grange, R.W., Chang, W.J., Kamm, K.E., Sarelius, I. and Stull, J.T. (1998). Skeletal muscle contractions stimulate cGMP formation and attenuate vascular smooth muscle myosin phosphorylation via nitric oxide. *FEBS Letters*, 431(1): 71-74.
63. Love, D.R., Byth, B.C., Tinsley, J.M., Blake, D.J., Davies, K.E. (1990). Dystrophin and dystrophin-related proteins. *Neuromuscular Disorders*, 3: 5-21.
64. Lowe, D.A., Warren, G.L., Ingalls, C.P., Boorstein, D.B. and Armstrong, R.B. (1995). Muscle function and protein metabolism after initiation of eccentric contraction-induced injury. *Journal of Applied Physiology*, 79(4): 1260-1270.
65. Lundberg, I., Brengman, J.M. and Engel, A.G. (1995). Analysis of cytokine expression in muscle in inflammatory myopathies, Duchenne dystrophy, and non-weak controls. *Journal of Neuroimmunology*, 63(1): 9-16.
66. Lynch, G.S., Rafael, J.A., Chamberlain, J.S. and Faulkner, J.A. (2000). Contraction-induced injury to single permeabilized muscle fibers from *mdx*, transgenic *mdx*, and control mice. *American Journal of Physiology. Cell Physiology*, 279: C1290-C1294.
67. McArdle, A., Edwards, R.H.T. and Jackson, M.J. (1991). Effects of contractile activity on muscle damage in the dystrophin-deficient *mdx* mouse. *Clinical Science*, 80: 367-371.
68. McCarter, G.C. and Steinhardt, R.A. (2000). Increased activity of calcium leak channels caused by proteolysis near sarcolemma ruptures. *The Journal of Membrane Biology*, 176: 169-174.
69. Matsumura, K., Ervasti, J.M., Ohlendieck, K., Kahl, S.D. and Campbell, K.P. (1992). Association of dystrophin-related protein with dystrophin-associated proteins in *mdx* mouse muscle. *Nature*, 360(6404): 588-591.

70. Matsumura, K. and Campbell, K.P. (1994). Dystrophin-glycoprotein complex: its role in the molecular pathogenesis of muscular dystrophies. *Muscle Nerve*, 17(1): 2-15. Review.
71. Matsumura, K., Arai, K., Zhong, D., Saito, F., Fukuta-Ohi, H., Maekawa, R., Yamada, H. and Shimizu, T. (2003). Matrix metalloproteinase activity that disrupts the dystroglycan complex: its role in the molecular pathogenesis of muscular dystrophies. *Basic Applied Myology*, 13(6): 299-304.
72. MedlinePlus. (2005). *Medical Encyclopedia: Immune Response*. Retrieved from <http://www.nlm.nih.gov/medlineplus/ency/article/000821.htm>.
73. Mendell, J.R., Sahenk, Z. and Prior, T.W. (1995). The childhood muscular dystrophies: disease sharing a common pathogenesis of membrane instability. *The Journal of Child Neurology*, 10: 150-159.
74. Menke, A. and Jockusch, H. (1991). Decreased osmotic stability of dystrophin-less muscle cells from the mdx mouse. *Nature*, 349(6304): 69-71.
75. Meryon, E. (1852). On granular and fatty degeneration of the voluntary muscles. *Medico-Chirurgical Trans (London)*, 35: 73.
76. Morrison, J., Lu, Q.L., Pastoret, C., Partridge, T. and Bou-Gharios, G. (2000). T-cell dependent fibrosis in the mdx dystrophic mouse. *Laboratory Investigation*, 80(6): 881-891.
77. Moss, R.L. (1992). Ca²⁺ regulation of mechanical properties of striated muscle. Mechanistic studies using extraction and replacement of regulatory proteins. *Circulation Research*, 70(5): 865-884. Review.
78. *Muscular Dystrophy Association*

79. Mukoyama, M., Kondo, K., Hizawa, K., Nishitani, H. and the DMDR Group. (1987). Life spans of Duchenne muscular dystrophy patients in the hospital care program in Japan. *Journal of the Neurological Sciences*, 81: 155-158.
80. Nakamura, A., Harrod, G.V. and Davies, K.E. (2001). Activation of calcineurin and stress activated protein kinase/p38-mitogen activated protein kinase in hearts of utrophin-dystrophin knockout mice. *Neuromuscular Disorders*, 11: 251-259.
81. Ohlendiek, K. and Campbell, K.P. (1991). Dystrophin constitutes 5% of membrane cytoskeleton in skeletal muscle. *FEBS Letters*, 283: 230-234.
82. Ohlendiek, K., Matsumara, K., Ionasescu, V.V., Towbin, J.A., Bosch, E.P., Weinstein, S.L., Sernett, S.W. and Campbell, K. (1993). Duchenne muscular dystrophy: deficiency of dystrophin-associated proteins in the sarcolemma. *Neurology*, 43: 795-800.
83. Pearce, M., Blake, D.J., Tinsley, J.M., Byth, B.C., Campbell, L., Monaco, A.P. and Davies, K.E. (1993). The utrophin and dystrophin genes share similarities in genomic structure. *Human Molecular Genetics*, 2(11): 1765-1772.
84. Petrof, B.J., Shrager, J.B., Stedman, H.H., Kelly, A.M. and Sweeney, H.L. (1993). Dystrophin protects the sarcolemma from stresses developed during muscle contraction. *Proceedings of the National Academy of the Sciences USA*, 90: 3710-1714.
85. Petrof, B.J. (1998). The molecular basis of activity-induced muscle injury in Duchenne muscular dystrophy. *Molecular and Cellular Biology*, 179: 111-123.
86. Petrof, B.J. (2002). Molecular pathophysiology of myofiber injury in deficiencies of the dystrophin-glycoprotein complex. *American Journal of Physical Medicine and Rehabilitation*, 81(11 Suppl): S162-S174.

87. Porter, J.D. (2000). Introduction to muscular dystrophy. *Microscopy Research and Technique*, 48: 127-130.
88. Porter, J.D., Khanna, S., Kaminski, H.J., Rao, J.S., Merriam, A.P., Richmonds, C.R., Leahy, P., Li, J., Guo, W. and Andrade, F.H. (2002). A chronic inflammatory response dominates the skeletal muscle molecular signature in dystrophin-deficient *mdx* mice. *Human Molecular Genetics*, 11(3): 263-272.
89. Porter, J.D., Merriam, A.P., Leahy, P., Gong, B., and Khanna, S. (2003a). Dissection of temporal gene expression signatures of affected and spared muscle groups in dystrophin-deficient (*mdx*) mice. *Human Molecular Genetics*, 12(15): 1813-1821.
90. Porter, J.D., Guo, W., Merriam, A.P., Khanna, S., Cheng, G., Zhou, X., Andrade, F.H., Richmonds, C. and Kaminski, H.J. (2003b). Persistent over-expression of specific CC class chemokines correlates with macrophage and T-cell recruitment in *mdx* skeletal muscle. *Neuromuscular Disorders*, 13(3): 223-35.
91. Porter, J.D., Merriam, A.P., Leahy, P., Gong, B., Feuerman, J., Cheng, G. and Khanna, S. (2004). Temporal gene expression profiling of dystrophin-deficient (*mdx*) mouse diaphragm identifies conserved and muscle group-specific mechanisms in the pathogenesis of muscular dystrophy. *Human Molecular Genetics*, 13(3): 257-269.
92. Rafael, J.A. and Brown, S.C. Dystrophin and utrophin: genetic analyses of their role in skeletal muscle. *Microscopic Research Technics*, 48(3-4): 155-66. Review.
93. Rando, T.A. (2002). Oxidative stress and the pathogenesis of muscular dystrophies. *American Journal of Physical Medicine and Rehabilitation*, 81(11): S175-186. Review.
94. Rezvani, M., Cafarelli, E. and Hood, D.A. (1995). Performance and excitability of *mdx* mouse muscle at 2, 5, and 13 wk of age. *Journal of Applied Physiology*, 78: 961-967.

95. Rittler, M.R. (2002). *Sarcoplasmic reticulum calcium handling in maturing skeletal muscle from two models of dystrophic mice*. Master's Thesis, Virginia Polytechnic Institute and State University, Blacksburg, Virginia.
96. Robert, V., Massimino, M.L., Tosello, V., Marsault, R., Cantini, M., Sorrentino, V., and Pozzan, T. (2001). Alteration in calcium handling at the subcellular level in *mdx* myotubes. *The Journal of Biological Chemistry*, 276(7): 4647-4651.
97. Roberts, R.G. (2001). Protein family review (dystrophin). *Genome Biology*, 2: 3006.1-3006.5.
98. Ruegg, U.T. and Gillis, J-M. (1999). Calcium homeostasis in dystrophic muscle. *TiPS*, 20: 351-352.
99. Rybakova, I.N., Patel, J.R. and Ervasti., J.M. (2000). The dystrophin complex forms a mechanically strong link between the sarcolemma and costameric actin. *The Journal of Cell Biology*, 150: 1209-1214.
100. Sacco, P., Jones, D.A., Dick, J.R.T. and Vrbova, G. (1992). Contractile properties and susceptibility to exercise-induced damage of normal and *mdx* mouse tibialis anterior muscle. *Clinical Science*, 82: 227-236.
101. Sewry, C.A., Dubowitz, V., Abraham, A., Luzio, J.P., and Campbell AK. (1987). Immunocytochemical localization of complement components C8 and C9 in human diseased muscle. The role of complement in muscle fiber damage. *Journal of Neurological Sciences*, 81(2-3): 141-153.
102. Spencer, M.J., Walsh, C.M., Dorshkind, K.A., Rodriquez, E.M. and Tidball, J.G. (1997). Myonuclear apoptosis in dystrophic *mdx* muscle occurs by perforin-mediated cytotoxicity. *Journal of Clinical Investigation*, 99: 2745-2751.

103. Spencer, M.J., Marino, M.W. and Winkler, W.M. (2000). Altered pathological progression of diaphragm and quadriceps muscle in TNF-deficient, dystrophin-deficient mice. *Neuromuscular Disorders*, 10: 612-619.
104. Spencer, M.J. and Tidball, J.G. (2001). Do immune cells promote the pathology of dystrophin-deficient myopathies? *Neuromuscular Disorders*, 11: 556-564.
105. Stange, M., Tripathy, A. and Meissner, G. (2001). Two domains in dihydropyridine receptor activate the skeletal muscle Ca^{2+} release channel. *Biophysical Journal*, 81: 1419-1429.
106. Stedman, H.H., Sweeney, H.L., Shrager, J.B., Maguire, H.C., Panettieri, R.A., Petrof, B., Narusawa, M., Leferovich, J.M., Sladky, J.T. and Kelly, A.M. (1991). The mdx mouse diaphragm reproduces the degenerative changes of Duchenne muscular dystrophy. *Nature*, 352(6335): 536-539.
107. Stevens, E.D. and Faulkner, J.A. (2000). The capacity of *mdx* mouse diaphragm muscle to do oscillatory work. *Journal of Physiology*, 522(3): 457-466.
108. Straub, V., Rafael, J.A., Chamberlain, J.S. and Campbell, K.P. (1997). Animal models for muscular dystrophy show different patterns of sarcolemmal disruption. *The Journal of Cell Biology*, 139(2): 375-385.
109. Strube, C., Tourneur, Y. and Ojeda, C. (2000). Functional expression of the L-type calcium channel in mice skeletal muscle during prenatal myogenesis. *The Journal of Biophysics*, 78(3): 1282-1292.
110. Tews, D.S. and Goebel, H.H. (1996). Cytokine expression profile in idiopathic inflammatory myopathies. *Journal of Neuropathology and Experimental Neurology*, 55(3): 342-347.

111. Thomas, G.D., Sander, M., Lau, K.S., Huang, P.L., Stull, J.T. and Victor, R.G. (1998) Impaired metabolic modulation of alpha-adrenergic vasoconstriction in dystrophin-deficient skeletal muscle. *Proceedings of the National Academy of Sciences of the United States of America*, 95(25): 15090-15095.
112. Tidball, J.G. and Law, D.J. (1991). Dystrophin is required for normal thin filament-membrane associations at myotendinous junctions. *The American Journal of Pathology*, 138: 13-21.
113. Tidball, J.G., D.E. Albrecht, B.E. Lokensgard and M.J. Spencer. (1995). Apoptosis precedes necrosis in dystrophin-deficient muscle. *The Journal of Cell Science*, 108: 2197-2204.
114. Tidball, J.G. and Spencer, M.J. (2000). Chaplains and muscular dystrophies. *The International Journal of Biochemistry and Cell Biology*, 32: 1-5.
115. Tinsley, J.M., Blake, D.J., Roche, A., Fairbrother, U., Riss, J., Byth, B.C., Knight, A.E., Kendrick-Jones, J., Suthers, G.K. and Love, D.R., et al. (1992). Primary structure of dystrophin-related protein. *Nature*, 360(6404): 591-593.
116. Tinsley, J., Deconinck, N., Fisher, R., Kahn, D., Phelps, S., Gillis, J.M. and Davies, K. (1998). Expression of full-length utrophin prevents muscular dystrophy in *mdx* mice. *Nature Medicine*, 4(12): 1441-1444.
117. Tkatchenko, A.V., Le Cam, G., Leger, J.J. and Dechesne, C.A. (2000). Large-scale analysis of differential gene expression in the hindlimb muscles and diaphragm of *mdx* mouse. *Biochimica et Biophysica Acta*, 1500: 17-30.

118. Tkatchenko, A.V., Pietu, G., Cros, N., Gannoun-Zaki, L., Auffray, C., Leger, J.J. and Dechesne, C.A. (2001). Identification of altered gene expression in skeletal muscles from Duchenne muscular dystrophy patients. *Neuromuscular Disorders*, 11: 269-277.
119. Turner, P.R., Westwood, T., Regen, C.M. and Steinhardt, R.A. (1988). Increased protein degradation results from elevated free calcium levels found in muscle from *mdx* mice. *Nature*, 335: 735-738.
120. Turner, P.R., Fong, P., Denetclaw, W.F. and Steinhardt, R.A. (1991). Increased calcium influx in dystrophic muscle. *The Journal of Cell Biology*, 115: 1701-1712.
121. Turner, P.R., Schultz, R., Ganguly, B., Steinhardt, R.A. (1993). Proteolysis results in altered leak channel kinetics and elevated free calcium in *mdx* muscle. *The Journal of Membrane Biology*, 133(3): 243-251.
122. Tusher, V.G., Tibshirani, R. and Chu, G. (2001). Significance analysis of microarrays applied to the ionizing radiation response. *Proceedings of the National Academy of the Sciences*, 98(9): 5116-5121.
123. Warren, G.L., Hayes, D.A., Lowe, D.A., Williams, J.H. and Armstrong, R.B. (1994). Eccentric contraction-induced injury in normal and hindlimb-suspended mouse soleus and EDL muscles. *Journal of Applied Physiology*, 77(3): 1421-1430.
124. Wehling, M., Spencer, M.J., Tidball, J.G. (2001). A nitric oxide synthase transgene ameliorates muscular dystrophy in *mdx* mice. *Journal of Cell Biology*, 155: 123-31.
125. Yoshida, M., Matsuzaki, T., Date, M. and Wada, K. (1997). Skeletal muscle fiber degeneration in *mdx* mice induced by electrical stimulation. *Muscle and Nerve*, 20: 1422-1432.

Appendices

Appendix A. Mouse Morphological Data

Mouse Number	Genotype	Age (days)	Gender	Mass (g)
C57BL6p2	Control	9	Male	4.7
C57BL6p3	Control	9	Male	4.3
2246a2	Control	9	Male	5.5
2246a3	Control	9	Male	4.7
2246a4	Control	9	Male	4.7
Mean				4.8
SD				0.4
2269ap2	mdx:utrn-/-	10	Male	4.5
1781ap4	mdx:utrn-/-	10	Male	4.3
1781ap7	mdx:utrn-/-	10	Male	3.9
2273ap1	mdx:utrn-/-	10	Male	4.4
1781ap1	mdx:utrn-/-	10	Male	4.6
Mean				4.3
SD				0.3
2246a8	Control	20	Male	10.7
2246a9	Control	20	Male	9.5
2246a10	Control	20	Male	10.1
2248a4	Control	21	Male	10.8
2248a2	Control	20	Male	6.6
Mean				9.5
SD				1.7
2262ap2	mdx:utrn-/-	21	Male	8.7
2262ap6	mdx:utrn-/-	21	Male	9.0
2262ap9	mdx:utrn-/-	21	Male	8.5
2206ap2	mdx:utrn-/-	21	Male	8.0
2206ap4	mdx:utrn-/-	21	Male	8.2
Mean				8.5
SD				0.4

Appendix B. Directions to download raw data.

The Microsoft Excel files containing the original signal intensity values, as calculated by Affymetrix[®] Microarray Suite 5.0, for all probes in each condition in this study are available to download from the Virginia Tech Electronic Thesis and Dissertation website containing this document. The website is <http://scholar.lib.vt.edu/theses/>.

The files are contained within AffyRawData.zip and contain:

1. **Affy SI_control 9-10d.xls** – signal intensity values for the control group at ages 9-10 days.
2. **Affy SI_mdx-utrn 9-10d.xls** – signal intensity values for the *mdx:utrn^{-/-}* group at ages 9-10 days.
3. **Affy SI_control 20-21d.xls** – signal intensity values for the control group at ages 20-21 days.
4. **Affy SI_mdx-utrn 20-21d.xls** – signal intensity values for the *mdx:utrn^{-/-}* group at ages 20-21 days.

Curriculum Vita

THOMAS G. GAINER

Born October 1, 1976 in Newport News, VA to Thomas and Sheila Gainer.

- Education**
- M.S., Human Nutrition, Foods, and Exercise with an emphasis in Muscle Physiology and Biochemistry**, May 2005, Virginia Polytechnic Institute & State University (Virginia Tech), Blacksburg, VA
- B.S., Human Nutrition, Foods, and Exercise with an emphasis in the Science of Nutrition, Foods, and Exercise**, May 2000, Virginia Tech, Blacksburg, VA
- Skills**
- | | | |
|----------------------------------|--------------------------------|----------------------------------|
| Affymetrix GeneChip® | Gel Electrophoresis | Laboratory Automation |
| PCR/RT-PCR | Protein Microarray Development | Fluorometry/Spectrophotometry |
| RNA/DNA Isolation & Purification | Piezoelectric Dispensing | Small Animal Handling |
| | ELISA | Tissue & Cell Culture Processing |
- Experience**
- Associate in Research – Duke Center for Drug Discovery, Department of Neurobiology, Duke University**, Durham, NC, September 2004 – Present
- Perform secondary compound screening for therapeutic agents to slow or stop the progression of Huntington disease using an *in vitro* brain slice assay.
 - Optimize methods to improve the transfection of brain tissue with DNA using gold particles and biolistic devices.
 - Develop assays to examine drugs effective against pathways involved in the pathology of Huntington disease
- Research Associate (Contract with Manpower Scientific) – Department of Technology Development, GlaxoSmithKline**, Research Triangle Park, NC, February 2003 – September 2004
- Designed and created protein microarrays using non-contact piezoelectric dispensing technology.
 - Programmed, operated, troubleshoot and maintained piezoelectric arrayers.
 - Developed and analyzed methods for multiplex cytokine and kinase immunoassays.
 - Established quality control methods for protein microarray manufacturing.
- Technologist (Contract with Manpower Professional) – Department of Serology, LabCorp**, Burlington NC, December 2002 – February 2003
- Performed the following assays on patient samples:
 - IFA for IgM antibodies specific to herpes simplex virus I and II
 - ELISA for *Legionella pneumophila* serogroups 1 through 6
 - Agglutination assay to detect *Treponema pallidum* antibodies (TP-PA)
 - Managed, analyzed and prepared reports for up to 500 patient samples daily.
- Research, Muscle Function Laboratory, P.I. - Robert W. Grange, Virginia Tech**, Blacksburg, VA, Nov 1999 – Aug 2002
- Research Focus:** Molecular mechanisms of pathophysiological onset in murine models of Duchenne muscular dystrophy (DMD).
- Profiled gene expression in dystrophin:utrophin knockout mice with Affymetrix GeneChip®.
 - Constructed spotted cDNA microarray to examine calcium handling and immune response in skeletal muscle of mdx and mdx:utrophin knockout mice.
 - Assessed rates of proteolysis by the ubiquitin proteasome complex in dystrophic skeletal and cardiac muscle and C2C12 cells.
 - Genotyped and cared for mdx and mdx:utrophin knockout mice.

Publications Grange R.W., Gainer T.G., Marschner K.M., Talmadge R.J., and Stull J.T. Fast-twitch skeletal muscles of dystrophic mouse pups are resistant to injury from acute mechanical stress. *Am. J. Physiol. (Cell 283)*, 2002. pp 1090-1101.